– Ph.D. Thesis –

Intelligent multi resolution wide area seafloor observation using a landing AUV

着底型AUVを用いた広域海底の知的多重解像度調査手法の研究

サンゲカー　メフル　ナレシュ
Sangekar Mehul Naresh (47-107643)

Supervisor: Prof. Shinichi Takagawa
Prof. Toshihiro Maki

Department of Ocean Technology, Policy and Environment
Graduate School of Frontier Sciences
The University of Tokyo

東京大学
THE UNIVERSITY OF TOKYO

Contents

List of Figures

List of Tables

Glossary

AUV	Autonomous Underwater Vehicle
IIS	Institute of Industrial Science
RESQ	Radiometric Environment Survey and Quantification
ROV	Remotely Operated Vehicle
Swath	A broad strip or area
^{137}**Cs**	Cesium-137 or radio-cesium
GHT	Generalized Hough Transform
FFT	Fast Fourier Transform
GUI	Graphical User Interface
PCA	Principal Component Analysis
CAD	Computer Aided Design
DST	Digital Sonar Technology
DVL	Doppler Velocity Log
FOG	Fibre Optic Gyroscope
MCU	Micro-controller
θ_h	Camera lens horizontal opening angle
θ_o	Mounting angle of camera
θ_v	Camera lens vertical opening angle
b	Baseline between camera and laser
P_h	Image horizontal pixels
P_v	Image vertical pixels
TCP	Transmission Control Protocol
XML	Extensible Markup Language
ϕ	Vehicle roll
θ	Vehicle pitch
ψ	Vehicle yaw
X_{rob}	Vehicle x position in earth frame
Y_{rob}	Vehicle y position in earth frame
Z_{rob}	Vehicle Z position in earth frame

1

Introduction

1.1 Motivation and aim of research

The ocean is the largest feature on Earth covering more than 72% of the planet. The hydrosphere of Earth is mainly comprised of the ocean and therefore is essential to all known lifeforms and influences climate and weather patterns. The extensive seafloor is the base for islands and also includes the continental shelves, slopes, canyons, oceanic ridges, trenches, fracture zones, abyssal hills and plains, volcanos and seamounts as can be seen in Fig. 1.1.

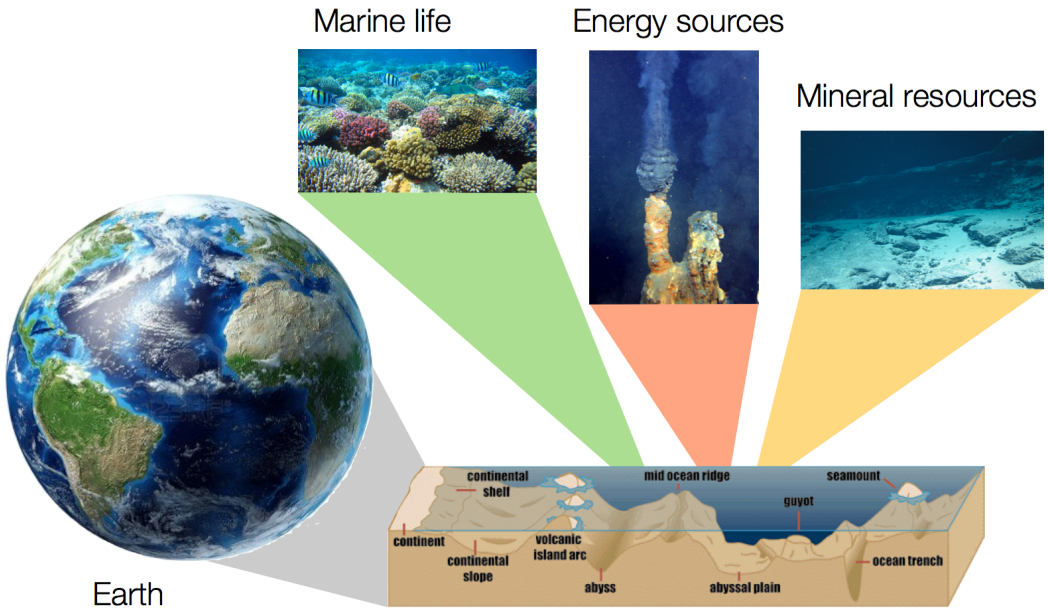

Fig. 1.1. Physical features of the seafloor such as seamounts, continental shelves, trenches, ridges, abyssal plains, etc. *Source: Museum of Science*; Resources found on the seafloor such as Manganese crusts *Source: research cruise NT*-09-02*Leg*2, hydrothermal vents *Source: weirdwarp* and marine life *Source: picture-newsletter*

The seafloor has been found to be rich in mineral deposits, marine life forms, energy products and other valuable resources which makes its exploration significant from an economic and scientific point of view. Exploration of the seafloor began as early as 1800s. Surveys was initially conducted mainly to identify the nature of the seafloor, detect features and study marine life. The first systematic deep sea exploration was carried out by *HMS Challenger* from the year 1872 to 1876 which lasted for 1000 days covering 68000 nautical miles [1]. On the shipboard scientists collected hundreds of samples, hydro-graphic measurements and specimens of marine life. They provided a first real view of the major seafloor features such as the deep ocean basins to the world and also discovered more than 4,700 new species of marine life, including deep-sea organisms. Seafloor analysis was then carried out mainly by dredging and collecting sediments using specially designed tools. Depth measurements were taken by attaching a weight to a long rope and suspending it from the ship. In order to cover larger areas and obtain higher resolution seafloor bathymetry to detect more intricate features, in the early 20th century, new methods for exploration were developed since the birth of the Electronics Age. In 1930s sufficiently accurate and compact shallow water echo sounders were developed which could be mounted on small survey crafts. Systematic surveys of the continental shelves and slopes were then performed mainly along the northeast Pacific Ocean. Even with these sensors, the survey times were quite significant often requiring a few tens of years to cover a substantial area. However a fair understand of the seafloor structure was now possible because of the bathymetry data collected from these measurements.

Fig. 1.2. Instruments for scanning the seafloor; Left: HMS Challenger survey *Source: NOAA Photo Library*, Centre: Simrad echo sounder *Source: Kongsberg Maritime AS*, Right: Multi-beam swath sounding sonar *Source: Qyudos Geosurvey*

To further reduce the survey times and generate accurate seafloor structures, in mid and late 20^{th} century, swath-sounding sonar systems were developed. A swath sounding sonar system is one that is used to measure the depth in a line extending outwards from the sonar transducer. These systems acquire data in a swath at right angles to the direction of motion of the transducer head. Technologies such as side-scan sonar [2], multi-beam sonars were

introduced which could measure seafloor bathymetry with high resolution while covering a wider area than a single beam sonar. These instruments can be seen in the Fig. 1.2.

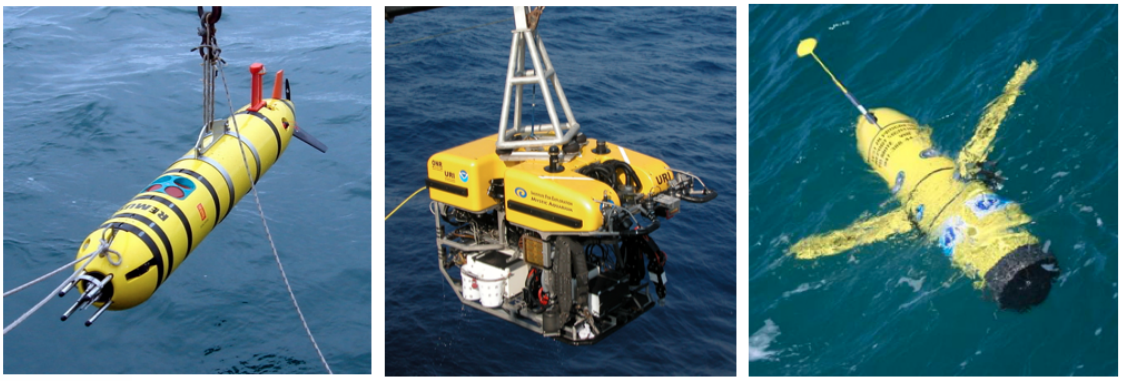

Fig. 1.3. Different types of underwater vehicles; Left: AUV Remus *Source: Hydriod Inc.*, Centre: ROV Hercules *Source: Wikipedia*, Right: Slocum glider *Source: Teledyne Webb research*

These sensors are either mounted on the bottom of a ship, towed behind or carried by an underwater vehicle. Unmanned underwater vehicles have proven to be a useful tool for ocean research by providing a reliable platform for acquiring valuable oceanic information without the need of human presence in the water as seen in Fig. 1.3. The Autonomous Underwater Vehicle technology has progressed rapidly over the past few decades to develop long endurance AUVs with cruising capabilities [3] [4]. Cruising type AUV are usually deployed for wide area mapping of the seafloor from altitudes of a few tens of meters and speeds of over a meter per second using acoustic sensors having a wide swath. At these speeds, using a lawn mower survey pattern, an AUV can cover a square kilometer area in about fifteen hours as shown by yellow lines in Fig. 1.4. Wide area bathymetry of the seafloor can provide a general overview of the nature of the seafloor. However, for detailed study and analysis of seafloor resources, higher resolution bathymetry, images and physical properties of the seafloor have to be measured.

Obtaining high resolution seafloor bathymetry or photos requires near seafloor operations using an underwater vehicle capable of slow precision maneuvers or hovering which cannot be performed using a cruising type AUV. Seafloor properties are usually studied by taking samples of rocks and sediments on the seafloor and processing them in the laboratory. In recent years, many groups have been involved in the development of in-situ sensors for obtaining seafloor properties such as gamma radiation detectors [5], underwater microscope for sediment grain size study [6], manganese crust measurement [7], chemical sensing [8] etc. Some of these can be seen in the Fig. 1.5. These sensors often require close proximity or contact with the seafloor for integrated measurements or stable contact for obtaining reliable results. Remotely Operative Vehicles (ROV) are typically used for precision slow speed maneuvers or hovering operations making them suitable for collecting high

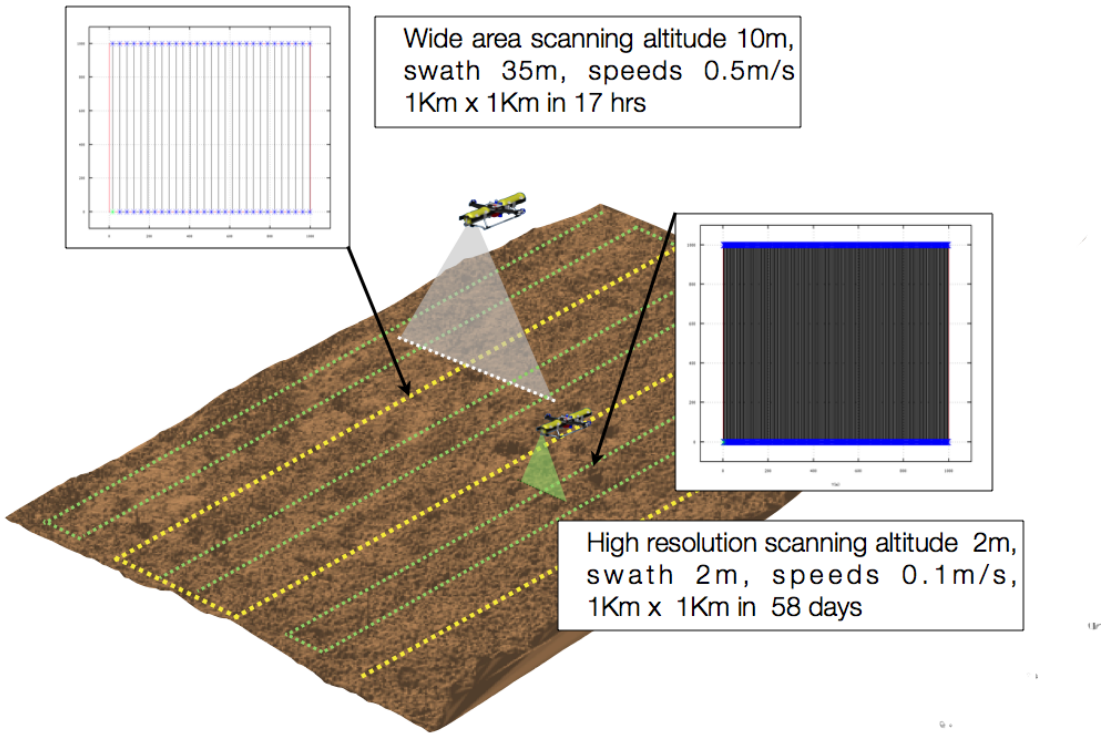

Fig. 1.4. Comparison between scanning the seafloor using an sensors with different swath lengths, scanning altitudes and speeds; Yellow line: scanning using sonar system with a wide swath, Green line: scanning using high resolution sensor with a narrow swath

resolution bathymetry, photo-mosaics, sampling or seafloor properties from in-situ sensors. For obtaining high resolution bathymetry or seafloor images, scanning is usually performed from an altitude of a few meters and speeds of few centimeters per second. At such slow speeds the vehicle would take around sixty days to scan a kilometer area of the seafloor. It would require a substantially large amount of time to obtain high resolution data, samples and measure seafloor properties all throughout the survey area. Since ship survey times are limited and costs are high, it is not possible to perform such high resolution observation in a large area. For understanding of seafloor process and marine life it is often necessary to obtain multiple resolution data and measure seafloor properties for better analysis and understanding as demonstrated with exploration scenario in real ocean environments.

The ocean has a complex combination of physical, chemical, biologic, and geologic processes that sometimes result in the formation of commercially viable wide range of minerals. Such minerals can be found around hydrothermal vents where hot chemically rich fluids pour out of the ground and deposit. On the slopes of underwater seamounts around the world, minerals precipitate out of the seawater to form thin crusts on rocky

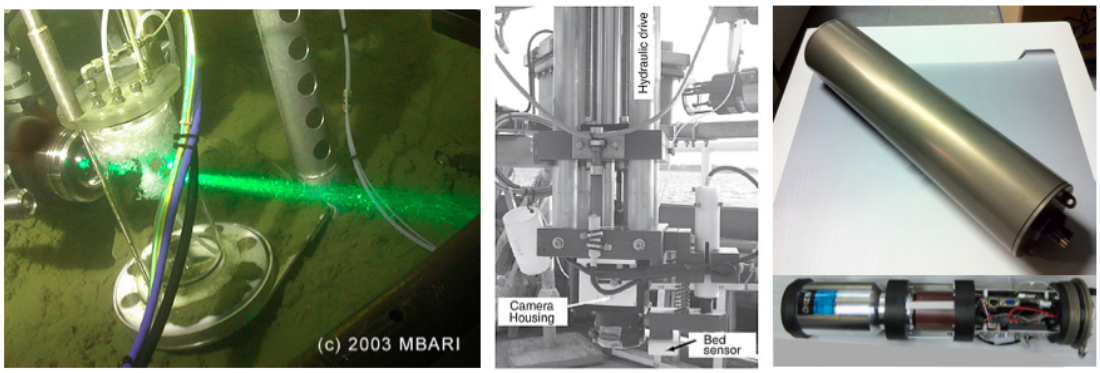

Fig. 1.5. In-situ measurement sensors; Left: DORISS - Deep Ocean Raman In Situ Spectrometer *Source: MBARI*, Centre: Underwater microscope for measuring spatial and temporal changes in bed-sediment grain size *Source: U.S. Geological Survey*, Right: Gamma ray spectrometer measuring full gamma spectrum *Source: Institute of Industrial Science, The University of Tokyo*

surfaces also known as ferromanganese crusts. These are found to be rich in iron and manganese and smaller amounts of cobalt. Manganese nodules are also found along some parts of this region which are rock concretions formed of concentric layers of iron and manganese hydroxides around a core. These minerals have high economic value with a possibility for mining for which their volumes and concentrations need to be measured to estimate profitability. Underwater seamounts are spread over hundreds of kilometers with resources scattered all throughout [9]. Bathymetry maps of these seamounts can be generated with the use of an AUV using an acoustic sonar with a wide swath by scanning at a high speed. However, to estimate the volume of manganese crusts it is necessary obtain thickness measurements from a specialized sensors. Since manganese nodules are of the order of a few centimeters, high resolution bathymetry and photo-mosaics also needs to be generated for their observation. These sensors require scanning from a low altitude and slow speed. Furthermore, to measure the concentrations of the mineral deposits, chemical measurements have to be taken which require contact with the seafloor. Since it is time consuming to obtain high resolution bathymetry and mineral properties, it is difficult to cover a wide area in limited ship time and perform analysis. Usually straight line transects are performed from a low altitude to survey unexplored area. An overview of such a survey can be see in Fig. 1.6.

Deep sea life with no access to sunlight depends strongly on the nutrients from the hydrothermal vents or seepage around which they establish colonies. Although life is very sparse at these depths, black smoker chimneys are the centers of entire ecosystems. Along with bacteria, more complex life forms, such as clams, tube-worms and crabs are also observed around these vents. The hydrothermal vents are therefore of significant importance for understand the origin of marine life. Hydrothermal vent fields are spread over wide areas and individual chimneys can be separated by tens of kilometers. By generating bathymetry from wide swath acoustic sensors using high speeds, the location

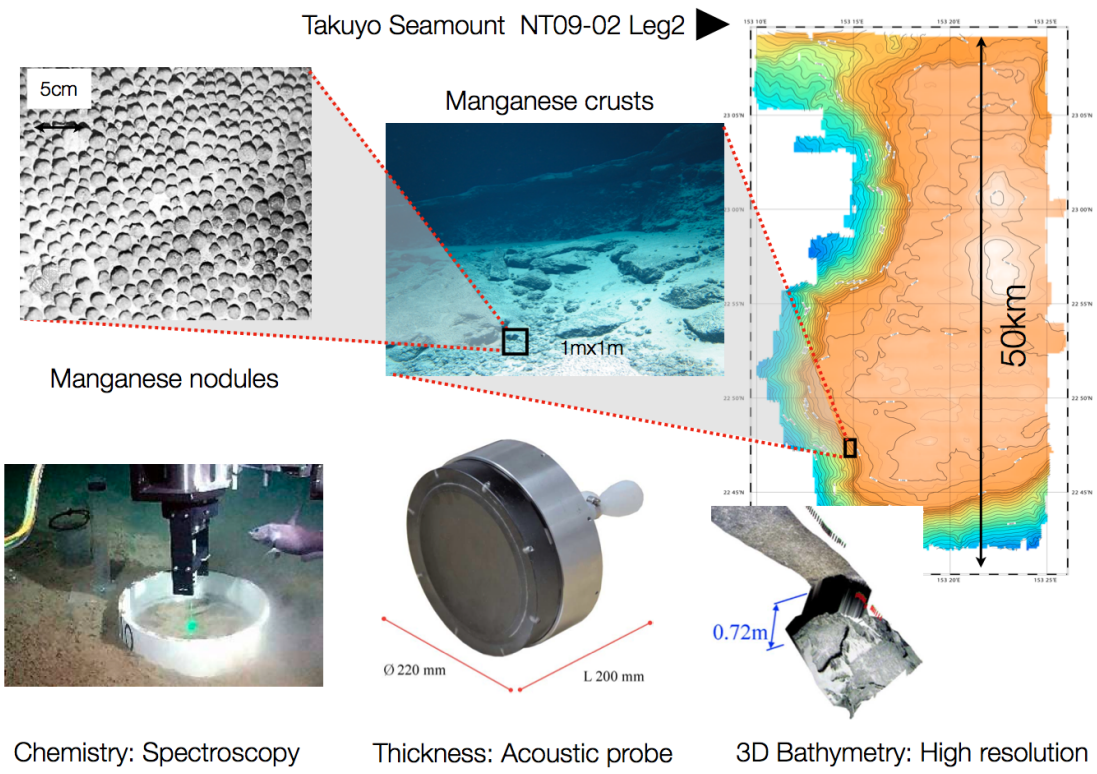

Fig. 1.6. Multi-resolution surveys required for measuring concentrations and thickness of mineral resources in areas with Ferromanganese crusts

of these vents can be identified [10]. To understand the marine life around these chimneys, high resolution bathymetry and color images have to be generated around these vents. Information from chemical sensors can also provide valuable information about their evolution. Obtaining such data is a time consuming operation and ROVs with suitable sensors are deployed at individual chimneys for performing operations. This limits the area to be covered substantially. Fig. 1.7 gives an overview of the multi-resolution surveys required to study hydrothermal vents.

Seafloor surveys become essential during disaster situations such as radiation leakage into the Ocean during the Fukushima No.1 nuclear plant incidence as see in Fig. 1.8. Nearly $0.5x10^{15}$ Bq of ^{137}Cs was leaked into the ocean after the nuclear accident following the Great East Japan Earthquake [11]. To understand the effects of radiation and its relation to seafloor bathymetry, wide area bathymetry has been generated using multi-beam sonar system. The radiation measurements are conducted using a towed system which is dragged from a boat on the seafloor along straight line transects [12]. The system consists of a gamma scintillator housed in a pressure cylinder and enclosed in a rubber hose called Radiometric Environment Survey and Quantification hose, or RESQ hose. From the data

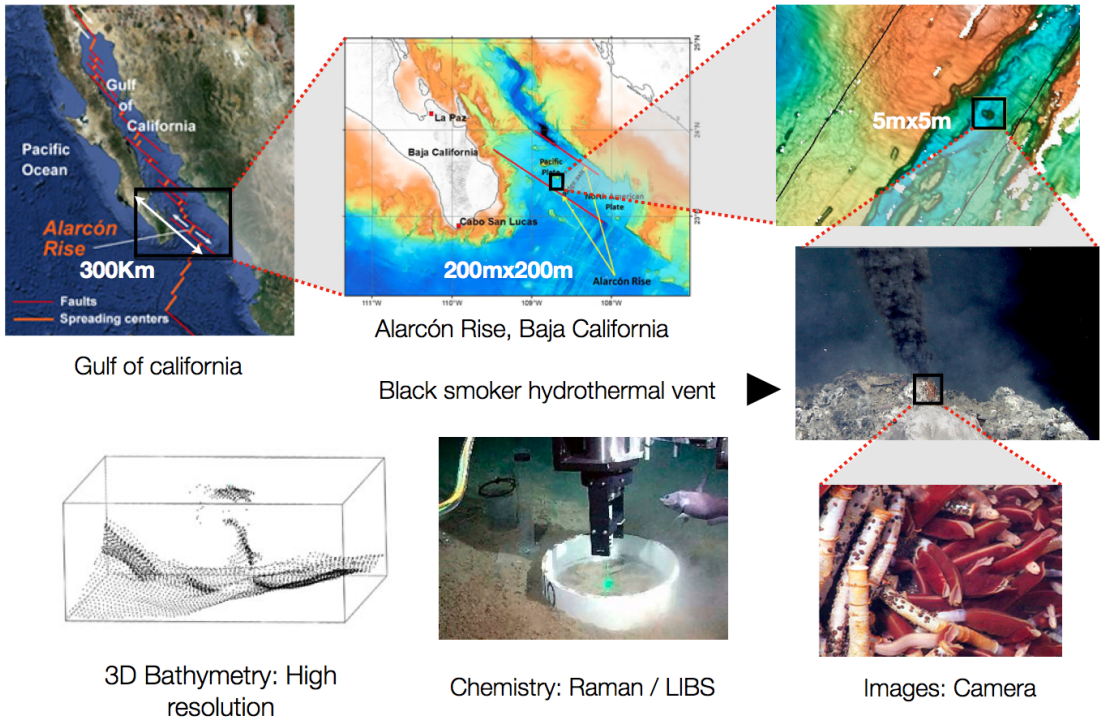

Fig. 1.7. Multi-resolution surveys required for observation and study of marine life and seafloor composition in areas around hydrothermal vents

collected it is evident that radiation hotspots have been observed at several location along the survey area with seafloor features such as artificial reefs. For further analysis of these areas, detailed high resolution bathymetry has to be generated along with seafloor images. Radiation measurements also need to be obtained around these features which cannot be performed by a towed system. A ROV mounted with a gamma scintillator detector and camera for generating photo mosaics can be used to obtain such data by precise manoeuvring. In areas free of complex structures, this is a very effective technique to study the hotspots. However in areas such as fishing reefs, the chances of the ROV tether getting entangled and severed are high which makes it unsafe for operation.

From the above seafloor exploration scenarios, it can be seen that it is difficult to obtain high resolution bathymetry, images and measure seafloor properties from the seafloor in a wide survey area. Most surveys are conducted by generating a wide bathymetry map of the survey area and manually identifying features where higher resolution data can be obtained. Within the wide survey areas, the regions where mode details need to be obtained are small and based on the seafloor properties being measured by the sensor. In the proposed method, an AUV at first scans the seafloor in the survey area using an acoustic sensor with a wide swath from a high altitude and fast speed to generate bathymetry with centimeter order resolution. This bathymetry data is then automatically analyzed in smaller sections by an

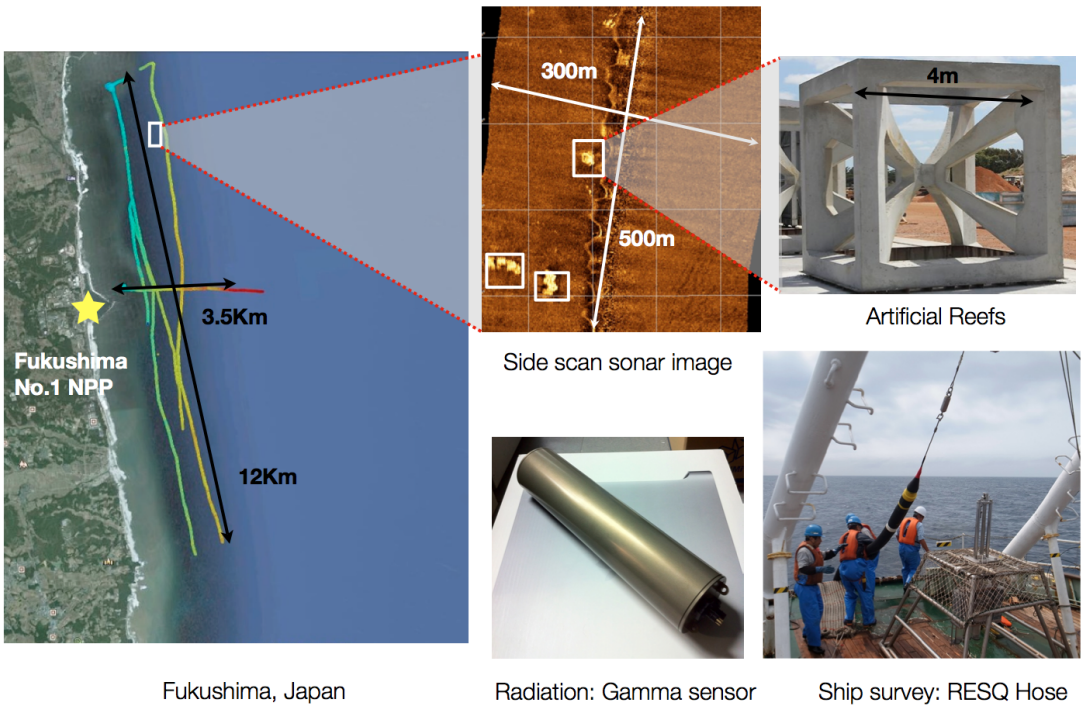

Fig. 1.8. Radiation measurement around man-made artificial reefs in waters around the Fukushima nuclear power plant No.1

algorithm to identify suitable areas for high resolution scanning based on the survey interest provided as survey rules. At these locations, higher resolution millimeter order bathymetry is then generated by scanning from a lower altitude and slow speed using a laser profiling system. Autonomous landing is also performed at some of these locations depending on the survey interest to obtain data from the seafloor using payload sensor. In this way, a multi-resolution map of the area can be generated efficiently and in a less period of time as compared to scanning the entire survey area with high resolution. By using a different payload sensor and modifying the survey rules depending upon the seafloor property being measured, the same vehicle can be used to perform surveys such as chemical plume tracing, radiation measurements around man-made structures and seafloor features, photo-mosaic underwater structures etc.

1.2 Background research on the subject

Most underwater surveys are carried out by pre-mission path planning to navigate the entire survey area under interest. Efficient path planning methods have been previously researched by various groups [13]. The survey path is only modified in case of obstacles found in the planned path or to navigate throughout ocean currents. Algorithms for efficient

re-path planning in presence of obstacles have also been developed previously [14]. During such surveys, the collected seafloor observation data is stored inside the vehicle and not used for real-time analysis. Pre-mission planned paths, such as lawn-mover patterns, can be effective for wide area scanning using acoustic sensors to generate an overall bathymetry of the area or high resolution scanning over a small survey site for collecting detailed information. It is not efficient when covering a wide area while trying to acquire high resolution bathymetry and measuring seafloor properties by landing at the same time due to limited ship times and costs.

Previous work has been done on adapting the vehicle route during surveys by analyzing the collected data in real-time. One such research is for sonar equipped vehicles to modify their planned path for adapting the AUV route to prevent portions of the mission area from being either characterized by poor image quality or obscured by shadows caused by sand ripples [15]. Simulations have carried tried out to demonstrate multiple AUV surveys [16] by analyzing the data collected in real-time to avoid sampling the sub-regions already explored [17]. Algorithms for analyzing the scanned bathymetry point cloud and detecting regions with poor mesh resolution for path planning have been previously developed. [18]. Although the data collected is analyzed and used for vehicle path planning in real-time, it is not used for adapting between scanning resolutions. Furthermore, the property of the seafloor measured does not influence the path-planning process.

Adaptive path planning based on the seafloor property measured has also been tried before. One work involves simulating adaptive path planning for bathymetry contour tracking using an AUV with downward looking altimeter and evaluating the expected utility [19]. Work has also been done for chemical feature tracking and localization using an AUV for processing the concentration levels measured by the sensor in real-time [20]. Chemical plume tracing by measuring the concentrations to locate the source have been demonstrated as well [21]. Simulations have also been performed to demonstrate the adaptive sampling technique by identifying locations of additional ocean measurements that would be most useful to collect [22]. Tracking based on the observed data features has also been performed [23]. In most cases only concentration of measurements previously collected are utilized in adapting the path, the features detected on the seafloor and their relationship to the parameters to be measured is not considered.

Algorithms for terrain classification and segmentation have been previously developed for sonar as well as image data [24] [25]. FFT based algorithms have been used for segmentation of objects on the seafloor mainly at archeological sites [26] [27]. Estimating seafloor properties and benthic classification based on sonar backscatter and reflection intensities have been studied by various groups [27]. Feature detection based on acoustic data has been demonstrated [28] [29]. Classification is mainly done to determine the nature of seafloor and its material characters. Not much application has been based on identifying the attributes of the features. Also most algorithms require substantial computation time and large processing power making them difficult to implement for real-time applications in underwater vehicles. Also use of the terrain classification information and its use

in adapting the survey based on the interest and sensor requirements has not been demonstrated.

Navigation of underwater vehicles by analyzing the scanned bathymetry in real-time has previously been demonstrated [30]. Feature matching has been performed for localization and accurate positioning of the vehicle using particle filter on profiling sonar data data [31] [32]. Similar algorithms have also been simulated for side-scan data [33]. However, features are not used for adapting the scanning resolutions and their relationship to the payload sensor and the seafloor property being measured are not considered. Bathymetry analysis is not performed for detecting high resolution scanning areas or performing landing at relevant locations. The use of sensor information and seafloor parameters measured in decision making for adapting the scanning resolution has not been implemented in a autonomous underwater vehicle.

The proposed research also allows the vehicle to land on the seafloor for obtaining measurements. Extensive work has been previously done for automatic landing of aerial vehicle [34]. Landing controllers for unmanned vehicles based on Fuzzy logic have been simulated [35]. Work has also been demonstrated on camera based landing with reinforced learning [36]. Autonomous landing of underwater vehicles on the seafloor has not been significantly explored. Experiments for seafloor landing have been performed by developing a control system for landing using variable buoyancy [37] [38]. Dynamics for seafloor landing have been studied and models have been developed [39]. Theoretical concept for use of camera [40] for detecting obstacles during landing has been proposed. Autonomous landing on the seafloor by detecting obstacles from high resolution scanned bathymetry has not been demonstrated before and performed for the first time in this study.

1.3 Research objectives

This research aims at developing a new survey method for allowing an autonomous underwater vehicle to cover a wide survey area while obtaining high resolution data at certain areas of interest in a single dive. The research aims to allow AUVs to change scanning resolutions and sensors based on the seafloor property being measured and sensor requirements. This will enable the use of AUVs in complex seafloor scenarios. As seen from the previous section, due to scanning speeds and sensor resolutions, it is difficult for a vehicle to obtain high resolution bathymetry and measure seafloor properties after landing while covering a wide survey area in a limited ship time.

To provide a solution to this problem, this study proposes to develop a survey method and hardware capable of intelligently adapting between scanning resolution in real-time based on the ocean properties being measured and the survey interest. For the vehicle to make appropriate decisions, it is necessary to detect the seafloor features from the scanned bathymetry data. Since the computational power on-board an underwater vehicle is usually limited, algorithms developed for detecting these features and making intelligent decisions need to be efficient and simple. This research shows the theoretical development of the

intelligent decision making technique and its practical implementation on an underwater robot.

To demonstrate the survey system, a vehicle suitable for high speed scanning as well as low precision manoeuvring has to be designed. For measuring properties of the seafloor using in-situ sensors, the research aims to develop a platform capable of performing autonomous landing on the seafloor. As seafloor can be bumpy, it is not safe for an underwater vehicle to land arbitrarily. When using ROVs for seafloor observation, vehicle landing is performed by a human operator using visual and sonar feedback. Automatic landing is a more complex operation and requires detection of obstacles on the seafloor and suitable flat area. For making this process automatic, a sensing technology with sufficient resolution along with an landing algorithm has to be developed which can perform safe landing. Since the data has to be collected from the seafloor, it is important not to disturb the underlying sand and sediments while performing autonomous landing. These points need to be considered while designing the vehicle to perform the survey.

1.4 Organization of thesis

The thesis is organized into eight chapters which includes this introduction. The chapters cover in detail the theoretical aspects of the proposed intelligent multi-resolution survey method as well as its implementation using a developed autonomous underwater vehicle. The manuscript also includes three Appendices to provide additional support to the chapters containing multi-resolution scanning hardware and vehicle development.

In Chapter 2 of the manuscript, the proposed method is described in detail with elaborate sections on each stage of the method. The concept of survey rules is explained along with an overview of the data processing algorithms required at each stage. Assumptions required for the method to work effectively and requirements for an underwater vehicle to performs such surveys are also mentioned. The applications of the method to real-world scenarios are shown with illustrations.

Chapter 3 explains the wide area scanning stage of the survey method in detail. Details are provided on the sensor initialization, assumptions and considerations for wide area scanning. Details of the hardware used for data collection are provided along with sensor specifications. The data processing techniques to generate bathymetry and filtering outliers are illustrated. The algorithm for seafloor feature identification and classification using this data is described in detail. The method for intelligently selecting an area for high resolution scanning based on the features detected and the survey rules is elaborated in detail along with necessary mathematical equations. The chapter also explains the automatic waypoint generation for covering the selected for high resolution scanning efficiently.

Chapter 4 continues over from the previous chapter and discusses in detail the method for high resolution scanning of the seafloor and automatic landing. The hardware used for obtaining the data is described and the processing techniques for generating high resolution bathymetry and removing outliers are explained. The algorithms for analyzing this bathymetry for detecting features and extracting their attributes are described and

corresponding mathematical equations are mentioned. The process of decision making for selecting the landing sites based on survey rules is explained with illustrations.

Chapter 5 gives details on the development of the landing vehicle which is used for demonstrating the proposed survey technique. The design considerations for the vehicle have been discussed. Specifications of the vehicle and the scanning sensors have been provided. The vehicle electronics architecture has been explained along with the basic software architecture and the control system. Details on implementation of the software for performing the proposed method have been provided along with its integration into the vehicles core software. The different modes of operation of the vehicle have been shown which are required to carry out the survey.

Chapter 6 describes the experimental procedures used to evaluate the proposed method. Initial sections of the chapter provide details on the individual experiments used to test the vehicle hardware, wide area scanning and high resolution scanning systems and algorithms. The experimental setup used is described and the results obtained are analyzed to evaluate the performance of the individual systems. The later part of the Chapter describes the assumptions and test objectives for evaluating the overall survey method proposed. Experiments are conducted in a tank environment at the Chiba experimental station with the IIS, University of Tokyo to test the decision making capability of the vehicle and computation speeds of the algorithms. The setup used and the scenarios made for the experiments are explained in detail. The results obtained from these experiments are also analyzed to evaluate the proposed method. The algorithm are evaluated for their intelligence based on the decisions made by the vehicle under different scenario. They are also evaluated for their accuracy and computation time.

Chapter 7 provides observations concerting the efficiency and accuracy of the proposed method for generating multi-resolution maps. The parameters affecting the performance of the algorithms and their effects are also analyzed. The vehicle hardware and software performance is analyzed in terms of adaptation to real ocean environments and scenarios.

Chapter 8 provides conclusion to the research and offers suggestions for future works and advancements that can be made to this research. This chapter is followed by the references used in this thesis as a support for arguments and discussions. The manuscript has Appendix A which provides further details on the wide area and high resolution scanning sensors and the bathymetry generation process. Appendix B provides CAD mechanical diagrams of the vehicle along with essential electronic circuits. Finally, Appendix C gives the format specifications of the vehicle initialization file and the survey rule file used for decision making and analysis. Examples of these files used during the experiments are also provided.

2

Proposed survey method

This chapter explains in detail the method proposed in this research for wide area high resolution scanning of the seafloor by intelligently adapting the scanning resolution. Initial section of the chapter gives an overview of the method and describes the various stages involved in performing the survey briefly. The assumption and conditions considered for the method to perform successfully have been elaborated. The specifications and requirements of an underwater vehicle capable of performing such a survey have also been discussed. Finally the practical applications where this method can be used in some of the scenarios described in chapter 1 have been illustrated. The following chapters thereafter describe the different stages in detail and provide an introduction to the algorithms developed for performing decision making and analysis.

2.1 Overview of the method

The proposed method involves the generation of wide area maps of the seafloor with high resolution data and seafloor properties measured at intermediate locations. The locations for high resolution data collection are automatically decided based on the interest of the survey and the property measured by the sensor after landing. The first stage of the survey involves scanning a suitable patch of the seafloor using an acoustic sensor with a wide swath such as a multi-beam sonar or a side-scan sonar. A vehicle is provided waypoint coordinates and safe operational area of the survey area within which the multi-resolution map has to be generated. The vehicle is prohibited from scanning outside the limits of the safe operational area. Scanning speeds and altitudes for wide area survey are also provided to the vehicle before the start of the survey.

Fig. 2.1 provides an overview of the wide area scanning stage of the proposed method. The vehicle first scans the region between the waypoints in small sections. Scanning altitude is typically set such that the resolution obtained in the horizontal direction is between 15cm-20cm. Altitude of about 10m or more is usually set for obtaining sufficient resolution. To obtain a similar resolution in the forward direction and a uniform footprint on the ground, the speed of the vehicle is usually set at about 0.5m/s. The length of the seafloor sections is usually kept to a few tens of meters at a time. This is done to prevent excessive

processing time and having the vehicle to traverse a long distances backward for high resolution scanning.

Once a suitable section of the seafloor has been scanned, three dimensional bathymetry is generated from the sonar data which has a resolution of a few tens of centimetres. This bathymetry data is then provided as an into to the algorithm which identifies seafloor features, slopes and roughness to segment the area into sections. A survey rule file is also provided to the vehicle which is a custom file providing information about the features to be identified where higher resolution bathymetry and seafloor properties have to be measured. Based on the survey rules and the features identified, the area for high resolution scanning where properties of the seafloor have to be measured after landing is selected. An algorithm then generates waypoints to cover the selected area effectively and efficiently. Finally high resolution scanning is performed at these area where properties of the seafloor have to be measured either by landing or slow speed navigation.

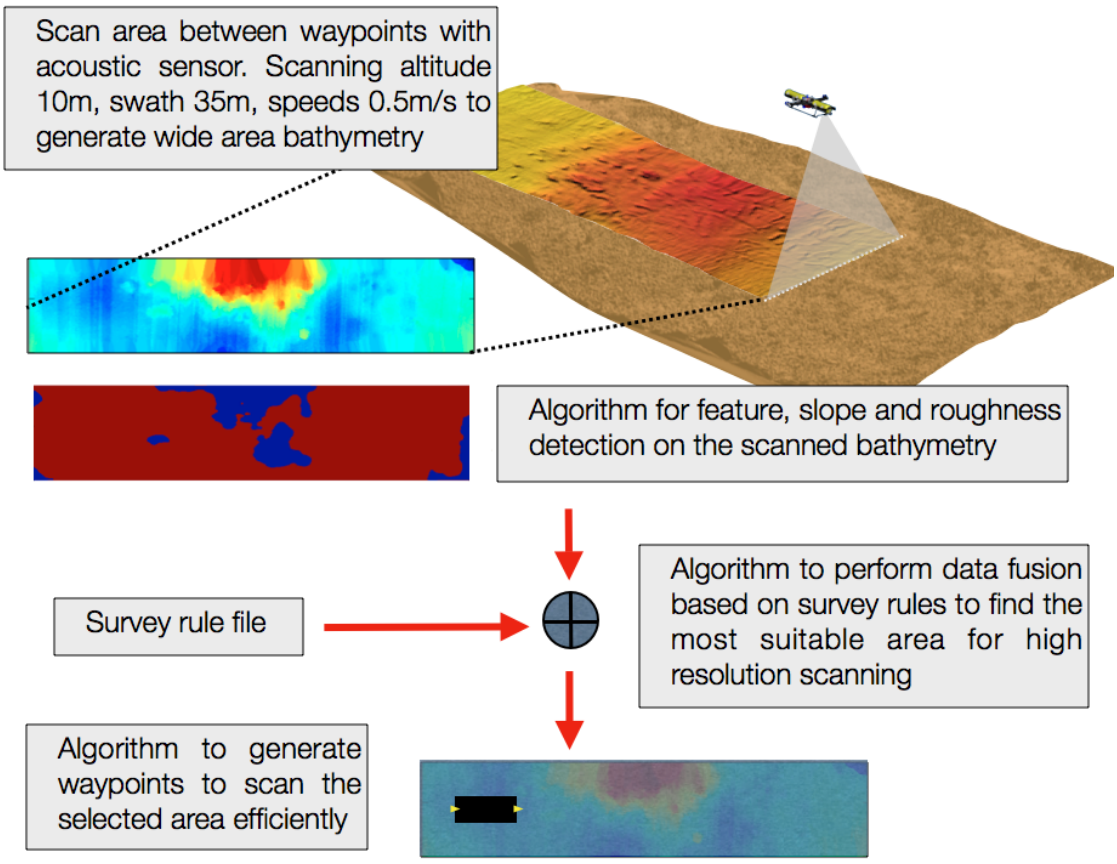

Fig. 2.1. Overview of the wide area scanning stage of the method using an AUV

After the waypoints for high resolution scanning within the survey area have been generated by the algorithm, the vehicle scans the area between the waypoints with slower speed and lower altitude. Fig. 2.2 provides an overview of the high resolution scanning stage. The scanning altitude and speeds for high resolution scanning are also provided to the vehicle before the start of the survey. Scanning sensors such as light sectioning based laser profiling system or stereo camera system are used for generating millimeter resolution bathymetry of the seafloor. The scanning altitude is set such that the resolution obtained across track is about 5mm-8mm. Typically for laser profiling system with camera resolution of 640x480, the scanning altitude is set to about 2.5m. In order to have a similar resolution in the forward direction and a uniform footprint, the forward scanning speed is set to about 0.1m/s. After scanning the entire selected area, high resolution bathymetry is generated.

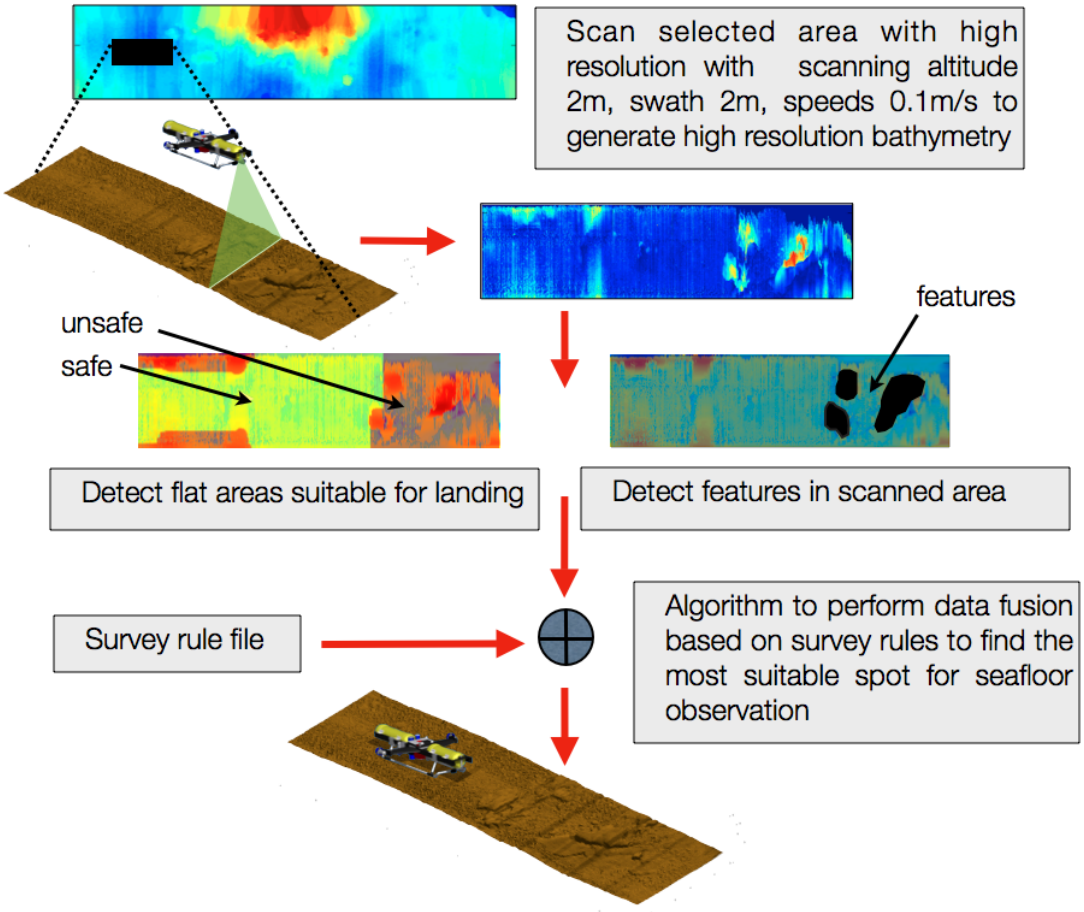

Fig. 2.2. Overview of the high resolution scanning stage of the method using an AUV with landing and slow speed navigation capabilities

This bathymetry is then analyzed in two separate ways to extract parameters from the scanned bathymetry. An algorithm first detects flat areas in the scanned bathymetry which are suitable for the size of the vehicle to land safely. A second algorithm detects features in the scanned high resolution data and measures their attributes such as shape, size, orientation, location and other parameters based on shape. Survey rules are provided to the vehicle which indicate the actions to be taken by the vehicle based on the features identified in the bathymetry. Based on the survey rules and the features and flat landing areas are detected, the landing points or navigation waypoints for performing seafloor observation are selected.

A landing algorithm generates the appropriate landing coordinate and heading for the vehicle. The survey rules might at times require the vehicle to detect additional landing spots. This is usually the case when seafloor properties measurements have to be compared between two areas with features. In case the landing spots have to be detected in areas not scanned previously, the algorithm generates new waypoints for the vehicle to scan a small region with high resolution. The newly scanned area is fused with the previously scanned area and new landing coordinates are generated using the landing algorithm. In case seafloor observation has to be performed by slow speed navigation, a path is generated for navigation with the right scanning heading.

2.2 Requirements and assumptions

The method requires the detection of features in the scanned bathymetry for making decisions. To be able to detect features in the acoustically scanned wide area bathymetry data, the collected data should have a minimum resolution of 20cmx20cm. At lower resolution it may not be possible to detect small features such as hydrothermal vents and rocky areas correctly. For high-resolution data analysis, the sensor should be capable of data acquisition with a resolution of about 8mmx8mm or lesser. High resolution is required for detecting the feature attributes accurately for making decisions. The algorithm for detecting the landing sites also utilizes this data. Since the size of the objects that can be detected on the seafloor for safe landing depends on the resolution of the data, it is important that the scanning resolution is high.

For an underwater vehicle to generate wide area maps, it should be able to perform high speed cruising. At the same time for generating high resolution maps and precision landing on the seafloor, the vehicle should be able to hover and perform slow speed maneuvers. For this a hybrid vehicle design and shape are essential. Since data has to be processed in real-time, the vehicle should have sufficient computational power with preferably more than one main computers. During data processing, it is required that the vehicle performs hovering and maintains its horizontal position. It is essential to have the data processing time and the computational time of the algorithms to be kept at a minimum to prevent substantial drift in the vehicle navigation sensors. It is assumed that during short processing, the drift in sensors is negligible and does not contribute substantially to the vehicle position error. For this reason, it is not possible to process large bathymetry areas at

the same time and the area has to be divided into smaller sections for processing. Since the main aim is to obtain reliable seafloor properties using in-situ sensors, the vehicle should be able to provide a stable footing for the sensor after landing. A vibration-free platform is essential for obtaining data such as microscopic images, integrated measurements using breakdown spectroscopy LIBS system etc. The vehicle should also prevent disturbing the underlying sediments and sand while landing before performing seafloor observations.

2.3 Application to real world scenarios

Radiation measurement: The proposed survey method can be easily applied to real world scenarios as describes in this section. One of the suitable applications of the method is to study the ^{137}Cs that was leaked into the ocean after the nuclear accident following the Great East Japan Earthquake. Currently measurements are conducted using a towed system which is dragged by a boat on the seafloor along straight line transects. The system consists of a gamma scintillator housed in a pressure vessel and enclosed in a rubber hose. From the data collected it is evident that radiation hotspots have been observed at several location along the survey area [41]. These hotspots have specially been observed in areas with seafloor features, man-made as well as natural. For further analysis of these areas, detailed high resolution observation is essential which cannot be performed by a towed system. Furthermore, it may not be possible to obtain measurements using the towed system at man made structures such as artificial reefs due to possible damages caused by the structure sensors.

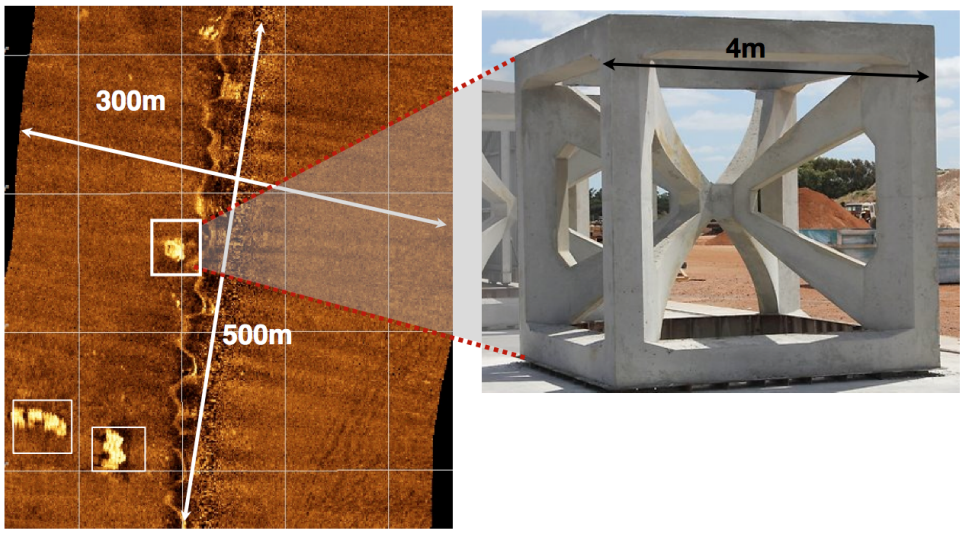

Fig. 2.3. Artificial reefs seen in a wide area side scan image taken in the waters around Fukushima

A ROV mounted with a gamma scintillator detector and camera for generating photo mosaics can be used to obtain such data by precise manoeuvring. In areas free of complex structures, this is a very effective technique to study the hotspots. However in areas such as fishing reefs, the chances of the ROV tether getting entangled and severed are high which makes the operation unsafe. Fishing reefs are effective in promoting marine life in areas which have generally featureless bottom. Reefs tend to increase fish yields and is an effective way for developing fishing areas.

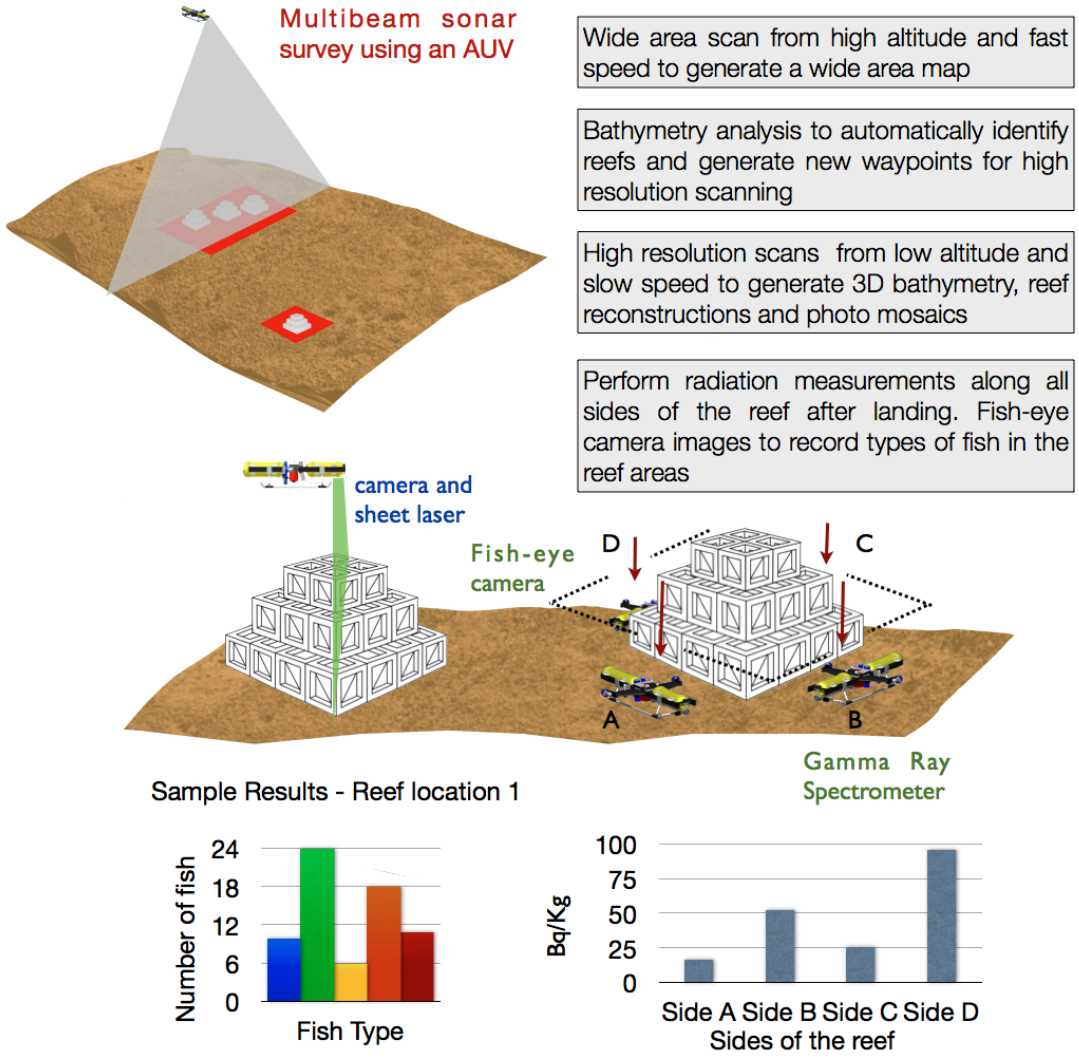

Fig. 2.4. Autonomous radiation measurements around artificial reefs; Observations made such as the types and quantities of fish measured and the radiation levels measured on all sides of the reefs

Artificial reefs are present in the vicinity of Fukushima and are likely to accumulate radioactive substances. Since these fish are caught for consumed, it can create a major health issue. As a result it is essential to observe these areas in detail and measure the radiation concentration levels around them. Along with this, it is essential to identify the species of fish and their population by scanning a large volume. The proposed method can be implemented on an AUV to perform the survey autonomously. The reefs under consideration are spread over a wide area as can be seen from the side scan image in the Fig. 2.3

The autonomous underwater vehicle can perform a wide area scan automatically in the survey area to generate bathymetry from a fast speed and high altitude scanning. This bathymetry can be then automatically analyzed to identify the location of features with similar shapes as the reefs. The vehicle can then select areas for high resolution scanning based on the location of the identified reefs and new waypoints will be generated as seen in Fig.2.4. The selected area with the reefs will be scanned with high resolution. Data from the camera will be used to generate photo mosaics of the area around the reefs automatically. The high resolution bathymetry will be generated around the reefs which will be analyzed by the algorithm. The algorithm will detect the reef as the featuring estimating its shape, size and other attributes. The landing areas will also be identifies. From the survey rules, the vehicle will decide to perform landing on all four sides of the reef to measure radiation levels. The landing algorithm will then process the scanned bathymetry to generate landing points and headings on all four sides for observation of seafloor properties. The radiation levels measured on all the sides can then be compared as a bar chart. The type of fish detected and their quantities can also be analyzed.

Mineral exploration: The method can also be easily applied for other seafloor exploration scenarios such as exploration of mineral resources at ferromanganese crusts seamounts. Exploration for mineral resources is essential for economic progress of nations. It is necessary to measure their volumes and concentrations. Underwater sea-mounts are spread over hundreds of kilometers and mineral resources are scattered. Long slabs of manganese crusts have been observed along the outer edges of these seamounts as can be seen in the Fig. 2.5. Bathymetry maps of these seamounts can be generated with the use of an AUV using an acoustic sonar with a wide swath by scanning at a high speed.

However, to estimate the volume of manganese crusts it is necessary obtain thickness measurements. These in-situ thickness measurements are possible today by the use of an acoustic probe by scanning from a low altitude and slow speed. Also to study manganese nodules, and estimate their quantity, it is necessary to generate high resolution bathymetry and photo-mosaics which also require scanning from a low altitude and slow speed. Furthermore, to measure the concentrations of the mineral deposits, chemical measurements have to be taken which require contact with the seafloor. Since it is time consuming to obtain high resolution bathymetry and mineral properties, it is difficult to cover a wide area in limited ship time and perform analysis. The proposed method can be used to perform such surveys autonomously by using the appropriate sensors and setting

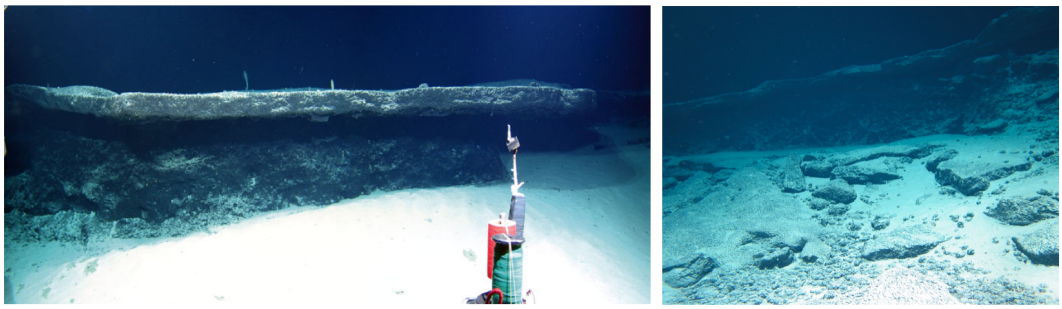

Fig. 2.5. Slabs of Ferromanganese crusts observed at the Takuyo seamount during the research cruise NT-09-02Leg2

up right survey rules. The rules can be designed to identify flat slab like features or nodules from acoustic bathymetry. At such flat areas and features, the vehicle can generate new waypoints for scanning with higher resolution to scan the bathymetry in detail. The vehicle can then perform landing at one or more locations along the slabs to measure concentrations and get thickness measurements. The vehicle can land on the top and bottom areas of the slabs for comparing measurement and concentration results.

Hydrothermal vent exploration: Application of this method can be easily extended to the study of hydrothermal vents for mineral resources and marine life exploration. Hydrothermal vents are the source of energy and nutrients for marine life which rarely receive energy from the sun. These vents are spread over hundreds of kilometers and can be easily detected using a multi-beam sonar. To understand them thoroughly and study the mineral and marine life, it is necessary to obtain high resolution information from a close proximity of the vents. The proposed method can be adapted to surveying such hydrothermal vent fields automatically. The vehicle can be made to scan a wide area automatically to detect features similar in shape to vents. This can be done using the rule file. Once the feature is detected, the vehicle can scan the area around the hydrothermal vents to generate high resolution bathymetry. This can then be analyzed to detect the vent features in high resolution and generate a three dimensional model by scanning from all directions around the chimney automatically. Also landing can be performed at one or more locations on the side of the vents to measure chemical compositions. Photographs can be taken by slow speed navigation around the vents to document marine life. The vehicle can be made to perform this survey by modifying the survey rules to detect hydrothermal vent like features and performing appropriate action. By performing such a survey, a wide area map of the survey region can be automatically generated showing the location of the chimneys with high resolution images and chemical data obtained around the vents.

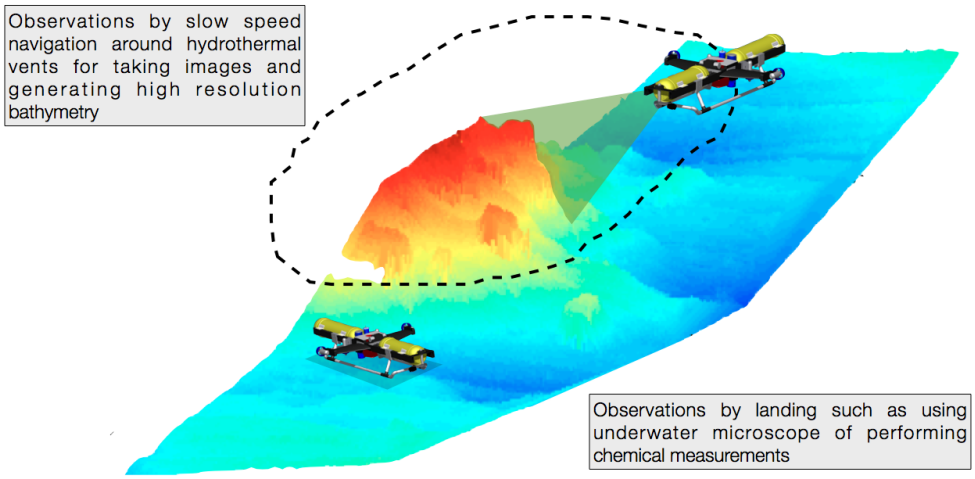

Fig. 2.6. Autonomous observations around hydrothermal vents by landing or slow speed navigation; Black line: observation track around the hydrothermal vent

2.4 Survey rules

The main objective of the survey is to be able to obtain seafloor properties efficiently over a wide area either by landing or by detailed high resolution observation. For this purpose, we consider a sensor driven approach to select the landing areas based on the features detected in the bathymetry. In an area where high resolution bathymetry is available, the landing points have to be decided which are most suited for the sensor carried by the vehicle. At these locations, seafloor observation can be performed after autonomous landing based on the attributes of the features. Some sensors may not require landing on the seafloor for data collection and observation. In such cases, the survey might require the vehicle to perform slow speed manoeuvring around specific features on the seafloor. For this purpose the survey rules exploits the known relationships between the seafloor features and the seafloor properties being measures. The rule dictate the features to be selected and the action to be taken by the vehicle when specific features are observed. The rules of the survey are defined in a custom format in the survey rule file. This file is provided to the vehicle before the start of the survey along with the initialization file. The rules define the behavior of the vehicle and the multi-resolution map generated during the survey. Details on the format of the file and its structure are provided as Appendix C at the end of the manuscript.

3

Wide area scanning

This chapter provide details on the wide area acoustic scanning stage of the proposed survey method. The acoustic sensors required for scanning the seafloor and their requirements are described. The method of seafloor scanning using these sensor is described. The decision making process to select high resolution scanning area based on the features detected is descried with illustrations. The purpose of the rule file in has been explained and its involvement in the decision making process is mentioned. Details of the feature detection algorithm are provided with further information on the techniques used during each step of the algorithm. The waypoint generation algorithm for scanning the selected area with high resolution was developed and explained with the help of examples and sample scenario. This chapter is also supported by the Appendix A which provides detailed information on the scanning sensor used for this research and the bathymetry generation and meshing techniques.

3.1 Wide area scanning process

This section describes the scanning process for acquiring wire area acoustic data in the survey area. The waypoints for wide area acoustic scanning are provided to the vehicle in the form of an initialization file. The file provides these waypoints in the earth frame of reference as north and east coordinates and depth information. The file also mentions the limits of survey area which are safe for the vehicle to operate as a bounding box. The initialization parameters for the sonar are also provided in the file. The parameters which are provided include the range of operation of the sonar, the scanning altitude, the scanning speed of the vehicle and the physical gain of the system. At present the gain of the sonar is fixed and is calibrated based on trial data taken at the experimental site. The details on the initialization file are provided in the Appendix C at the end of the manuscript. The vehicles waypoint navigation system performs scanning between the points provided in the navigation file in a straight line. The initialization file may contain more than one pair of waypoints for scanning multiple sections of the seafloor. In this case, the observation is performed one section at a time.

The obstacle avoidance system is used for obstacle detection and collision avoidance since no previous information about the survey area is available. The heading, depth and velocity controller of the vehicle is commanded by the navigation system after calculating the required heading to reach the next waypoint. While navigating between the waypoints, the vehicle records individual sonar scans as well as the vehicle navigation data. The navigation data recorded by the vehicle contains the three axis position and three axis orientation information. The obstacle avoidance system measures the range of any obstacle in the path of the vehicle. Preventive measures are taken if an obstacle is found within a certain range of the vehicle. The safe distance value for obstacle avoidance is also included in the vehicle initialization file. Three dimensional bathymetry is generated after the vehicle performs scanning using the data collected during the scan. During this time, the vehicle performs station keeping by maintaining its horizontal position and depth.

3.1.1 Wide area scanning hardware

For generating wide area bathymetry, an acoustic scanning sensor with a wide swath is used. Sensors capable of such scanning are side-scan sonar, multi-beam sonar, SAS or mechanically steered profiling sonar. These systems can generate bathymetry with the resolution of a few tens of centimeters depending on the scanning altitude and other sensor parameters. A multi-beam sonar is used for this research however the algorithms developed can be easily applied to a point cloud generated using any other acoustic sensor with sufficient resolution. The resolution obtained from a multi-beam sonar depends on the beam fan angle and the number of beams. The scanning altitude of the vehicle decides the swath obtained along the direction of the forward motion of the vehicle. This altitude has to be fixed based on the sonar specifications and the resolution required. The sonar scanning rate is usually low and also depends on the scanning altitude. The vehicle scanning speed is set based on the scanning rate of the sensor to obtain sufficient resolution in the forward direction. For the algorithms proposed in this research to work effectively, the seafloor should be scanned with a minimum bathymetry resolution of 20cmx 20cm in the horizontal plane. The vertical resolution is usually much higher but also depends on the scanning altitude. The scanning mechanism of the multi-beam sonar and the data processing techniques to generate bathymetry are explained in detail in the Appendix A of this manuscript.

3.2 Wide area bathymetry analysis

The data obtained using the wide area acoustic scanning sensor is analyzed to identify areas for high resolution scanning based on the interest of the survey. The survey rules are provided to the vehicle in the form of a rule file which is explained in the Appendix C of this manuscript. The survey rules are determined based on the sensor used for seafloor observation and the seafloor parameter being measured. High resolution scanning areas are identified such that the seafloor properties measured in these areas best satisfy the

survey interest. The algorithm developed should be easy and fast to execute on the limited computation power available when implemented on an underwater vehicle. In order to make decisions, it is necessary to detect features on the seafloor from the scanned bathymetry data. The features can be used to decide the area which are of interest to the survey. Since the resolution obtained by the acoustic sensor is of few tens of centimeters, it is difficult to determine small scale features. However since the area covered during the scan is wide, larger features can be identified. The features identified by the algorithm correspond to sea scenario such as hydrothermal vents, manganese crust slabs, man-made features such as foundations of underwater structures or artificial reefs etc. Based on the features detected and the survey rules, high resolution scanning area is selected. Once a suitable area has been identified, an algorithm generates waypoints by taking into account the scanning swath of the high resolution system to scan the area effectively. The overview of the process can be seen in the Fig. 3.1.

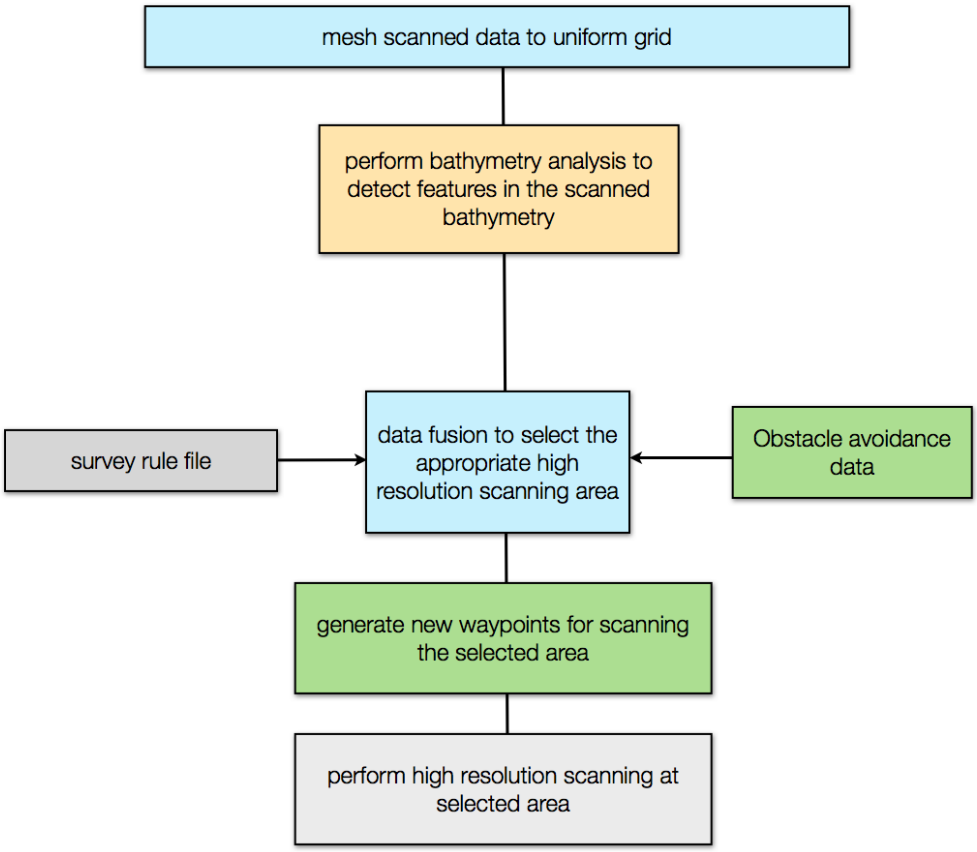

Fig. 3.1. Overview of the wide area data analysis and decision making process

The bathymetry generated by the acoustic scanning sensor is non-uniformly spaced in the horizontal plane. The first step involves meshing the bathymetry to a uniform grid. It is necessary to have the bathymetry uniformly sampled for the purpose of implementing the algorithm by data and image processing. To mesh the bathymetry to an uniform grid the maximum and minimum coordinates in the x and y direction of the original point cloud are identified. The scanned point cloud is meshed into a grid of size $n \times m$ where n is the number of points across track and m is the number of points in the forward scanning direction. The number of points in the across track direction is the number of beams of the sonar while the number of points in the forward direction of scanning is the number of scans. The new coordinates on a uniform mesh are determined by splitting the minimum and maximum values of x and y into $n \times m$ number of points respectively. The meshing algorithm used is explained in the Appendix A at the end of the manuscript. The meshed data is then used as an input for the other algorithms.

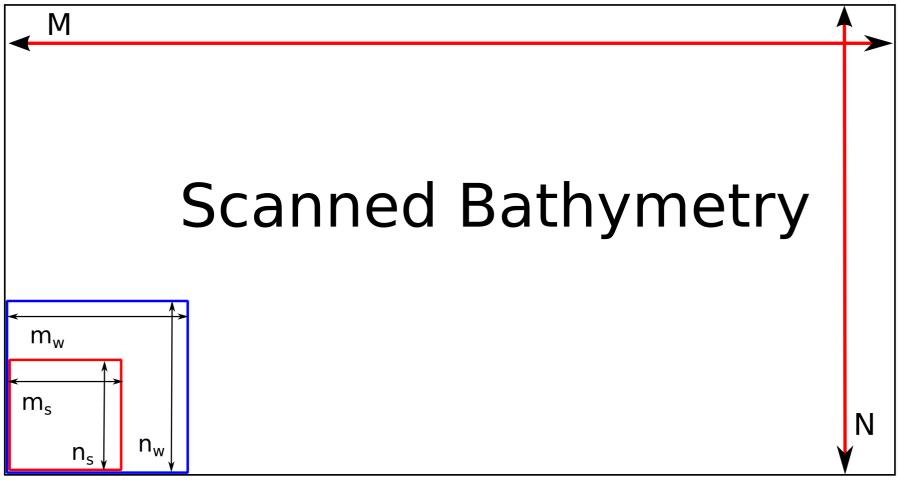

Fig. 3.2. Variance taken over the scanned bathymetry; Variance applied over windows of different dimensions. The larger 2D window has dimensions $m_w \times n_w$ and narrow window $m_s \times n_s$

3.2.1 Detecting features in scanned bathymetry

This section explains in detail the feature detection and selection process using the acoustically scanned bathymetry data generated by scanning a wide area of the seafloor. Since the swath length of the sensor used for generating the bathymetry is a few tens of centimeters, the features identified are also larger in size and low in detail. To perform analysis on this data, an simple algorithm is developed which can be easily implemented on a reasonably fast computer on an AUV. For this research, the algorithm has been implemented to recognize features potentially representing seafloor scenario.

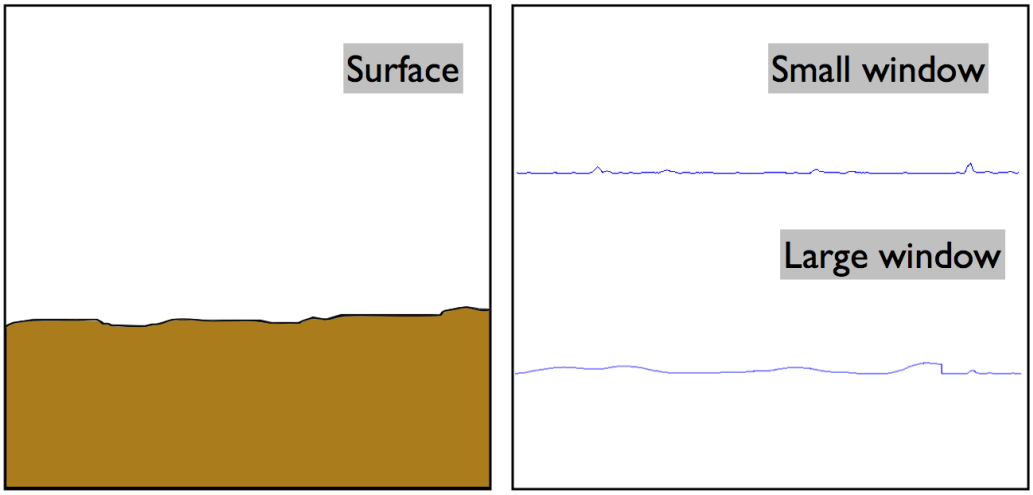

Fig. 3.3. Variance applied on flat surfaces; Small and large window variance taken over a nearly horizontal surface. The variance observed is low in flat areas.

The algorithm developed in this case uses bathymetry variance for detecting features and analyzing the seafloor bathymetry. The concept of bathymetry variance is explained in detail in this section of the chapter. The bathymetry grid comprises of x and y points with a z value for each point on the grid. Variance of bathymetry measures how far individual points on the z axis of the bathymetry grid are spread away from the mean. The data variance is extended to bathymetry by performing computations over a 2D window. All the points in the window are used for calculating the variance and assigning it to the central grid point. The concept of application of 2D window over a bathymetry can be seen in the Fig. 3.2. The bathymetry is considered to be a meshed data image of size $M \times N$. The variance is applied over windows of different sizes. The size of the window used for calculating the variance determines the nature and attributes of the feature identified. The features that need to be determines are potential flat areas, peaks such as isolated boulders and hydrothermal vent chimneys, edges of man-made features and artificial slabs and rifts.

Variance taken over 2D windows of different sizes can provide different information about the features such as their nature and sizes. For instance, a large window provides bathymetry variance over a wide area as seen in Fig. 3.3. A flat area will generate low variance values for a large window as well as a small window. The smaller window can reveal more undulations in the flat area. Small windows also detect the location of individual peaks such as large rocks and boulders or hydrothermal vents by identifying points where peak high variance is observed. The larger window sizes can reveal the outer boundaries of the features around the peaks. This is seen in the Fig. 3.4(right). In case of slabs with edges, a small window can revel the exact location of the edge of the slab. The larger window can identify the location of the slab or artificial man-made feature. This can be seen in the Fig. 3.4(left).

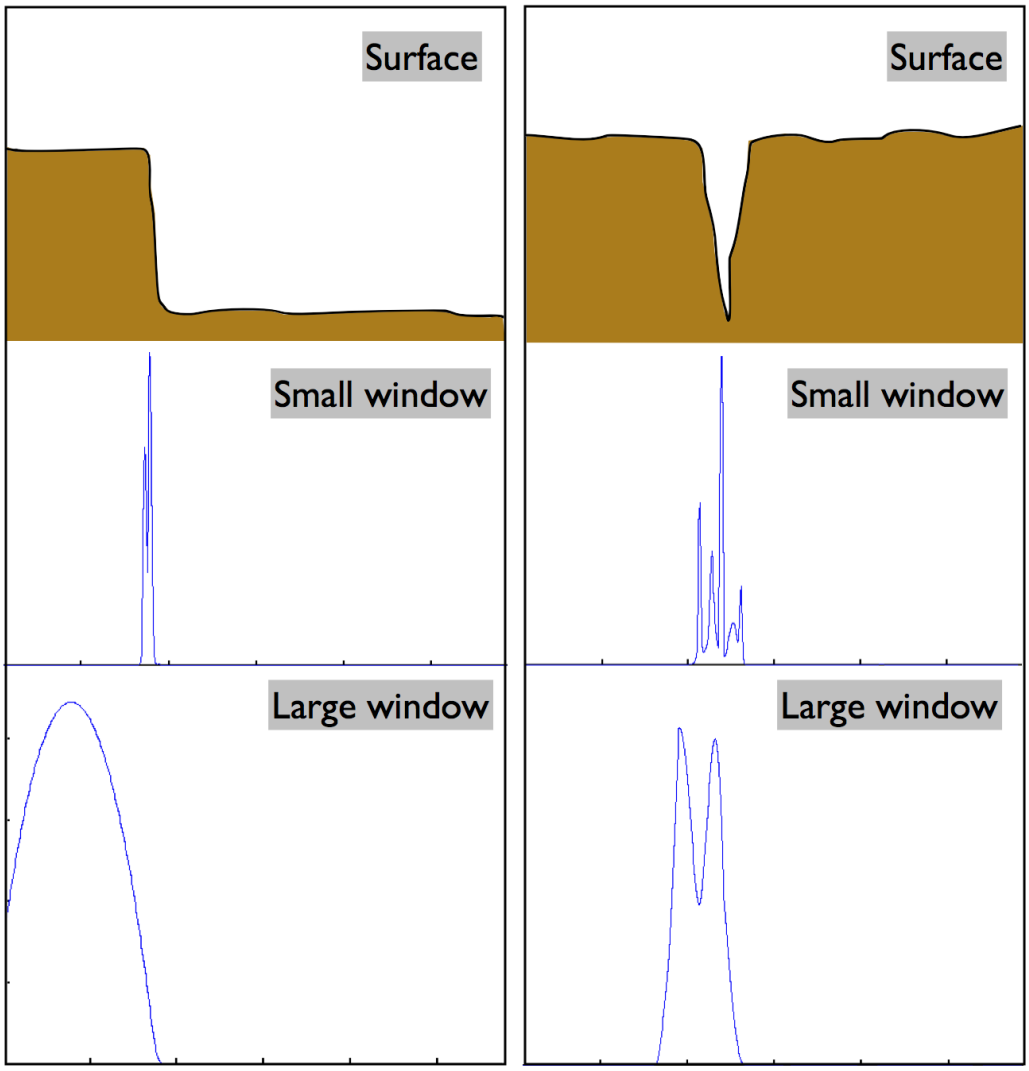

Fig. 3.4. Variance applied on different surfaces; Left: Small and large window variance taken over a slab with edge. Right: Small and large window variance taken over a rift. Different window sizes reveal different information

By performing variance analysis over windows of different sizes on the same bathymetry, different parameters are extracted. The data from different sizes is then combined to estimate the features in the scanned bathymetry. To understand the concept, let us consider a bathymetry scanned in as seen in Fig. 3.5. The bathymetry has been collected at the Kagoshima bay in Japan. The bathymetry is meshed into a uniform grid of $M \times N$ as seen. The window used for variance mapping is decided based on the swath of the data, the resolution of the data, the size and nature of the features to be identified. Variance is taken over windows $W_i$of different sizes $m_i \times n_i$. For every analysis, all the points in the meshed bathymetry data inside the window are first collected and an average is taken.

If z_i are all the points inside the window used for analysis and n is the total number of points then:

$$\mu = E[z_i]$$

$$Var(z_i) = \frac{1}{n} \times \sum_{i=0}^{i=n-1} (z_i - \mu)^2$$

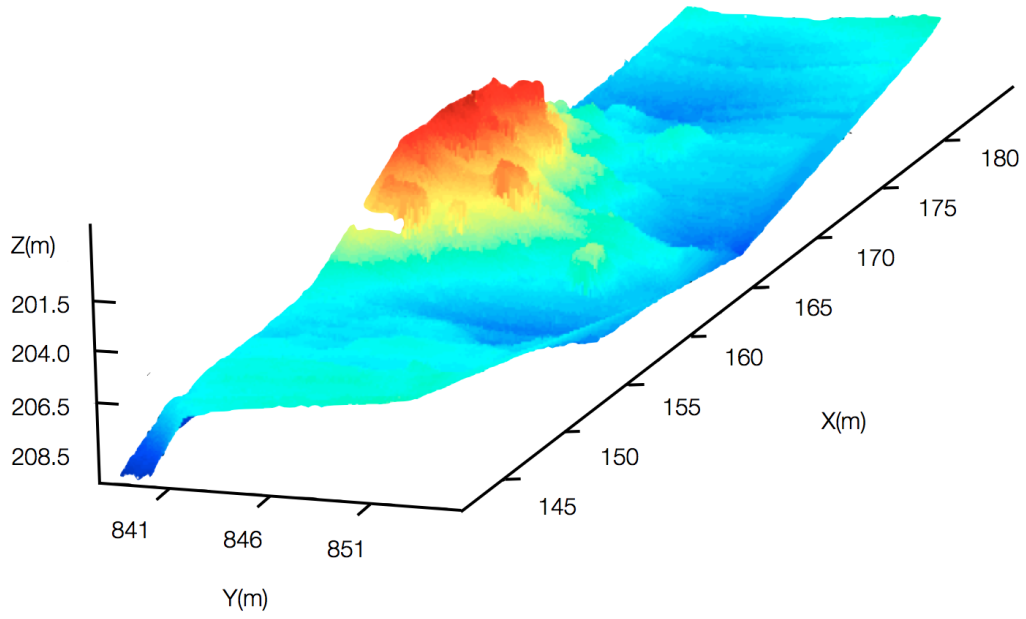

Fig. 3.5. Bathymetry data for analysis using variance maps scanned at Kagoshima bay, Japan

Different window sizes revel different information from the scanned bathymetry. Variance taken over a small window revels the location of small boulders and rocks. Along with the rocks, the peaks of the mount are also clearly visible in the small window variance. These are then be extracted by filtering the highest variance areas as seen in the Fig. 3.6. Variance taken over a larger window identifies the location of larger features such as the main mount. This is then separated by filtering the high variance area. This process can be seen in the Fig. 3.7. In all the variance maps, the area with the lowest variance is the one with least undulations. It is considered as potential flat area and is also separated as seen in the Fig. 3.8

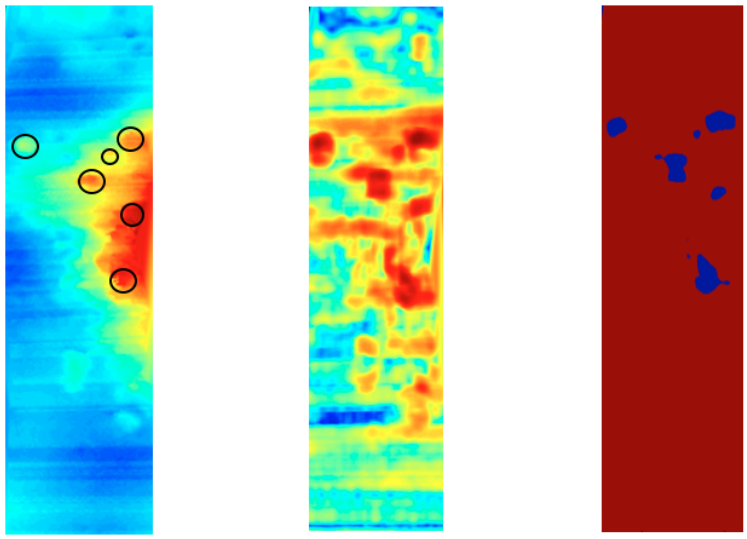

Fig. 3.6. Left: Original bathymetry. Black circles indicate the locations of the peaks of the mounts and boulders, Centre: Variance map generated by over a small size window. The high variance peaks indicating the boulders and mount peaks are identified, Right: After thresholding and extracting the areas with high variance to detect features

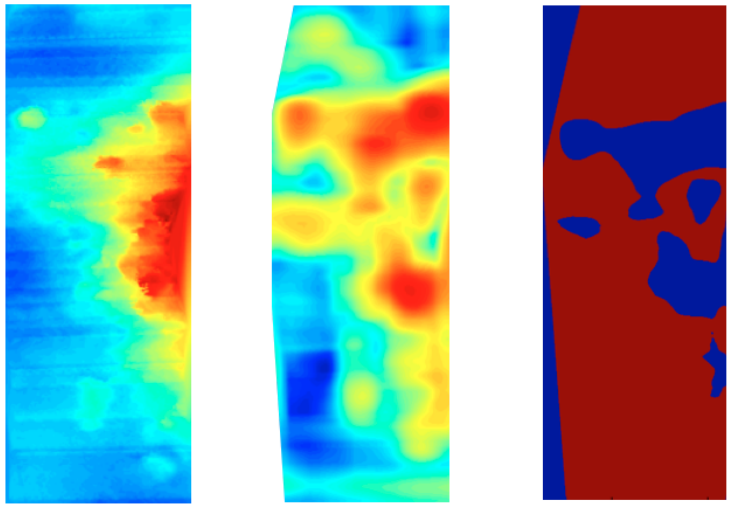

Fig. 3.7. Left: Original bathymetry. The main mount is identified from scanned bathymetry, Centre: Variance map generated by over a large size window. The high variance area indicating the location of the main mount identified, Right: After thresholding and extracting the areas with high variance to detect the main feature

3.2.2 Selecting area for scanning

The features detected are first stored in a custom database which is used later in the decision making process. The database includes the type of features and some of their

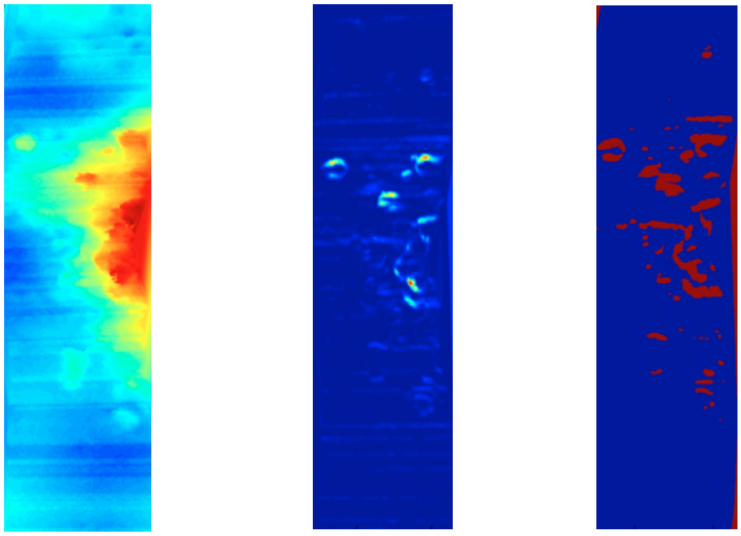

Fig. 3.8. Left: Original bathymetry, Centre: Variance map generated using a very small size window to reveal small undulations in bathymetry, Right: After thresholding and extracting the areas with very low variance to detect flat area ares

attributes. The data is also stored in the form of a map with different colors representing different features which can be seen in the Fig. 3.9. This is useful for image processing operations for selecting the area for high resolution scanning. Once the analysis of the seafloor has been completed decision to perform observations is based on the features identified and the survey rules. The features required by the survey are extracted from the rules and identified in the created feature database. These are then compared with those identified and stored in the feature database. Their location on the map is then marked for analysis. By using image processing operators, the area within these features for high resolution scanning is selected.

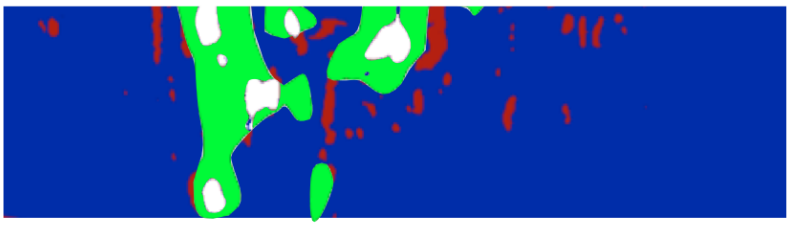

Fig. 3.9. Detected features and attributes stored as a map; Green: main seamount, White: boulders, Red: rough areas, Blue: flat areas

3.3 Generating waypoints for scanning area

This section explains the method for generating waypoints for scanning the area selected for high resolution observation by the previous algorithm. A fast and less computationally intensive method has to be developed since the algorithms have to to be executed in real-time using the computers on-board an underwater vehicle. Since the newly selected area is scanned using an underwater vehicle, the algorithm should give preference to straight line transects over turns when deciding the waypoints. A high resolution scanning sensor is used by the vehicle to observe the seafloor at these locations. The swath of the high resolution scanning sensor in the direction normal to the forward direction of the vehicle should also be considered while generating the waypoints. The area selected for high resolution scanning by the previous step of the algorithm is considered as a binary image of size $M \times N$ having selected and unselected points. This is possible since the bathymetry used is meshed to a uniform grid and each pixel has a definite coordinate in the horizontal plane. The selected area could either be one single continuous patch or a series of small areas. Once the new waypoints are computed, they are stored in a waypoint file automatically and provided to the vehicle. At these locations, the vehicle performs waypoint navigation to obtain data using a high resolution scanning sensor. Consider the region of the scanned area shown in the Fig. 3.10 in red where high resolution observation has to be performed.

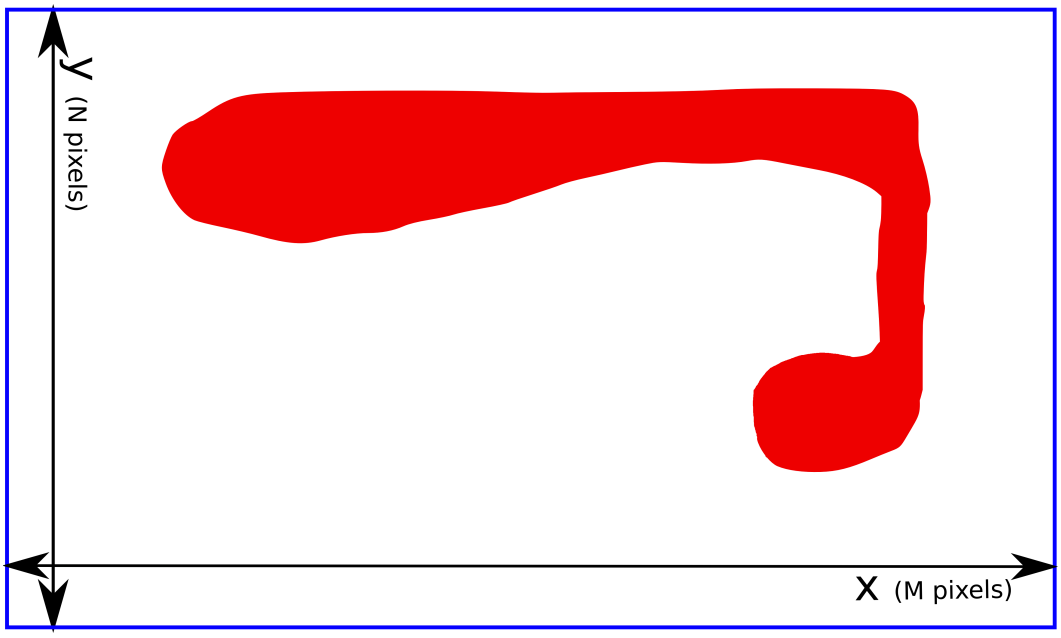

Fig. 3.10. Area selected for high resolution scanning (red) using the algorithm in the previous section

The first step involves making a bounding box around the selected area as can be seen in the Fig. 3.11. The outer edges of the box are generated using the extremities of x and y

(x_{max} ,x_{min}, y_{max}, y_{min}). Since the data is considered as an image, let $M_s \times N_s$ be the number number of pixels representing the data. The swath of the sensor used for high resolution scanning is then estimated in terms of number of pixels. If σ is the swath of the sensor, then the number of pixels P representing the swath are calculated as:

$$dx = \frac{x_{max} - x_{min}}{M_s}$$

$$P_x = \frac{\sigma}{dx}$$

$$dy = \frac{y_{max} - y_{min}}{N_s}$$

$$P_y = \frac{\sigma}{dy}$$

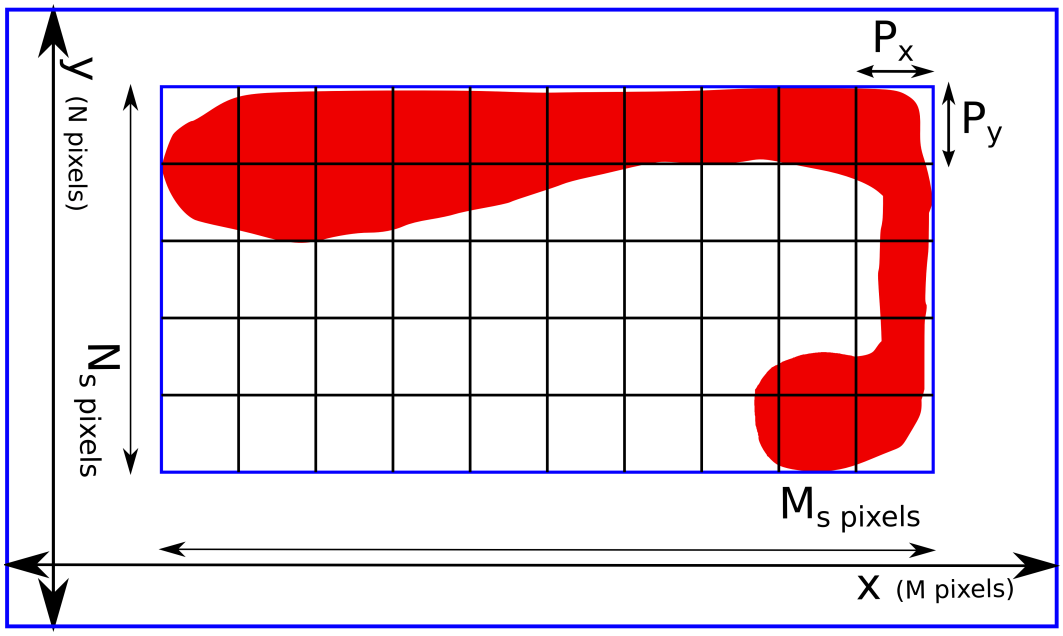

Fig. 3.11. Bounding box and new mesh applied based on the swath of the high resolution scanning sensor

The values of P_x and P_y are floored to the closest integer. The swath of the scanning system, σ is considered smaller than the actual swath to introduce overlap in the scanned bathymetry. The area to be scanned is then divided into a mesh with grid size $P_x \times P_y$. To illustrate the method, consider a sonar with a scanning swath of 15m and the distance scanned in the forward direction to be 30m. The number of beams of the sonar are considered as 120 and the scanning rate is 5scans/second at speed of 0.5m/s. The resolution of the area generated can be considered as 120×300. Assume that $x_max - x_min$ is 10m and represented by 200 pixels. Also $y_max - y_min$ is 10m represented by 80 pixels.

The laser swath is then calculated as:

In x direction:

$$dx = \frac{10}{80}; P_x = \frac{2.0}{0.125}; P_x = 16 pixels$$

In y direction:

$$dy = \frac{20}{200}; P_y = \frac{2.0}{0.1}; P_y = 20 pixels$$

Area is then enclosed in a bounding box. A new grid is then generated with size 16×20 to enclose the entire are as seen in the Fig. 3.11.

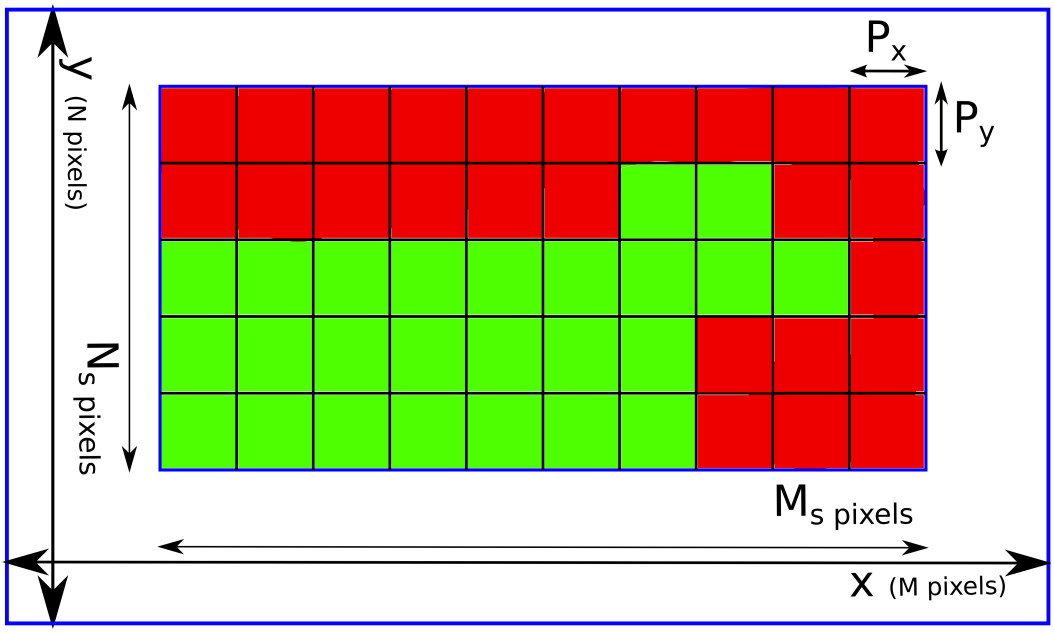

Fig. 3.12. Blocks assigned colors based on areas to be scanned; Red: Blocks that need to be scanned, Green: Blocks that do not need scanning

The squares now including areas to be scanned are filled as red and those where no scanning has to be performed are filled green as can be seen in the Fig. 3.12. Once the area to be scanned has been converted into blocks, the path planning sequence for scanning the area is established. The overview of the process is given in the Fig. 3.13. The waypoint generation is started from one of the four corners. Corner with block where scanning has to be performed (red) is given priority for start of scanning. If no such corner is available, the corner nearest to the current position of the vehicle is considered. The algorithm starts generating waypoints along the side with larger number of blocks. For connected blocks in the same direction, no intermediate waypoints are generated. In the case of our example,

the waypoint generation is carried out in the X direction with 10 blocks. This is done so that the vehicle can scan a larger patch at length without having to turn, thereby improving efficiency.

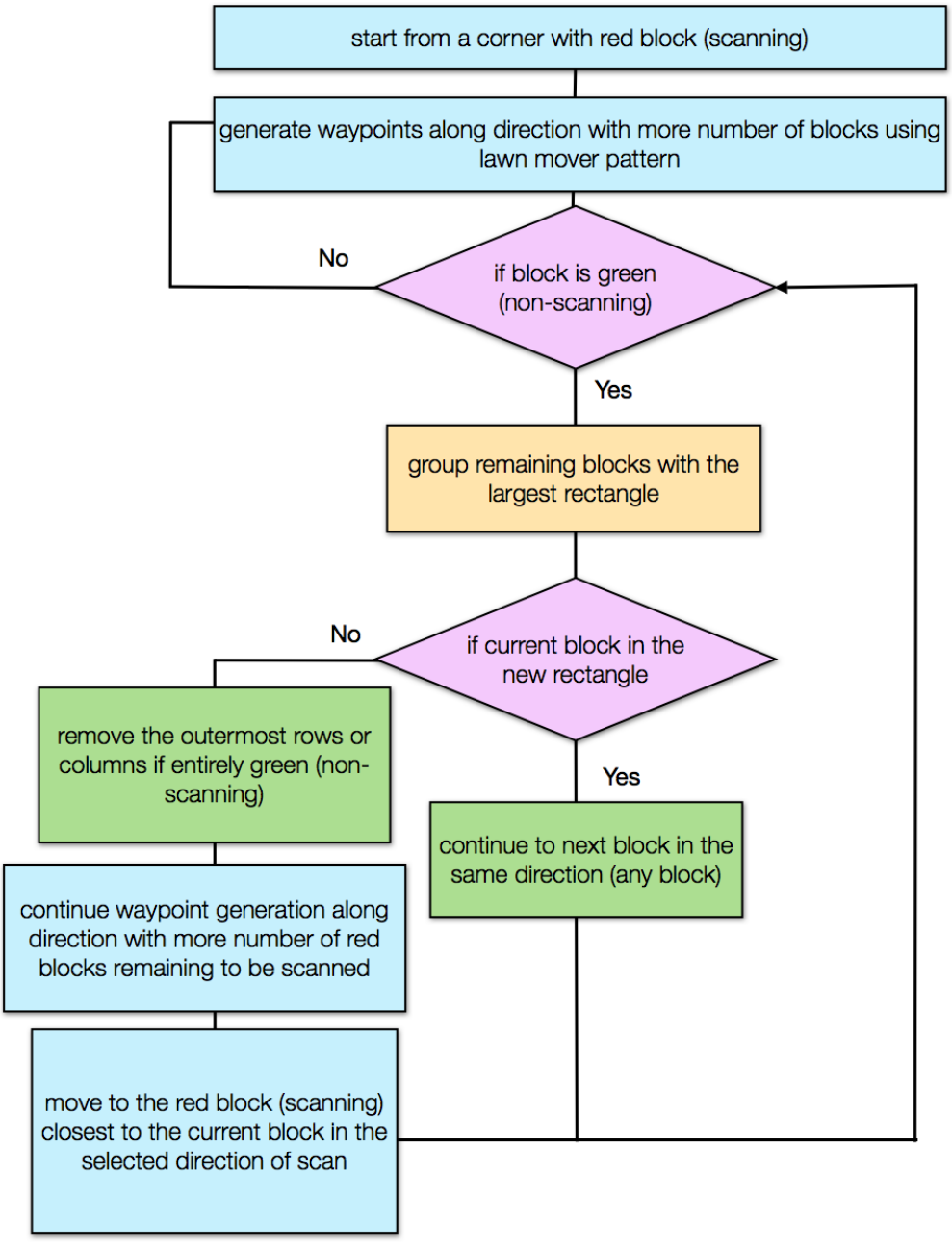

Fig. 3.13. Overview of the block selection and waypoint assignment algorithm

The algorithm generates waypoints in a lawn mower pattern until it reaches a patch of land which does not have to be scanned (green block). Once the green block has been reached, the blocks remaining to be scanned (red blocks) are located as seen in Fig. 3.14.

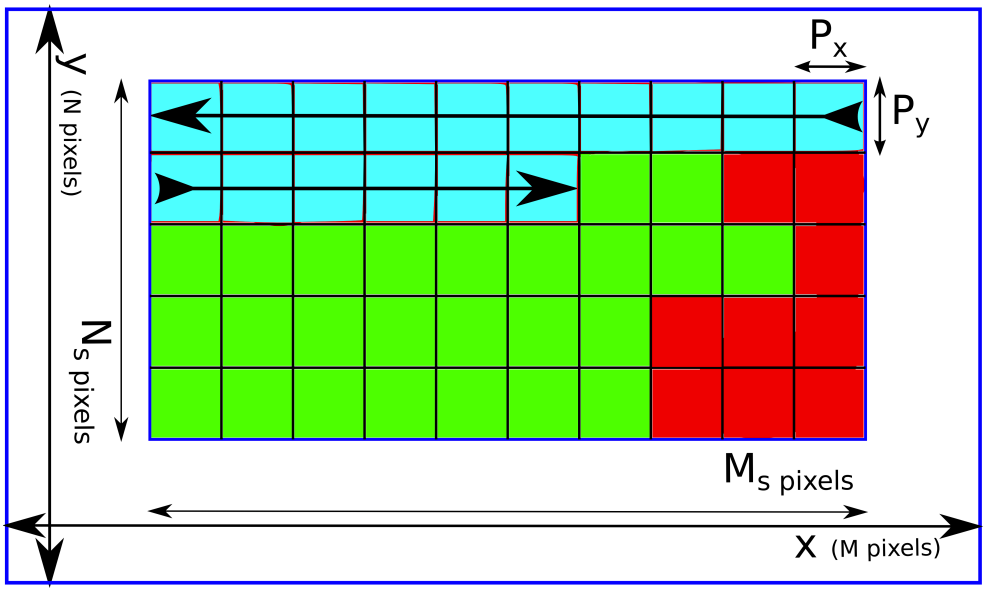

Fig. 3.14. Generation of waypoins; Red: Blocks that need to be scanned, Green: Blocks that do not need scanning, Blue: Blocks scanned so far

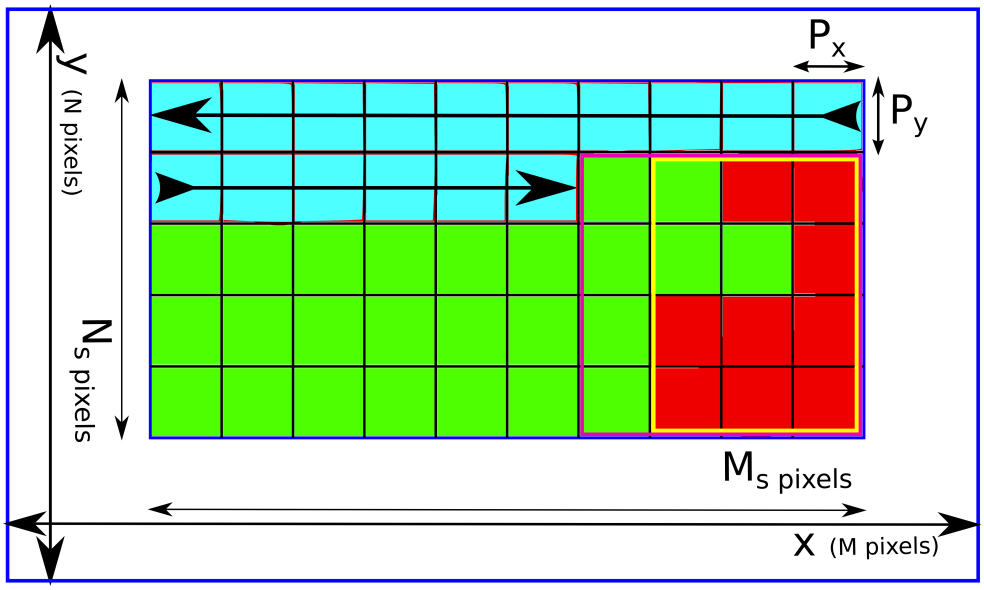

Fig. 3.15. Pink rectangle: encloses all the remaining blocks to be scanned (red blocks). Yellow rectangle: grouping remaining blocks after eliminating the first row

A largest rectangular region enclosing all the remaining blocks is drawn as seen in the Fig. 3.15. The pink rectangle has been drawn to enclose all the remaining red blocks. If the new region contains an outer row or column which does not have to be scanned, it is removed from the newly selected region. After eliminating the first column which does not have to be scanned, the remaining blocks are regrouped using a new yellow rectangle. If the current block is a part of the newly generated rectangular group, then waypoint generation is continued in the same direction as before.The algorithm then generates waypoints in the direction of the larger number of blocks as in the beginning of the algorithm. The next point generated on the block which is nearest to the current block in the required direction of scanning. In this case, the first block along Y direction is now considered since it has 4 remaining blocks as compared to 3 in the X direction. Waypoint generation is then continued in the lawn mower pattern until the next green block is detected as seen in the Fig. 3.16

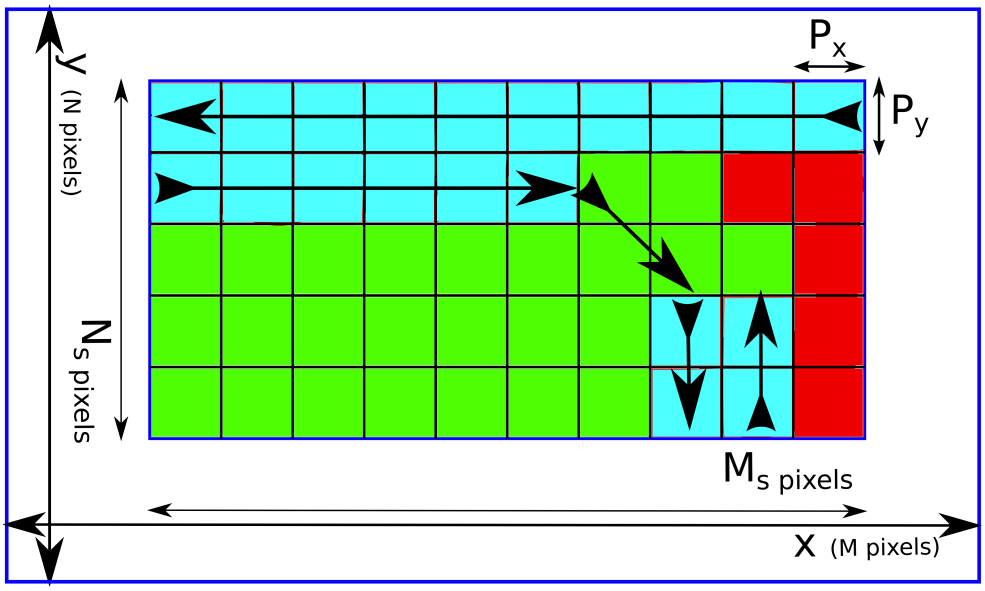

Fig. 3.16. Generating waypoints for remaining blocks. Scanning direction is changed since the number of remaining blocks in the y direction is greater

After reaching the next green block, the remaining blocks are regrouped by a new largest rectangle. The yellow rectangle is the Fig. 3.17 groups all the remaining red blocks. Since the current block is also included in the newly generated region, scanning is continued in the forward Y direction.

Finally all the blocks in the region are analyzed by using the algorithm as seen in the Fig. 3.18. Once all the blocks have been analyzed by the algorithm, waypoints are generated along the centers of each block in the direction of scanning. The algorithm was tested during the experiments conducted in the tank environment to evaluate the survey method. Details on the experiments have been provided in the chapter 6 of this manuscript.

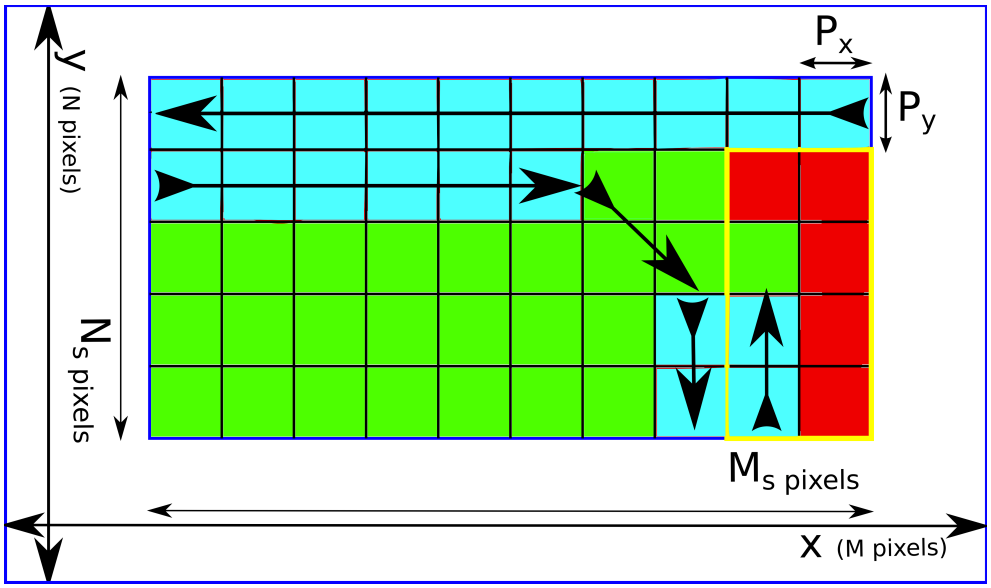

Fig. 3.17. Blocks assigned colors based on areas to be scanned (Red: Blocks that need to be scanned, (Green:) Blocks that do not need scanning

Once the waypoints for high resolution scanning have been generated, the vehicle scans the region using waypoint navigation. A suitable high resolution scanning sonar is used for generating high resolution bathymetry. The high resolution scanning stage has been explained in the next chapter.

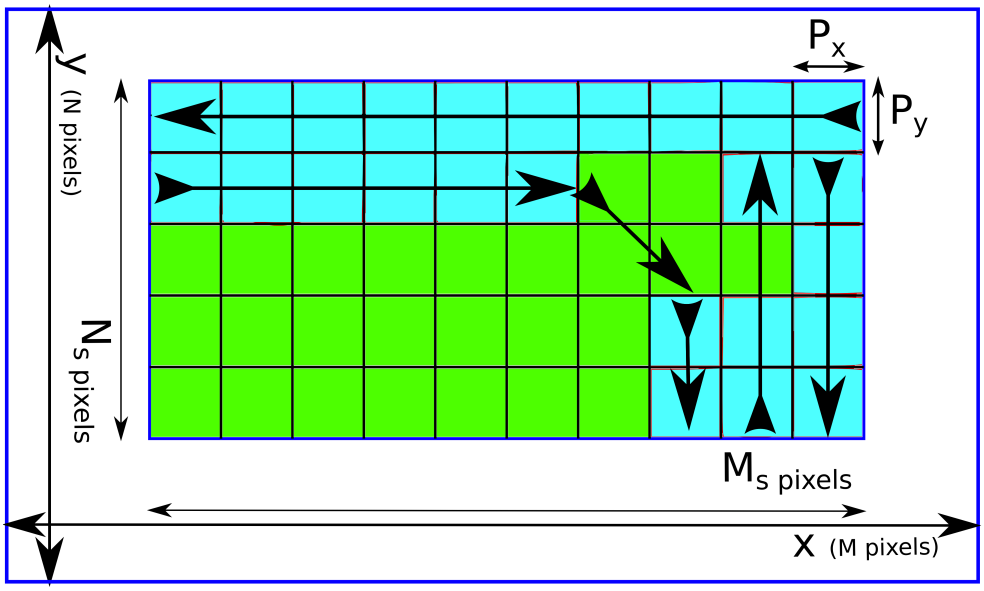

Fig. 3.18. Generating waypoints for remaining blocks to cover the entire selected area for high resolution scanning efficiently

4

High resolution scanning

This chapter provides details on the high resolution scanning stage of the proposed survey method. The initial part of the chapter provides an overview of the scanning process for generating high resolution bathymetry using a suitable scanning sensor. The requirements of the sensor for obtaining high resolution bathymetry to perform analysis using the algorithms proposed are described. Detailed information on the intelligent decision making process to select a suitable area for seafloor observation is provided. The algorithm for detecting features in the scanned bathymetry and estimating their attributes is described with mathematical equations. The algorithm for detecting flat potential areas for landing operation is also elaborated. The final sections of the chapter describe the decision making process based on the features and flat areas detected in the scanned bathymetry. The involvement of the survey rule file in the decision making process is also explained. This chapter is also supported by the Appendix A which provides detailed information on the high resolution scanning sensor used for this research and the bathymetry generation and meshing techniques.

4.1 High resolution scanning process

In the previous chapter, the process of selecting areas for high resolution scanning in the scanned acoustic bathymetry has been described in detail. The waypoints generated are provided to the vehicle in the form of a new waypoint file generated by the algorithm. The vehicle scans the area between the new waypoints with high resolution using a suitable scanning sensor. The waypoints are provided in the earth frame of reference as north and east coordinates and depth information. In this research, a laser profiling system is used for scanning the seafloor with high resolution. The details on the scanning system are provided in the Appendix A of this manuscript. The scanning parameters for the system are provided in the initialization file uploaded into the vehicle. The parameters which are provided include the opening angles of the camera and the laser, the baseline between the camera and the laser, the scanning speed of the vehicle, scanning altitude, camera gain and resolution. At present the gain of the camera is operated in automatic mode. The details on the initialization file are provided in the Appendix C at the end of the manuscript.

The vehicles waypoint navigation system performs scanning between the points provided in the new waypoint file to record camera images of the laser profiles projected on the bottom. The vehicle navigation data is also recorded in a separate file. The navigation data recorded by the vehicle contains the three axis position and three axis orientation information. The obstacle avoidance system measures the range of any obstacle in the path of the vehicle. Preventive measure is taken if an obstacle is found within a certain range of the vehicle. The navigation and obstacle avoidance system of the vehicle move the vehicle between the waypoints provided safely. Once scanning is completed, the three dimensional bathymetry is generated and analysis is performed while the vehicle maintains its last horizontal position and depth.

4.1.1 High resolution scanning hardware

To generate bathymetry with a high resolution, sensors such as laser profiling system [42] or stereo vision [43] can be used. These systems are capable of generating bathymetry with a resolution of a few millimeters. In this research, the light sectioning based laser profiling system is being used for bathymetry generation. The algorithms developed could however be easily applied to any other system which can generate a three dimensional point cloud with the required resolution. The implementation of the system on the developed underwater vehicle used for experiments in this study is explained in chapter 5 of this manuscript. The horizontal resolution of the scanning system depends on the opening angle of the camera lens, the camera CCD resolution, the baseline length between the camera and the laser, the laser swath and the vehicle scanning altitude. Since the camera and laser parameters are fixed, the vehicle scanning altitude is set to obtain sufficient resolution in the cross-track direction. The along-track resolution of the system depends on the rate of acquisition of the camera and the vehicle speed. The necessary requirements for the algorithm to perform analysis and detect suitable flat areas is that the scanned bathymetry has a minimum footprint of 8mmx 8mm in the horizontal plane and about 5mm in the vertical plane. The scanning mechanism of the laser profiling system and the bathymetry generation techniques is explained in detail in the Appendix A of this manuscript. Sample bathymetry scanned using the laser profiling system can be seen in the Fig. 4.1.

4.2 High resolution bathymetry analysis

The data obtained by high resolution scanning using a suitable sensor is then analyzed with an algorithm to make intelligent decisions based on the interest of the survey provided to the vehicle in the form of a rule file. The survey rules are made based on the sensor carried by the vehicle for seafloor observation. The relationship between the seafloor properties being observed and the features detected is explored. Based on the features detected, the vehicle may either be required to land on the seafloor or perform observations around the features to obtain the correct data. The overview of the process involved in decision making can be seen in the Fig. 4.2.

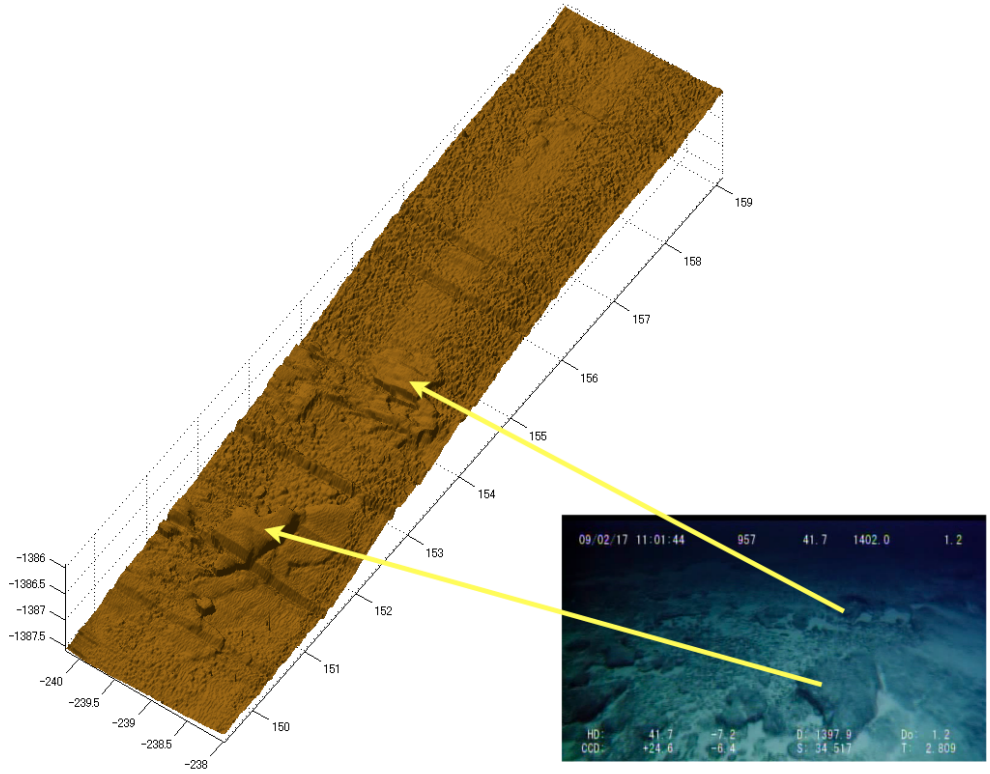

Fig. 4.1. Bathymetry scanned using the light sectioning based laser profiling system during NT09-02Leg2 Cruise. The detailed features on the seafloor can be clearly observed in the data.

To make intelligent decisions, the vehicle has to first know the nature of the bathymetry scanned and its features. The algorithm first segments the bathymetry scanned into seafloor features and flat areas. Since the bathymetry has a resolution of a few millimetres along every axis, it is possible to detect the features in high level of detail. At first, the bathymetry is analyzed to identify flat areas on the seafloor. This is done to identify areas on the seafloor where the vehicle can potentially land to obtain seafloor properties from in-situ observation payload sensors. Since the seafloor can be rough and varies abruptly, it may not be possible for the vehicle to land arbitrarily and hence flat areas need to be detected. The next stage of the analysis identifies features in the areas which are not considered flat. The essential physical attributes of the features such as the shape, size, orientation etc are analyzed and a database is created. The survey rule file decides the action to be taken by the vehicle for seafloor observation. Decisions are taken based on the features detected and the location of the flat areas. The survey might require the vehicle to land on the seafloor to perform observations using an in-situ sensor or observe a particular area by maneuvering using a suitable sensor. The individual algorithms are explained in detail in the next part of this section.

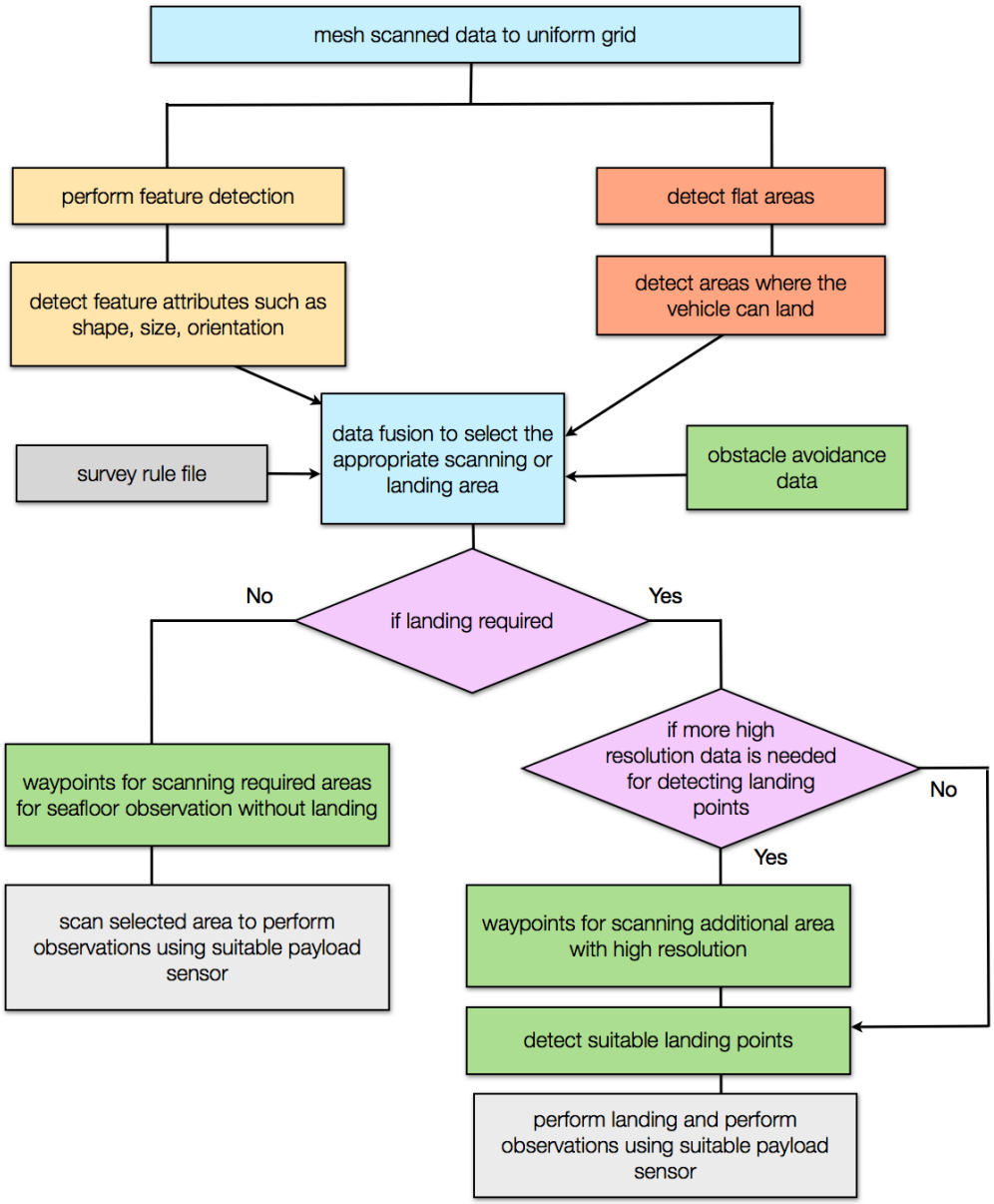

Fig. 4.2. Overview of the high resolution data analysis and decision making process

The bathymetry generated by the scanning sensor is non-uniformly spaced. The first step involves meshing the bathymetry to a uniform grid. It is necessary to have the bathymetry uniformly sampled for the purpose of implementing the algorithm by data and image processing. To mesh the bathymetry to an uniform grid the maximum and minimum coordinates in the x and y direction of the original point cloud are identified.

The scanned point cloud is meshed into a grid of size $n \times m$ where n is the number of points across track and m is the number of points in the forward scanning direction. The number of points in the across track direction is the horizontal resolution of the camera while the number of points in the along-track direction of scanning is the number of scans acquired in the area. The new coordinates on a uniform mesh are determined by splitting the minimum and maximum values of x and y into $n \times m$ number of points respectively. The meshing algorithm used are explained in the Appendix A at the end of the manuscript. The meshed data is then used as an input for the other algorithms.

4.2.1 Detecting flat areas in scanned bathymetry

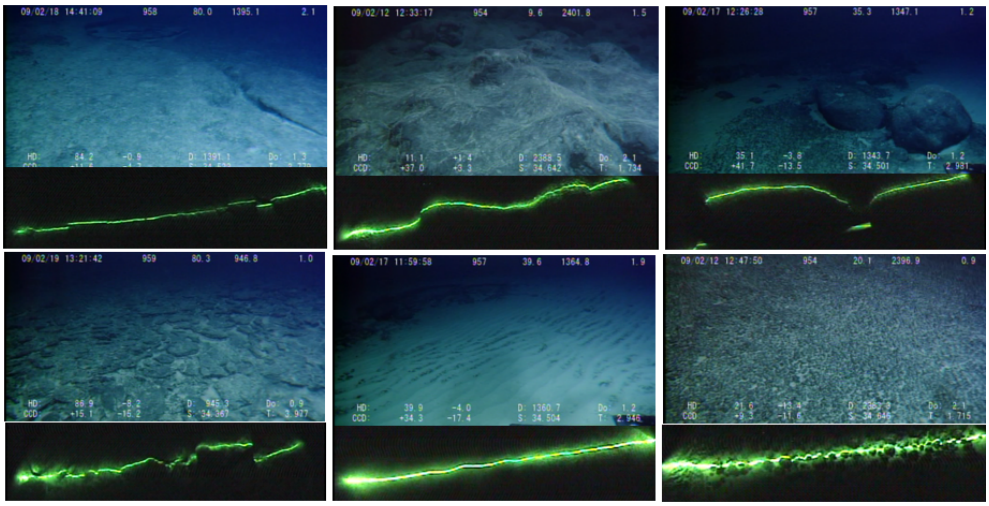

Fig. 4.3. Laser profiles of different types of surface taken during NT09-02Leg2 Cruise. Upper section of each images shows the seafloor surface and the bottom shows the corresponding laser profile

The laser profiles of a few types of surfaces can be seen in the Fig. 4.3. These were acquired during the NT09-02Leg2 survey cruise of R/V Natsushima. In each image, the upper section shows the surfaces photographed by the forward looking camera of the ROV used during the survey. The bottom part shows the corresponding profiles captured by projecting a sheet laser vertically downwards. If these profiles are considered as data points, their frequency domain analysis can provide useful information about their shape and roughness. Each laser line can be individually processed for identifying whether the surface is flat or not, but this method has an inherent problem in the analysis. Even if the laser profiles might appear flat in the cross-track direction, they may have features in the along-track direction of the vehicle. These features would only raise or lower the level of the laser line in the camera image and not change its shape. Since the seafloor contains a wide variety of three dimensional objects, it is essential that the algorithm remains unbiased towards bumps along a particular orientation. From this it is apparent that a single line by line laser analysis is not suitable for analysis of the terrain to detect flat areas.

Frequency analysis can provide a simple means of identifying flat areas from bumpy areas as the frequency components associated with these are entirely different [44]. Flat areas are represented by low frequency components. The high frequency components represent the sharp edges, rough surfaces and rocks. Fast computational algorithms for performing frequency analysis of data have been developed over the years and can be easily implemented on a reasonably fast computer. To overcome the problem of performing frequency analysis on one profile at a time, the entire scanned area is considered for analysis by taking a 2-dimensional (2D) Fast Fourier Transformation (FFT). The DC component in the point cloud can leak into to the neighboring low frequencies and make it difficult to identify them. For frequency analysis to work effectively, it is essential to realign the point cloud so that the DC component is brought to the x-y surface. This is achieved by first moving the point cloud to the center of mass and then realigning the data by rotating it along its eigenvectors by principal component analysis (PCA).

4.2.1.1 DC normalization

The eigenvector of a square matrix is a non-zero vector that produces a constant multiple of the matrix, when the matrix is multiplied by the vector. In short, the eigenvalues provide information about the direction of orientation of the point cloud and can be used for DC normalization by PCA. The data collected from the point cloud can be represented in three dimension as x_d,y_d and z_d. If the means values the point cloud are represented by $\bar{x}, \bar{y}, \bar{z}$ respectively, then the point cloud can be shifted to its centre of mass:

$$
\begin{aligned}
x_m &= x_d - \bar{x_d} \\
y_m &= y_d - \bar{y_d} \\
z_m &= z_d - \bar{z_d} \\
U &= \begin{bmatrix} x_m \; y_m \; z_m \end{bmatrix} \\
\Sigma &= \frac{U^T U}{(N-1)}
\end{aligned}
$$

U^T represents the transpose of the matrix U then the covariance matrix (Σ) of the mean centered data with number of points N can be calculated. The eigenvalues and eigenvector matrix E are then computed which are then used to rotate the mean centered point cloud to generate the transformed data set x_r, y_r, z_r. The DC normalized original bathymetry can be see in the Fig. 4.4.

4.2.1.2 2D Fourier analysis

The scanned bathymetry consists of objects with different shapes and dimensions which have different frequency signatures. The scanned bathymetry can be considered as a series of shapes which can be split into their fundamental sinusoidal and co-sinusoidal components

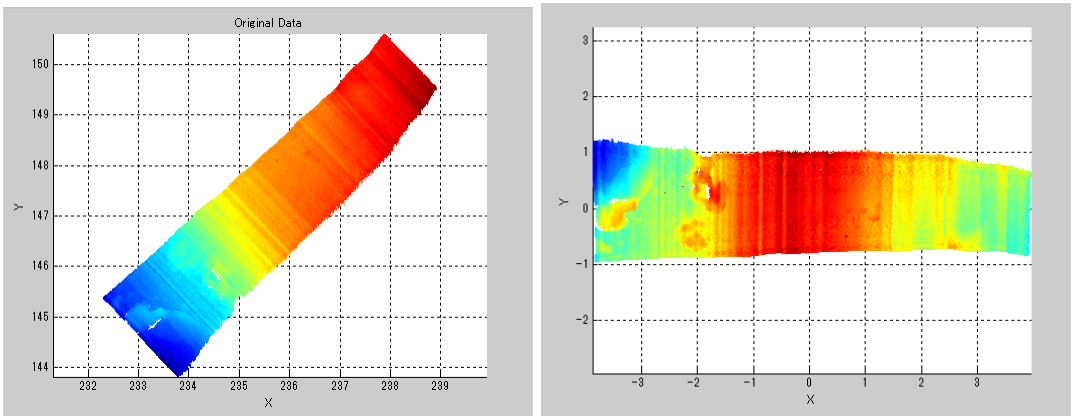

Fig. 4.4. Left: Data scanned using high resolution meshed to an uniform grid, Right: Same data after DC normalization

using frequency domain analysis such as 2D FFT. For the purpose of performing analysis, the data is divided into smaller sizes of $M \times N$. It is easier to perform computation on a smaller data segment and the analysis performed produces better results. Assuming M to be the number of mesh points along x_r direction and N is the number of mesh points along y_r direction. A FFT-shift function is used to centre the Zero-frequency component. A 2D FFT is performed on the bathymetry data to determine its frequency components. The bathymetry data is converted into frequency domain data $Z_f(x_u, y_v)$ where x_t and x_t are coordinates in the transformed data for each Z_f.

$$Z_f(x_t, y_t) = \frac{1}{\sqrt{MN}} \sum_{x_r=0}^{M-1} \sum_{y_r=0}^{N-1} z_r(x_r, y_r) e^{-j2\pi\left(x_t \frac{x_r}{M} + x_t \frac{y_r}{N}\right)}$$

The 2D FFT of the bathymetry scanned can be seen in the Fig. 4.5. The two axes of FFT represent the frequency components along the two dimensions of the scanned bathymetry. The underlying ground surface is represented by low frequency components. The rocks and bumps are represented by higher frequency components. The pebbles are represented by even higher frequency components with low amplitudes. It is possible to separate the nature of the underlying bathymetry from the features by using a filter and cutting of the appropriate frequencies.

To filter out the higher frequencies which represent the edges of surfaces and the pebbles, we need to design a suitable filter. The filter should have a linear phase response with nearly even response in the pass band. A filter similar to Butter-worth filter is used whose response can be seen in the Fig. 4.6. By multiplying the FFT data with the filter, element by element, we can mask the high frequency components which represent the bumps, rocks and pebbles to generate the underlying bathymetry. An inverse 2D Fourier transform can then be applied to produce a smooth bathymetry representing the underlying basic terrain,

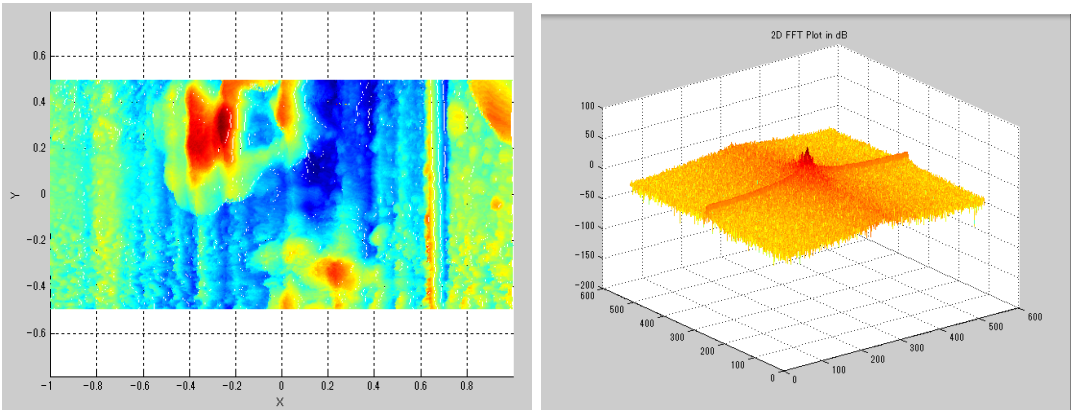

Fig. 4.5. Left: Small section of the original data used for performing Fourier analysis, Right: 2D-FFT plot of the data in dB. The two axis represent the frequency components along the X and Y direction

also seen to the right of Fig. 4.6. The smoothened bathymetry represents the underlying ground surface.

$$Z_g(x_r, y_r) = \frac{1}{\sqrt{MN}} \sum_{x_t=0}^{M-1} \sum_{y_t=0}^{N-1} Z_f(x_t, y_t) e^{j2\pi\left(x_t \frac{x_r}{M} + x_t \frac{y_r}{N}\right)}$$

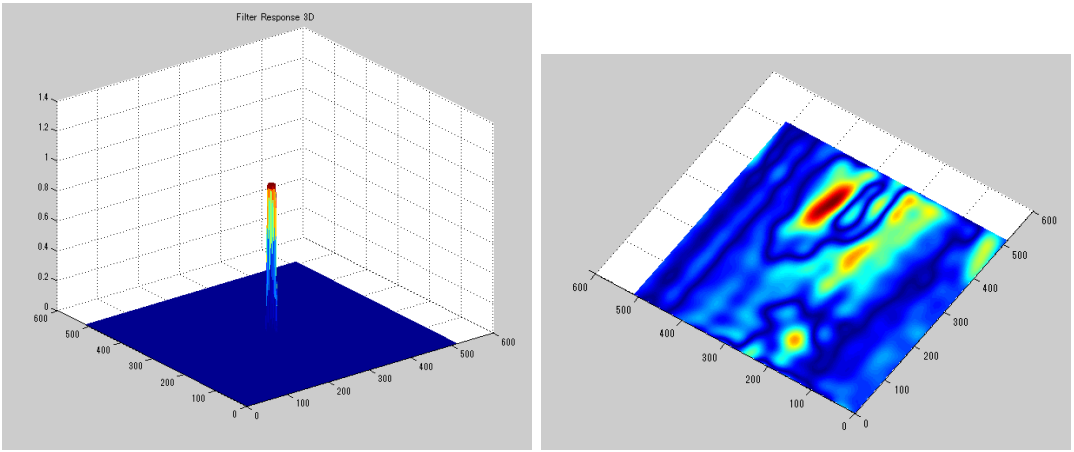

Fig. 4.6. Left: Response of the filter used to remove the high frequency components from the 2D FTT, Right: Smooth bathymetry generated after taking inverse fourier transform

This smooth bathymetry is then subtracted from the original bathymetry point by point to identify points which belong to the ground or the features placed on top of the ground. The subtracted bathymetry of the original data can be seen in the Fig. 4.7. From this we can identify the underlying ground from the features. A threshold is used to separate the

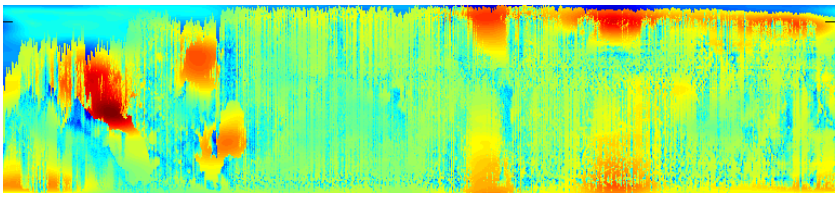

Fig. 4.7. Data generated by subtracting smoothened bathymetry from original bathymetry

flat region from the bumpy non landing areas and to generate a binary data as seen in the Fig. 4.8. In this figure, the blue areas represent the features while the red areas indicate the flat areas. The threshold to qualify a region suitable for landing remains fixed and is decided based on the cut-off frequency of the filter response. The threshold is decided based on the size of the features to be identified which will affect the landing characteristics of the vehicle. Since the scanned bathymetry has a resolution of a few millimeters, fine bathymetry features can also be detected. The threshold may be lowered to find the best site within the detected flat areas, if this would improve the quality of data obtained by seafloor observation. Within the flat areas detected, it is then required to identify areas where a vehicle of a particular dimension can land or perform observations. For this analysis, the threshold bathymetry is considered as a binary scaled image and simple image processing operators are used.

Fig. 4.8. Flat areas and features detected after applying threshold; Red: flat area, Blue: features

4.2.1.3 Image processing for flat areas

To identify flat areas where an underwater vehicle of a particular dimension can fit image morphological operations are used. For this purpose, the bathymetry data is considered as an binary image. The two binary components of the image are the flat area (red) and features (blue). The concept of finding a suitable flat areas where the vehicle can fit is equivalent to fitting an object of a given size into a continuous flat region of the scanned area.

The opening morphological image processing operator can be used to fit a structuring element into an image and find regions where it fits completely within a boundary. The image opening operation requires a structural element. The structural element chosen corresponds to the size of the underwater vehicle. A square footprint is considered by calculating the number of pixels equivalent to the largest dimension of the vehicle.

Considering the area to be represented by a an image with pixels $M \times N$, each point of the image is then indicated by $B(i, j)$ with i going from 0 to $M - 1$ and j going from 0 to $N - 1$. The structural element R is a mask of the size of the vehicle which is trying to land. $x_r(min)$ and $x_r(max)$ are the extreme values in the x direction and $y_r(min)$ and $y_r(max)$ are those in the y direction. If the largest dimension of the vehicle is l then the number of pixels representing it can be calculated as:

$$dx = \frac{x_r(max) - x_r(min)}{M}$$

$$P_x = \frac{l}{dx}$$

$$dy = \frac{y_r(max) - y_r(min)}{N}$$

$$P_y = \frac{l}{dy}$$

Opening operation is performed by an erosion process followed by a dilation process. The operation is performed by using the structural element R of size $P_x \times P_y$ on the data B.

$$B \circ R = (B \ominus R) \oplus R$$

where $\ominus$ indicates erosion and $\oplus$ indicates dilation.

Fig. 4.9. Detected flat area where the vehicle of a particular size can fit. Red: unsafe area with features, Yellow: flat area where vehicle can fit

By performing opening operation multiple times until the result no longer changes, we can find a suitable flat area where the vehicle can fit within the detected flat area as seen in the Fig. 4.9. The detected location of the flat areas suitable for the vehicle to perform landing or seafloor observations is then stored in a database as explained in the later sections of this chapter.

4.2.2 Detecting features in scanned bathymetry

The first part of the algorithm detects flat areas in the scanned high resolution bathymetry. The algorithm also determines areas where a vehicle of a particular dimension can fit within the flat area to perform seafloor observations. To make decisions for selecting the appropriate area for seafloor observation, the algorithm has to identify features on the seafloor and estimate their attributes. The features and attributes determined are used in the decision making process. Attributes currently considered are the shape, size, orientation and properties based on the shape such as radii, length, breadth etc which are explained in detail in this section. Once the flat areas are identified in the scanned bathymetry, the remaining area which is considered unsuitable for observations by landing is processed to detect features. Analysis is performed only in this part of the scanned bathymetry to detect the features and estimate their attributes. The feature detection used in this research is restricted to two dimensions and features are not identified by analyzing a three dimensional point cloud. One of the reason for doing this is the fast computational time required for real-time implementation of the algorithms in an underwater vehicle.

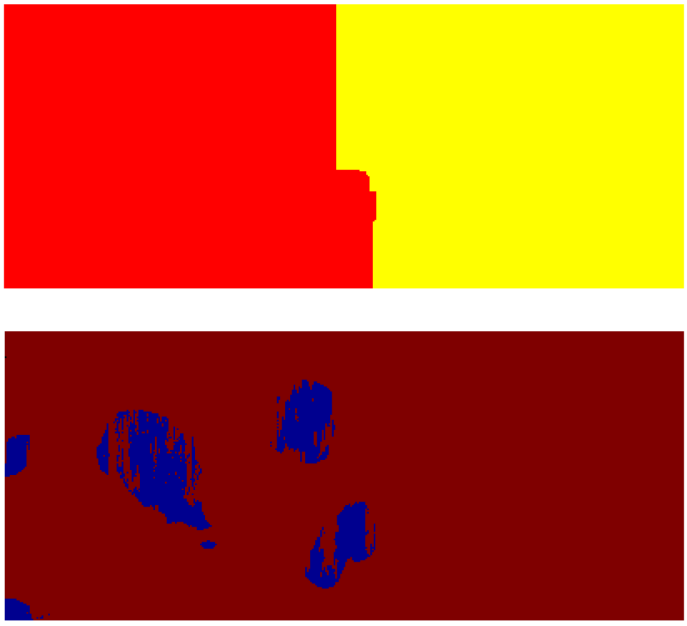

Fig. 4.10. Feature binary image; Top: Detected flat areas as seen in Fig. 4.9 (Red: area with features, Yellow: flat area), Bottom: Selected features in the area not considered flat. The detected rocks can be clearly seen.

A simple feature detection and attribute estimation algorithm has been implemented into the vehicle. The algorithm is based on Hough transform. Hough transformation is a technique for detecting imperfect instances of an object in a certain class of shapes by a voting process. The Generalized Hough Transform or GHT, is the modification of

the Hough Transform using the principle of template matching. This enables the Hough Transform to be used for not only the detection of an object described with an analytic equation (e.g. line, circle, etc.) but also arbitrary objects using a model. For estimating the features, the scanned bathymetry is considered as an image of $M \times N$ pixels similar to previous analysis. This is possible since the bathymetry has been meshed to an uniform grid and each pixel has a definite coordinate in the horizontal plane. The binary bathymetry image, Fig. 4.8, generated in the previous algorithm indicating the detected flat areas and non flat areas is used for analysis. The feature binary image generated using the scanned bathymetry and removing selected flat areas and resampling can be seen in the Fig. 4.10. The features in the scanning bathymetry can be clearly seen.

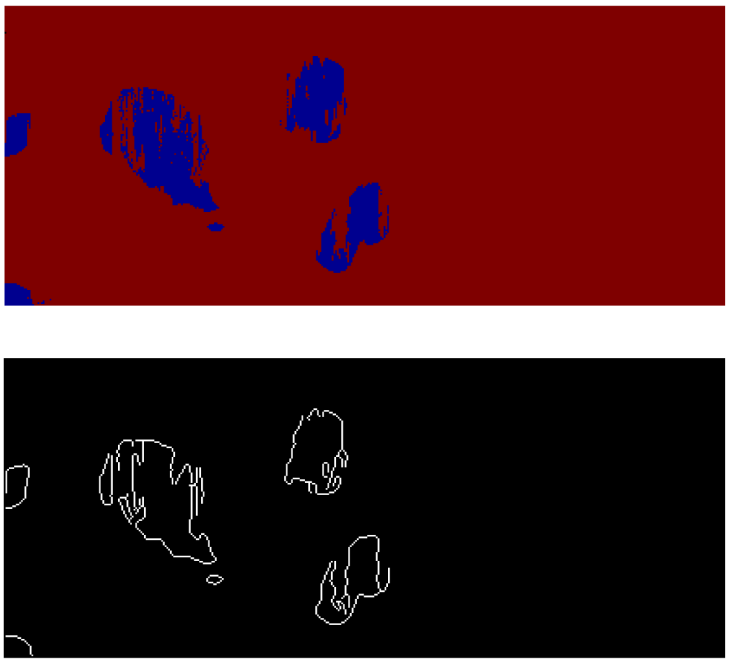

Fig. 4.11. Edge detection on identified features; Top: Rock features in the original bathymetry, Bottom: Edges of the rocks detected using image processing

The feature binary image created is first processed for detecting edges of the features. Edge detection is essential for Hough transform for extracting their attributes requires the edges of the features to be identified. A canny edge detector is used for extracting the edges of the features. The canny edge detection algorithm is considered as the optimal edge detection algorithm. It is also fast and efficient in computational time. The Canny edge detector is an edge detection operator that uses a multistage algorithm to detect a wide range of edges in images. The algorithm is efficient in good detection, good localization and minimal response to a single edge. The algorithm uses the calculus of variations.

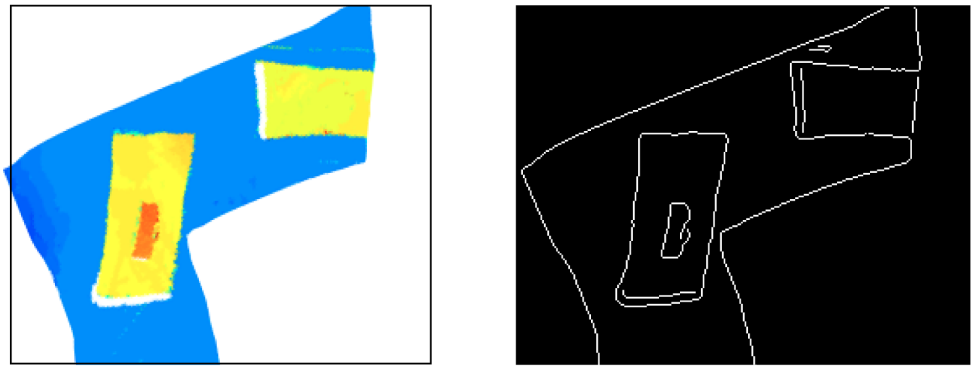

Fig. 4.12. Edge detection on identified features; Left: Rectangular features in the scanned bathymetry image, Right: Edges of the rectangular table detected using image processing

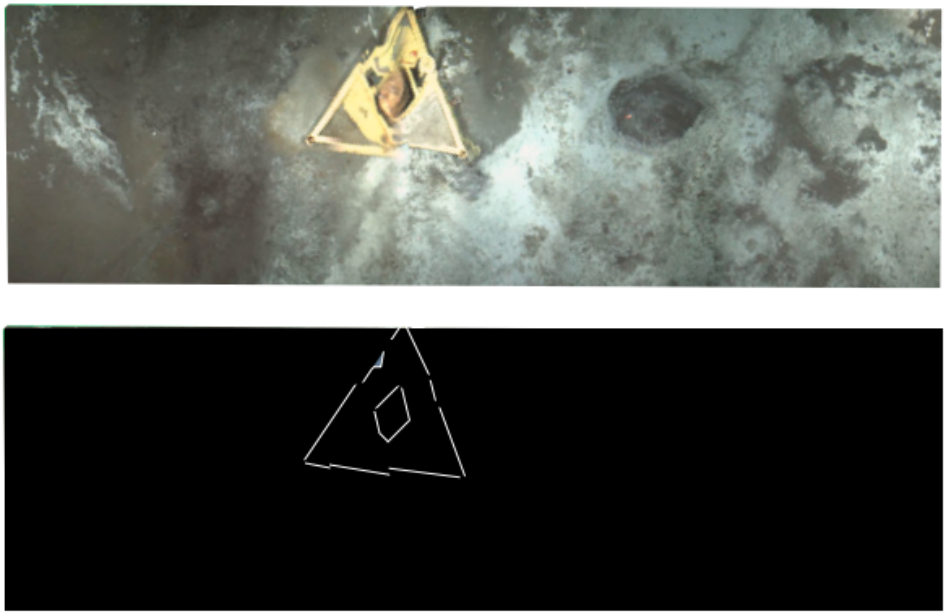

Fig. 4.13. Edge detection on identified hydrothermal vent feature; Left: Features in the binary bathymetry image, Right: Edges of the triangular hydrothermal vent detected using image processing

The optimal function in Canny's detector is described by the sum of four exponential terms, but it can be approximated by the first derivative of a Gaussian. Because the Canny edge detector is susceptible to noise present in raw unprocessed image data, the original image is convolved with a Gaussian filter. Is it important that the feature information is not lost in this process. The result is a slightly blurred version of the original image. This reduces the effect of small unscanned patches in feature detection. The features extracted using edge detection can be seen in the Fig. 4.11. To demonstrate the method, analysis is

also performed on other scenarios. A flat table scanned by high resolution scanning system is seen in the Fig. 4.12(left). The data used here is collected from the experiments performed at the Chiba experimental station, IIS. After detecting the flat area, the remaining area is then processed for feature detection. Canny edge detector is applied to detected the edges of the table. The original bathymetry data and the edges detected can be seen from the Fig. 4.12(right). Analysis performed on another data set collected at the triangular artificial hydrothermal vent C0014G during the cruise NT-12-27 can be seen in the Fig. 4.13.

After the edges have been detected, the Hough transformation is applied to extract the features and their attributes. At present the algorithm is only implemented to detect standard shapes in the features such as straight lines, circles and ellipses. The shapes of features such as triangles, rectangular shapes, quadrilateral, circular and elliptical are then estimated by the transform based on their connections and locations. The other attributes are then extracted based on the shape of the features. The attributes that are required are the size, orientation, X-Y location, major axis, etc. The output of the transformation applied to different scenario can be seen in the Fig. 4.14. The algorithm has been modified to enclose rock structures into elliptical regions.

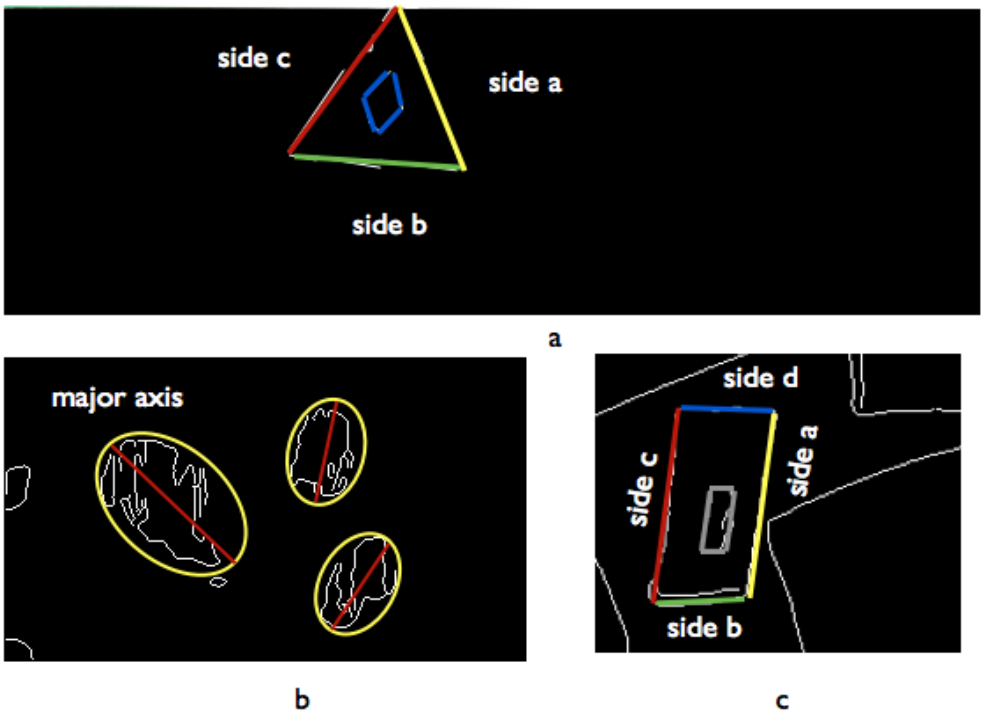

Fig. 4.14. Detected features and their attributes; a) Detected triangular shape of chimney and its sides b) Detected rocks as elliptical shape with major axis to understand the orientation c) Detected rectangular shape of the table and its sides

Once the features and their attributes have been identified, they are stored in a database file which is used during the decision making process. The features are named by their shape followed by an identification number. The position of the centre of mass (centroid) of the feature is stored. The area of the feature is also computed. Attributes of the feature based on its shape are stored as seen in the Table. 4.1. Along with the database file, information is also stored in the form of an colored image map as seen in Fig. 4.15. Featured with different shaped are given different colors. The edges are colored white and the flat are is colored yellow. The map file is useful for performing image processing operations for detecting landing points of observation area.

Table 4.1. Feature storage database

Type	**Map color**	**Nomenclature**	**Attributes**
Circuar	Brown	c	$Xpos$, $Ypos$, radius, area
Square	Cyan	s	$Xpos$, $Ypos$, side a, side b, side c, side d, area
Rectangular	Blue	r	$Xpos$, $Ypos$, side a, side b , side c, side d, area
Elliptical	Orange	e	$Xpos$, $Ypos$, area, major axis
Triangular	Green	t	$Xpos$, $Ypos$, side a, side b, side c, area
Flat area	Yellow	-	-

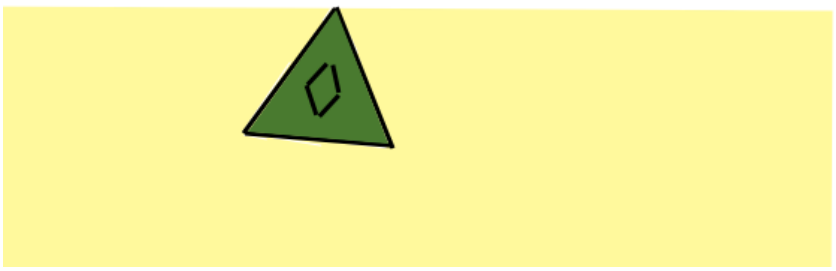

Fig. 4.15. Detected features and attributes stored as a map; Green: Triangular feature, Black: Edges, Yellow: Fat area

4.3 Performing observations

Once the analysis of the seafloor has been completed decision to perform observations is based on the features identified and the survey rules. The survey rules explore the relationship between the sensor used, the seafloor properties measured and the seafloor features. The features that suite the survey are selected from the feature database and

map. The decision to select the appropriate area for seafloor observation is then made based on the survey rules provided in the survey rule file. The format of the survey rule file is provided in the Appendix C of this manuscript.

The vehicle might have to perform landing on the seafloor for obtaining measurements from sensors that require contact or close proximity with the target. The landing points are determined in the flat areas and with specific relationships to the features identified. To explain this better, we can consider the case of seafloor radiation measurement where measurements after landing need to be taken from top and bottom of the rocky features. In case of rectangular artificial reefs, measurements will be taken by landing along all sides of the rectangular structure. Also in case of the triangular artificial reefs, landing will be performed on each side of the triangle to measure chemical contents and concentrations. In some other cases, the vehicle may not have to land on the seafloor but perform observations around the features by slow speed navigation. An example of such a case is the generation of high resolution three dimensional bathymetry of hydrothermal vents, surveying the rectangular columns of underwater foundations, etc.

4.3.1 Performing landing observations

To perform landing operations, the landing points are detected in the flat areas where observation has to be performed. The location of the landing points is identified based on the survey rules and features. The survey rules are extracted from the rule file to determine the required features and matching them to the feature database generated in the previous step. Based on the location of the flat areas and the features, flat suitable areas for observation are determined. The landing coordinate can be detected by image processing operation.

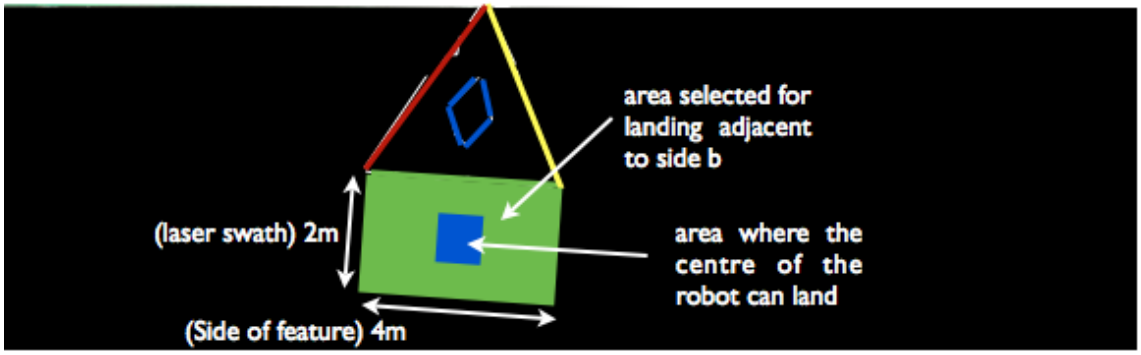

Fig. 4.16. Selected landing area on Side c of the triangular feature; Required rectangular region has been already scanned and landing point can be generated

To select the landing flat area, the feature around which observation has to be performed are first identified. The sides along which landing has to be performed are taken as reference for landing point calculation. Incase of features with straight line edges, a rectangular box

with one side equal to the length of the side of the feature is considered. If this side is longer than the swath of the high resolution scanning laser, the other side of the rectangle is considered equal to the swath. If the length of the edge is smaller than the sensor swath, then the area selected is a square of side equal to the largest size of the vehicle. The suitable landing area for the centre of the vehicle to land in the area suitable is then identified in the selected rectangle. To performing landing, a sufficient flat area is essential. It is necessary to verify if the entire selected area of the seafloor has been scanned with high resolution.

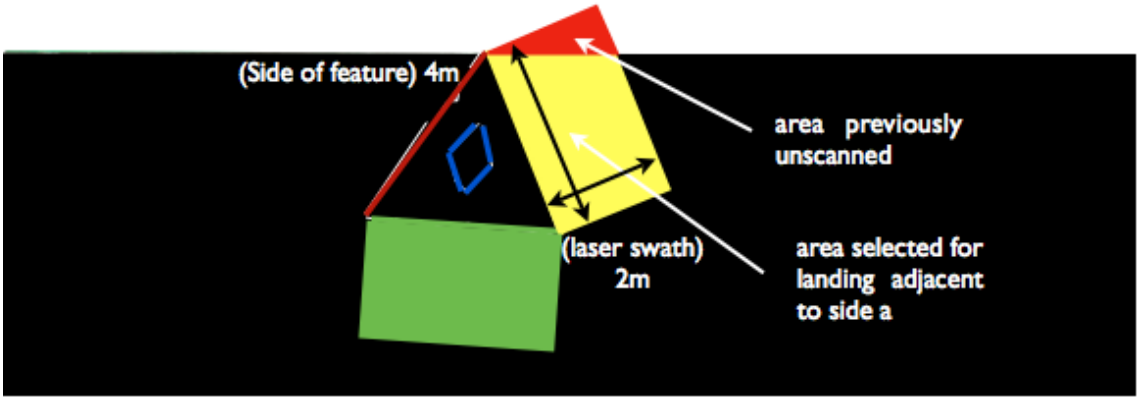

Fig. 4.17. Selected landing area on Side a of the triangular feature. Unscanned region is observed which has to be scanned first before generating a landing point

In case the area has not been scanned with high resolution, new waypoints have to be generated for the vehicle to first acquire high resolution bathymetry data in the unscanned area. Once, the required area has been scanned by the vehicle, the landing point is computed in the area selected for seafloor observation using the landing algorithm. To explain the concept in detail, we can assume that a landing point has to be identified along the side b of the triangular hydrothermal vent as seen in Fig. 4.16. A suitable flat patch of the land adjacent to the side b is analyzed. The rectangular area selected depends on the length of the side of the chimney. Since the side of the chimney is longer than the swath of the laser sensor, it is considered as the larger side of the rectangle. It if then verified that all the points in the required rectangular area have been previously scanned. Since they have been scanned in case of side b of the feature, the area suitable for landing for the centre of the vehicle is estimated. The opening morphological image processing operator is used to fit a structuring element into an image and find regions where it fits completely within a boundary. The image opening operation requires a structural element. The structural element chosen corresponds to half the size of the underwater vehicle. This is done since the area for landing of the centre of the vehicle has to be identified. The point in the landing area of the centre of the vehicle nearest to the centre of the side of the feature is then considered as the landing point.

To find a landing point adjacent to side a of the triangular hydrothermal vent as seen in Fig. 4.17, a rectangle of similar dimensions is considered. It can be seen that some of the area required for landing point detection is outside the unscanned. The unscanned area is first separated form the scanned area. New waypoints are generated to scan the required area with high resolution where features and obstacles are identified. The waypoint generation algorithm similar to the one is wide area analysis is used. After scanning the required area, the algorithm then generates the necessary landing point adjacent to side a of the triangular feature using image processing as in the previous case.

4.3.2 Performing observations by navigation

In cases where the vehicle has to perform slow speed maneuvers to obtain observation data, the areas where data need to be collected and the orientation of the vehicle have to be selected. This is done by comparing the requirements of the survey rule file and matching them with the feature database created from those identified. The feature around which the observation has to be performed is first selected in the bathymetry image and a bounding box is drawn around it. The obstacles in the area which are known are also marked in the image. Image processing is then done to detect a region around the features where the vehicle of a particular size can fit. The operator used for this is an image morphological operator called dilation. The mask used for this operation is a circular mask with diameter equivalent to the largest side of the robot. By performing image dilation on the feature image, we can find an area around the features where the vehicle has to navigate. The outer edge of this area is the path which the vehicle has to take for performing observations by navigation. Once the area for observation has been identified, the algorithm generates waypoints for scanning the selected area.

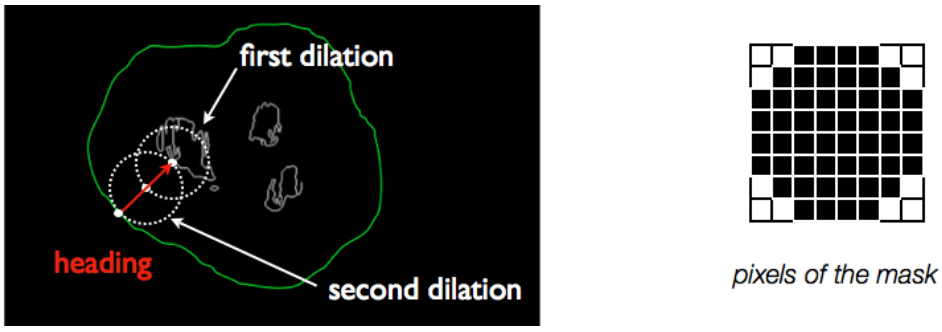

Fig. 4.18. Performing observations around rocks without landing; Green: Scanning path identified by image processing, Red: Scanning heading to face the target

The area selected for observation can be outside the currently scanned bathymetry. In this case, the unscanned region has to be first scanned to generate a high resolution bathymetry. The features on the floor and obstacles which could interfere during observation have to be identified. After obtaining the required unscanned bathymetry, new waypoints are generated

5

Development of landing AUV

This chapter explains in detail the design and construction of the prototype autonomous underwater vehicle developed with specialized hardware and software to demonstrate the proposed multi-resolution survey method. The requirements and considerations taken into account during the design of the the vehicle are discussed in detail along with the solutions applied to overcome these issues.

This chapter also elaborates on the hardware construction of the vehicle and provides details on the various features implemented for multi-resolution bathymetry scanning and landing. The electronics hardware of the vehicle are explained in detail with suitable connection diagrams. The integration of sensors used for vehicle navigation and for scanning the seafloor with different resolutions is described and their specifications provided. Details on the core software architecture of the vehicle, data acquisition and processing and the control system are provided. The software implementation of the survey method using various modes of vehicle operations is explained in detail. This chapter is also supported by Appendix B containing the mechanical drawings for vehicle constructions and Appendix C containing details about the vehicle initialization file and the survey rule file.

5.1 Vehicle design considerations

The proposed survey method requires the underwater vehicle to traverse at high speeds while acquiring acoustic bathymetry data with a wide swath [45]. For an AUV to cruise at high speeds, it is necessary to have a streamlined shape with small forward cross section to generate minimum forward drag. At the same time, while acquiring high resolution bathymetry, the vehicle has to perform slow speed precision manoeuvring. The vehicle also has to hover before vertical landing or real-time data processing for decision making. In order to make the AUV streamlined, protrusions have be kept at a minimum. Single thruster, torpedo shaped vehicles can generate a very low drag coefficient but are unable to hover or perform slow speed navigation. Box shaped vehicles, typically ROVs, can perform slow speed precision manoeuvring but have large cross section areas thereby restricting high speed cruising. The designed vehicle should therefore have the capability to cruise at relatively high speeds but also perform slow speed operations. From previous exploration

work carried out at sea [46], it can be seen that vertical landing using thrusters can disturb the underlying sand on the seafloor. Once the sand is agitated, it is not easily possible to obtain good quality data from the seafloor and it is often necessary to wait for a substantial amount of time to make any observations.

Since our main objective is to measure properties of the seafloor, the vehicle should have the capability to land on the seafloor by using minimum use of its vertical thrusters. The sensors for seafloor observation should be provided with a stable footing after landing for integrated data acquisition for which a special structure has to be designed. Since the algorithms implemented for decision making in the vehicle should process the data in real time, it should be equipped with a high speed computers. A software architecture capable of real-time data management and processing has to be developed and implemented. As this vehicle has a capability of cruising close to the seafloor and also landing, it is called as *Bottom Skimmer*.

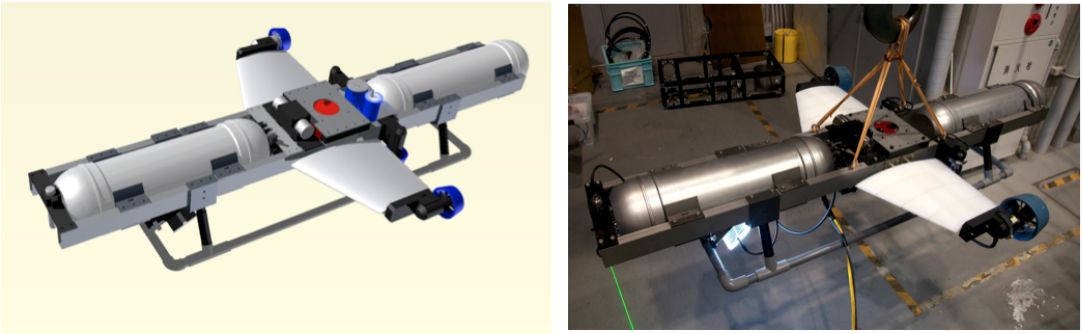

Fig. 5.1. Left: CAD drawing (Autodesk Inventor V9.0) of the vehicle, Right: Fully assembled vehicle

5.2 Bottom Skimmer vehicle overview

The bottom skimmer vehicle was designed as seen in the Fig. 5.1 by taking into account the required design considerations. The vehicle hardware structure was designed using Autodesk Inventor v 9.0. Stress analysis was performed on all key components to check for their tolerance and integrity. The vehicle was manufactured in the workshop belonging to IIS, The University of Tokyo. The fully assembled vehicle is about 2m in length and 1m breadth with a depth rating of 750m. For keeping the forward cross section at a minimum, the vehicle hull and sensors have been mounted in one straight line. The vehicle has independent thrusters for surge and heave motion allowing it to perform slow speed maneuvers as well as hover when necessary. The vertical thrusters have been inclined to 22.5° for performing sway movement. The inclined thrusters also direct the vertical thrust away from the area exactly below the vehicle hull preventing the underlying sand

and sediments from being disturbed during landing. The vehicle has been made slightly negatively buoyant so that it can land on the seafloor with minimum use of its vertical thrusters. To compensate for this negative buoyancy, NACA winged shaped foils are designed which generate lift during forward motion and also provide stability against roll. Landing skids similar to helicopter skids, have been designed for providing a stable footing for landing on the seafloor to perform measurements. The completed vehicle hardware and the mounted sensors can be seen in the Fig. 5.2.

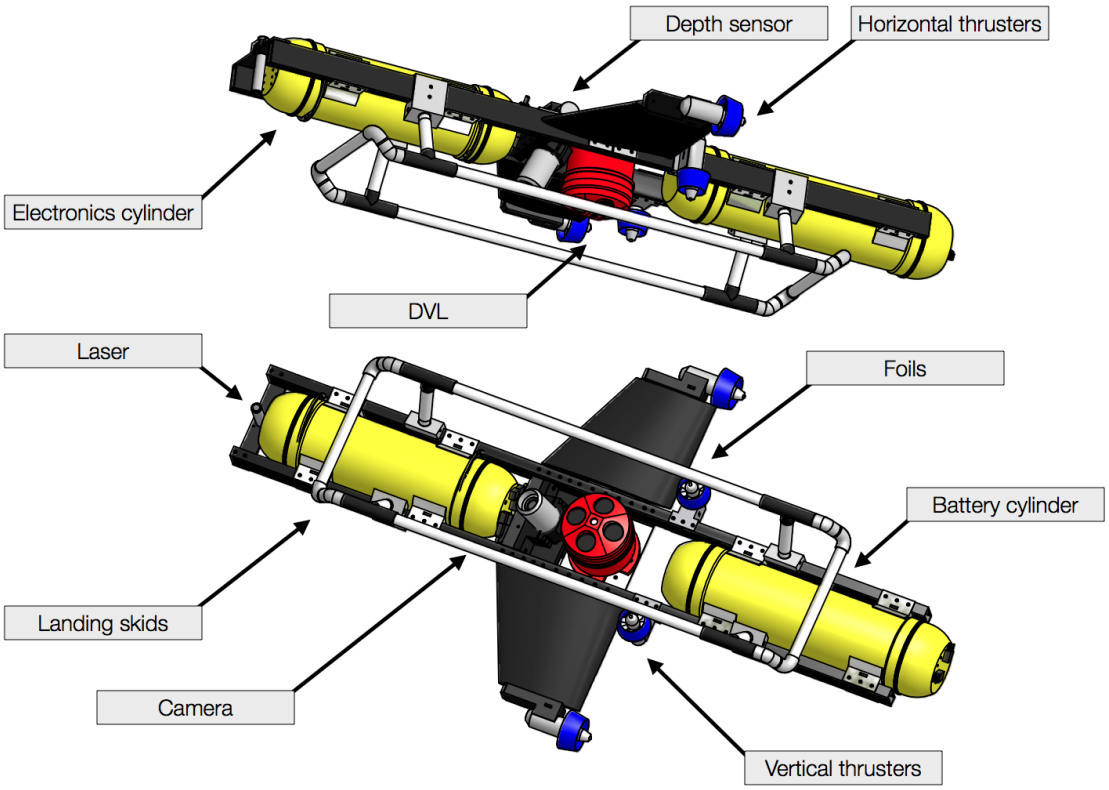

Fig. 5.2. Bottom Skimmer CAD drawing (Autodesk Inventor V9.0) showing different parts and sensors of the vehicle

5.3 Hardware construction

The main structure of the AUV comprises of two horizontal hollow rectangular pipes made from Aluminum. The hollow spaces inside the bars are filled with Nylon blocks for additional strength. Further details on the vehicle assembly and parts are provided in the Appendix B at the end of the manuscript. Holes are made on the top and bottom for mounting the main hull cylinders, thrusters, wings and other sensors. The individual parts of the vehicle hardware can be seen in the Fig. 5.3 and are described below:

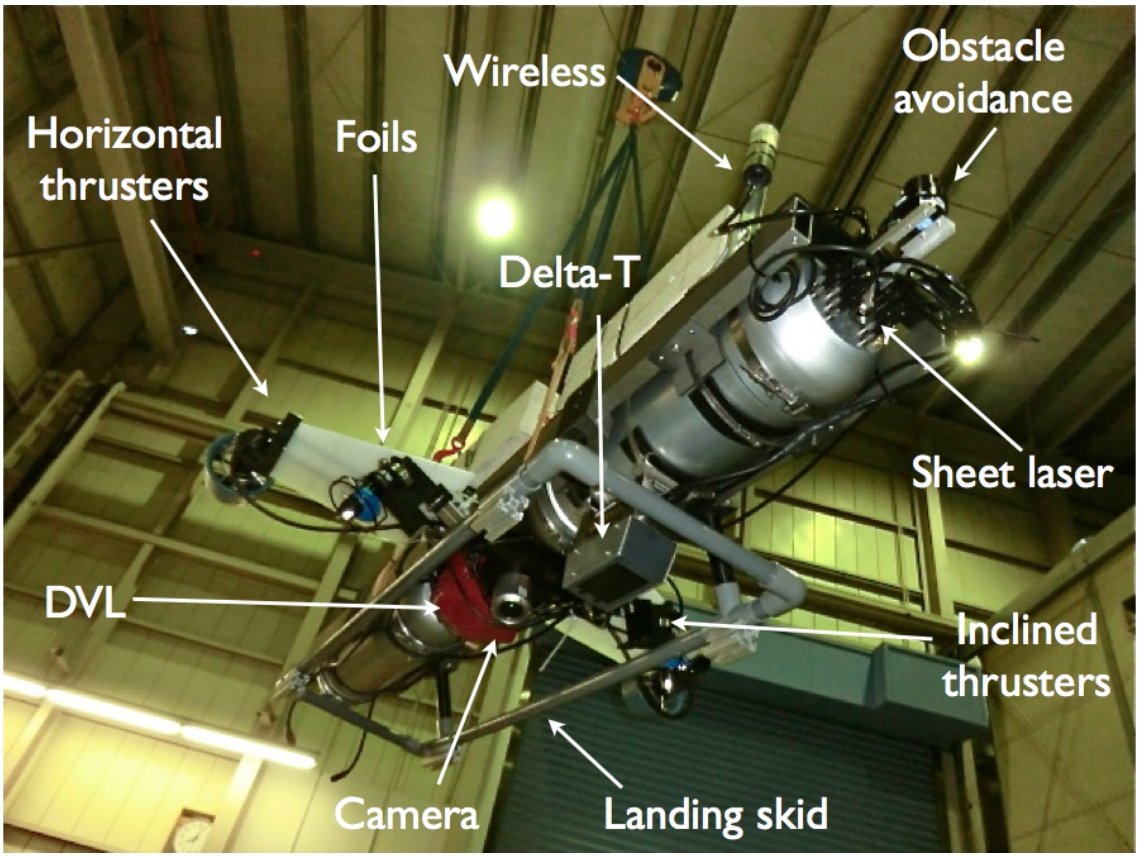

Fig. 5.3. Various components mounted on the final assembly of the Bottom Skimmer vehicle

5.3.1 Hull sections

The main hull is divided into two parts, the electronics and the battery cylinder constructed using 5056 grade Aluminum. The hull is divided into central section and two end caps. Trays for mounting components inside the hull are designed. Sealing is provided by use of O-rings (190mm No. JIS B 2401 G190) between the end-caps and the main cylinder. The end plates have a flat section for mounting underwater connectors and vent screws. The two end sections are connected to the main hull by the use of V-Bands (YMV12745). Each cylinder is attached to this frame by four clips and a jubilee band. CAD drawings of the hull assembly are provided in Appendix B.

5.3.2 Propulsion

The vehicle has two horizontal thrusters, 220W each, for surge motion. The thrusters are mounted on the ends of the winged structure. ABS holding clamps are designed and the thrusters are connected to this clamp using jubilee bands. Two thrusters, 100W each, inclined at 22.5° with the vertical are used for sway and heave motion. The initial design

of the vehicle had thrusters for heave motion mounted vertically without the possibility of generating sway motion. They were later inclined so that the vehicle can also perform sway motion. These thrusters are mounted equidistant from the centre of mass of the vehicle to avoid pitching and rolling during motion. The initially designed mounting location of the thrusters was changed as new components were added to the vehicle changing its centre of mass.

5.3.3 Wings and landing skids

A winged foil structure is designed to generate lift during forward motion to compensate for the negative buoyancy of the vehicle. The wing design is based on standard NACA651412 profile in order to generate lift even at zero angle of attack. Optimum lift is generated at speeds of about one knot. The wings are made from nylon with a Aluminum skeleton for strength and stability.

The design of skids was adopted from standard helicopter design with two long horizontal bars to provide stable footing on relatively flat surfaces. Skids have been designed from standard PVC piping and Nylon footings. The skids also provide protection to the sensors which are mounted along the underside of the vehicle. Details on the foil design and assembly as well as the landing skid assembly are provided in the Appendix B at the end of the manuscript.

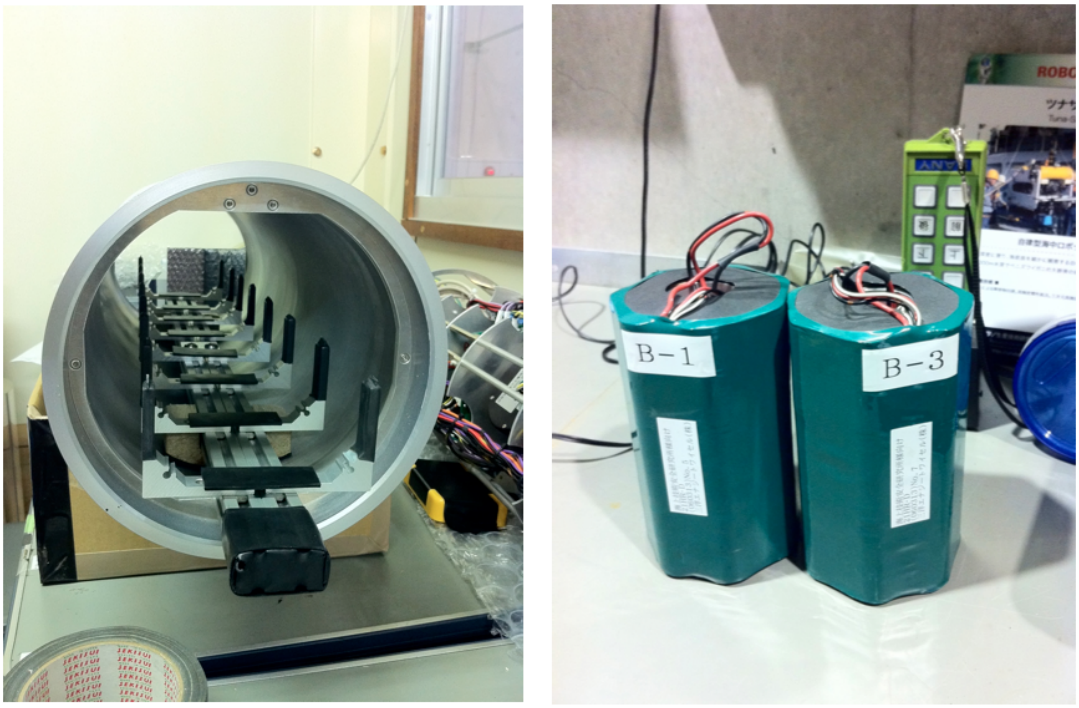

Fig. 5.4. Vehicle power system; Left: Tray for holding the battery packs, Right: Individual battery packs

5.3.4 Power source

The vehicle can be powered using internal batteries or external power supply. An relay switch chooses the source of power to be used. The power provided in the external mode comes from a tether. This powers all the vehicle electronics except the thrusters which are always driven by internal batteries. This is done to keep the amount of current flowing through the tether cable at a minimum. In the internal mode, all the vehicle electronics and thrusters are powered using a Li-ion battery rack as seen in the Fig. 5.4. The vehicle can house four Li-ion batter packs each with a capacity of 24V, 10Ah which are charged externally. A fully charged battery set can provide a four hour operational endurance.

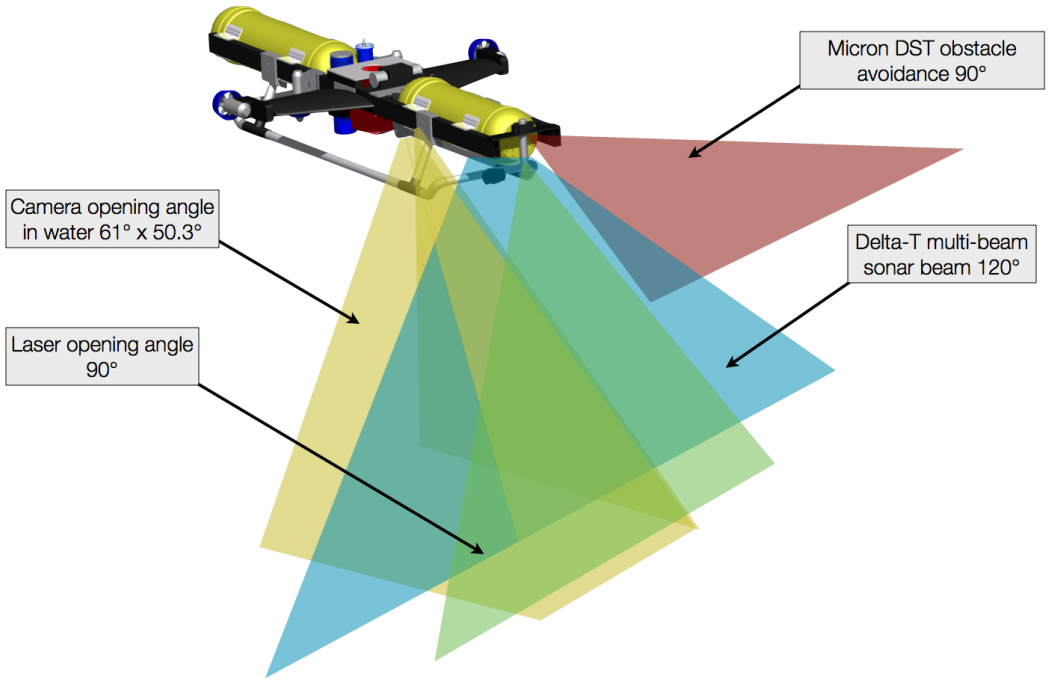

Fig. 5.5. Placement of navigation, scanning and obstacle avoidance sensors and their coverage swath lengths

5.4 Vehicle sensors

The sensors for navigation and scanning the seafloor with different resolution are integrated into the hardware design of the vehicle. The placement of the sensors on the vehicle main structure was determined based on their functionality. The placement and the coverage swaths of the different sensors can be seen in the Fig. 5.5.

5.4.1 Navigation sensors

The vehicle performs navigation by dead reckoning. Velocity of the vehicle in x and y robot frame is measured using a Doppler Velocity Log (DVL). The orientation of the DVL is such that two beams look forward and two backward relative to the direction of motion of the vehicle. The DVL also integrates the velocity measurements to generate X_{rob} and Y_{rob} position in the world frame of reference. The DVL has an internal compass and attitude sensor which gives the heading, roll, pitch and yaw measurements. The Z_{rob} position or depth is measured using a depth sensor. The electronics hull also houses a single axis Fibre Optic Gyro (FOG). The FOG is mounted horizontally in the central part of the section. The rate measurements from the gyro are integrated to obtain the vehicle heading as well as for the heading controller. The specifications for individual sensors are provided in the section 5.7 of this chapter.

5.4.2 Scanning sensors

The vehicle is designed with sensors for scanning the seafloor with different resolutions. A multi-beam sonar is mounted along the lower front section of the vehicle looking vertically downwards with the beam normal to the direction to the forward motion of the vehicle. The sonar used is an Imagenex Delta-T sonar. For high resolution scanning a laser profiling system is used. The system consists of a camera and laser arrangement integrated into the vehicle design. The detailed working of the profiling system has been explain in the Appendix A of this manuscript. The scanning resolutions of the sensors can be seen in the Table. 5.1.

Table 5.1. Scanning sensor specifications

Sensor	**Horizontal resolution**	**Vertical resolution**	**Scanning altitude**	**Scanning speed**
Multi-beam sonar	12.5cm × 12.5cm	2cm	10m − 15m	0.4 − 0.5m/s
Laser profiling	5mm × 5mm	8mm	2m − 3m	0.1m/s

5.4.3 Obstacle avoidance

The AUV uses a Micron Digital Sonar Technology (DST) using CHIRP pulses as the mechanically scanning forward looking obstacle avoidance sonar. The sonar is mounted in the front of the vehicle with the sonar beam in a horizontal plane. The reflection information is converted into real world position of obstacles using the vehicles current position information. The sonar is typically operated with a scanning range of 5m and a beam angle of 90°. The sonar typically takes precautionary actions when targets less than 1m from the vehicle are detected.

5.5 Vehicle Electronics

A modular hardware architecture has been designed for the vehicle [47]. The electronics are housed inside the main hull of the vehicle on a specially designed tray. The main components in the system comprise of the DC-DC converters for power conversion, control switches, computers for processing data, hub for Ethernet etc. The connections between the different key electronic components have been shown in the Fig. 5.6. DC-DC converters are used to step down the battery voltage for the sensors and internal computers. The AUV has a distributed architecture with two main computers, one for acquiring data from different sensors and processing it and the other for vehicle core control. A low powered micro-controller (MCU) is used for generating the control signals for the thrusters and control the power switches. External sensors are connected to the computer using underwater connectors. The AUV uses Ethernet as its main form for communication between the computers and the external world. The detailed schematics of the vehicle electronics are attached in Appendix B of the report.

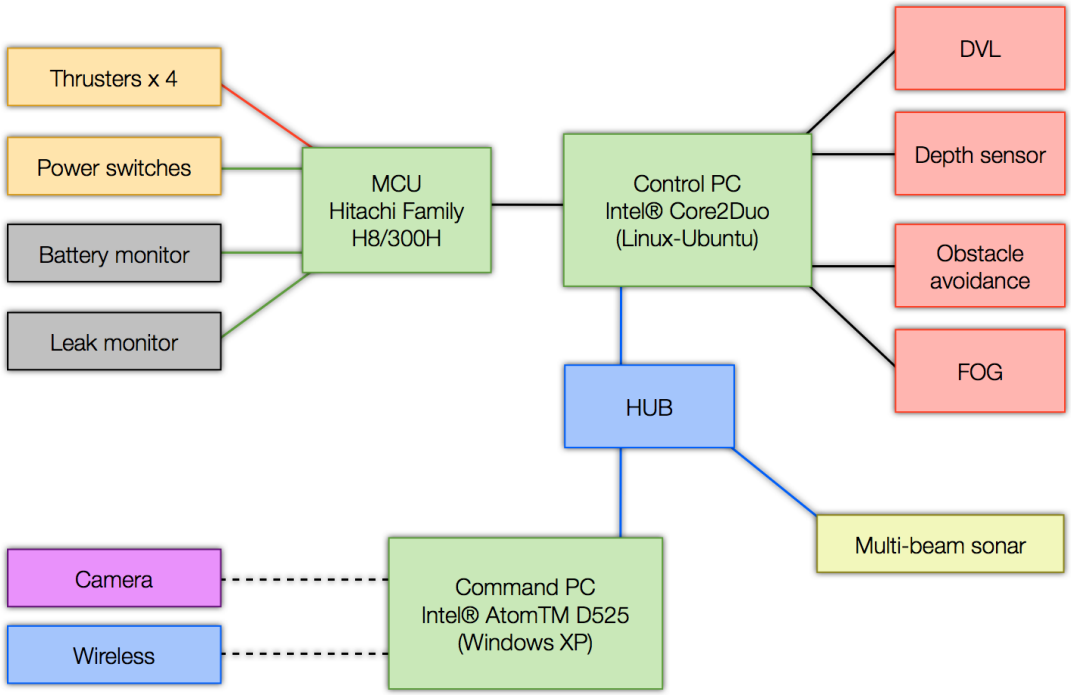

Fig. 5.6. Overview of the electronic components and their interconnections; Connection lines Black: RS232, Blue: Ethernet, Black dotted: USB, Green: Analog output, Red: GPIO

5.5.1 PCs and MCU

The vehicle is equipped with two computers for acquiring data from the sensors, controlling the vehicle navigation and processing data in real-time. The main computer (Control PC) is an Core2Duo Advantech Board for performing core system operations such as vehicle navigation and obstacle avoidance. The computer runs a Linux Ubuntu 12.04 operating system. Drivers for obtaining data from the navigation sensors are programed. A second computer (Command PC) running Windows Xp on an Advantech Board with Intel Atom performs data acquisition from the scanning sensors and also runs the vehicle command and control software. The data processing algorithms for bathymetry generation decision making are programmed in this computer using Visual C++. The vehicle also has a MCU which provides the necessary control signals to the four thrusters to set the speed and direction. The MCU receives serial communication from the Command PC with a control packet to control the thrusters and switches. The Command PC sends data commands to the micro-controller to set the thruster speed or to cut them off. It generates a PWM signal and passes it to the digital to analog converter module as the thruster control signal. The MCU also toggles the control switches connected to it by the GPIO ports to switch power to the vehicle sensors. The command to toggle switches for lights, laser and ballast release is obtained from the Control PC serial packet.

5.5.2 Ethernet network

The vehicle uses Ethernet as its main means of communication between the computers also with the external world. The AUV has an Ethernet hub which connects the devices together. A special protocol for data communication is developed to share important vehicle data between the computers. The data can also be accessed outside the vehicle over a wireless communication or tether. External communication can be used for testing the vehicle and also for getting data from the AUV after the mission is completed. A static IP has been assigned to the AUV network for connecting it to an external computer over the network. A remote desktop connection client is used for controlling the vehicle or transferring files using external Ethernet connection.

5.6 Software architecture

5.6.1 Vehicle computer programs

The vehicle has core software written for initializing sensors, data collection, controlling thrusters, etc. Most of the software programming is done using C++ programming language for its speed of execution. The vehicle software has a distributed hierarchical approach. The MCU has drivers written in assembly language for sending control signals to the vehicle thrusters, adjusting power switches, monitoring temperature and battery voltage as seen in the Fig. 5.8. Overview of the core software programmed into the Control PC is seen in Fig. 5.9.

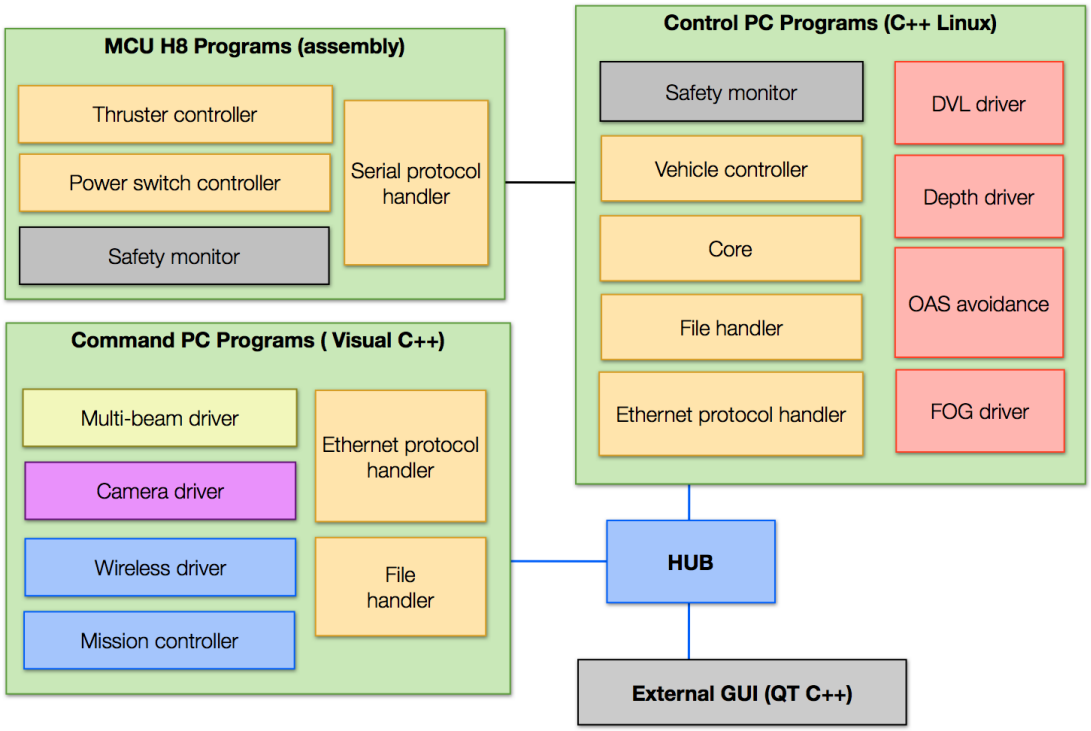

Fig. 5.7. Overview of the software architecture as implemented on the vehicle; Programs for acquiring data, vehicle control or data management for different components of the vehicle can be seen as individual blocks

The core software in the Control PC of the vehicle communicates with the MCU over a self made protocol. The Control PC can set the thruster speeds and toggle the power switches using this protocol. On powering up, the Control PC enables all the vehicles sensors and actuators based on an initialization file. Drivers for initializing, acquiring data and logging from the DVL, FOG and Micron DST sonar have been programmed in the Control PC. The vehicle position and orientation data is also received from the DVL by the driver and places in a shared memory segment for other process to access. The entire vehicle position and orientation data is automatically logged in a new file whenever the vehicle is powered up. The Micron DST driver receives individual scans and converts them into position data in real-time using the vehicles navigation information. The DST driver communicates with the vehicle control system using a file which provides information about the vehicle security level and obstacle status. In case of obstacles detected in the vehicles path, the safety level is made critical allowing the control system to stop the vehicle. An Ethernet handler manages communication between the Command PC and Control PC and also with the external world. It communicates the vehicles current navigation information. This data can also be received using wireless or tether to monitor the vehicles progress.

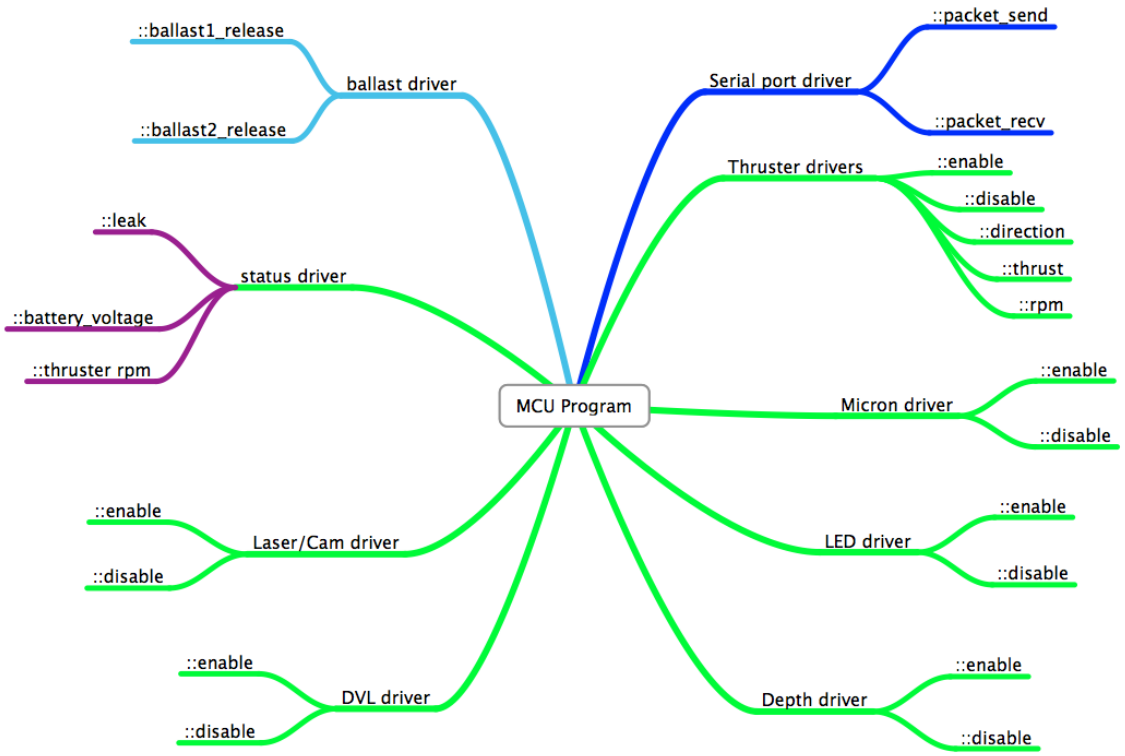

Fig. 5.8. MCU software structure; Functions and libraries implemented using assembly language

The programs in the Command CPU have been written using Microsoft Visual Studio and can be seen in the Fig. 5.10. The Command CPU is connected to the two sensors, camera and Delta-T used for scanning the seafloor. The Delta-T multi-beam sonar has a proprietary software for beam forming which can be executed only on Microsoft Windows. The Delta-T driver programmed requests the host program to transmit and receive one acoustic pulse which is then logged. Camera driver using the manufacturers API for fast image acquisition has been programmed which logs images. Ethernet handler has been programmed which managed communications between the CPUs, Wireless and external cable for sharing data and controlling the vehicle remotely if necessary. The Ethernet driver receives the vehicle position information from the Control PC in real-time.

5.6.2 Vehicle motion control

The vehicle motion controller is programmed into the Command PC and runs as an independent thread for high speed operation. The controller can directly communicate to the thrusters through the MCU thereby prevent any delay in operation. The controller also receives an emergency signal from the forward looking Micron DST sonar in case the vehicle has to be stop. The vehicle has a PD controller for heading control and depth control. A velocity PD controller has been made for surge and sway motion of the vehicle.

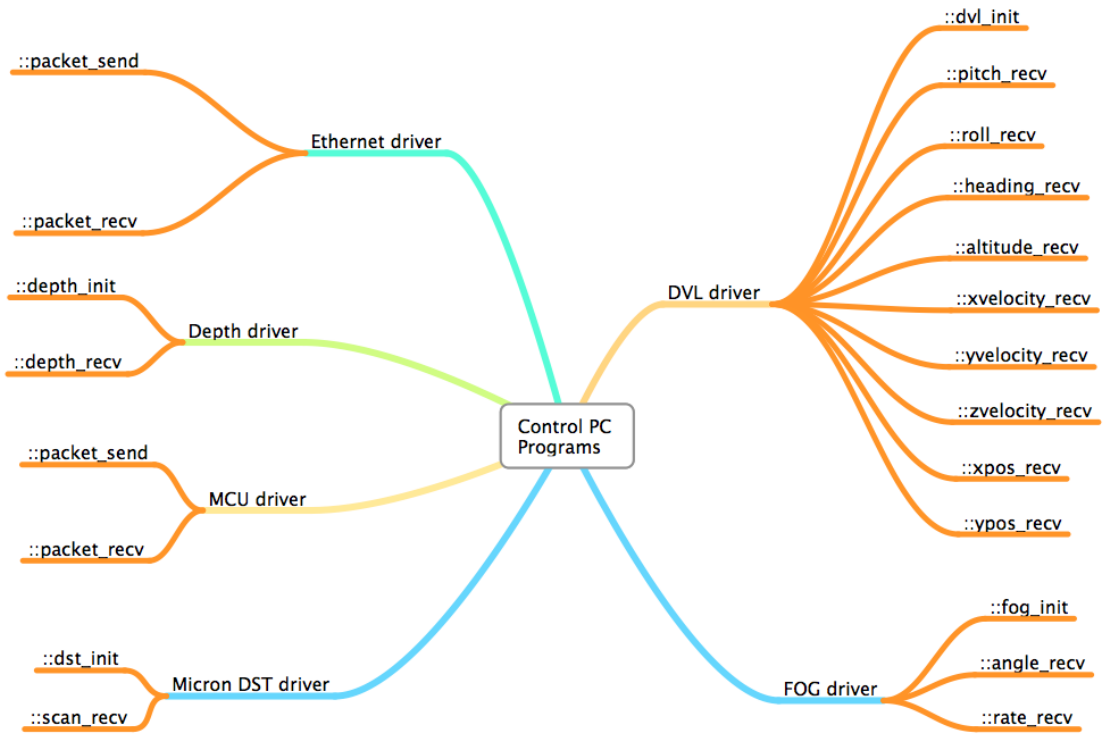

Fig. 5.9. Control PC software structure; Functions and libraries implemented using C++ programming language in Linux make

A waypoint navigation system has been developed over this controller. The navigation system calculates the heading required to reach the next waypoint and performs navigation at a constant velocity and altitude. A waypoint priority system has been implemented to decide the time-out before which the vehicle gives up on reaching the waypoint in case of difficulty.

5.6.3 Implementation of the survey technique

The survey method is implemented in the vehicle by writing the software and programs for the different algorithms involved in the process. The programs are integrated into the main core of the vehicle and use its command and control and waypoint navigation for performing the mission. The entire survey is broken down into different operational modes based on functionality as can be seen in the Fig. 5.11. The modes of operation define the state of the vehicle and the next action to be taken such as performing scanning or data processing. The scanning speed of the vehicle, the scanning altitude and the sensors used are set according to the mode. Programs are made to parse and read the initialization parameters from the file provided to the vehicle and also the survey rule file. A mission controller has been programmed which conducts the entire mission by operating the vehicle under the right modes and processing the collected data in real-time.

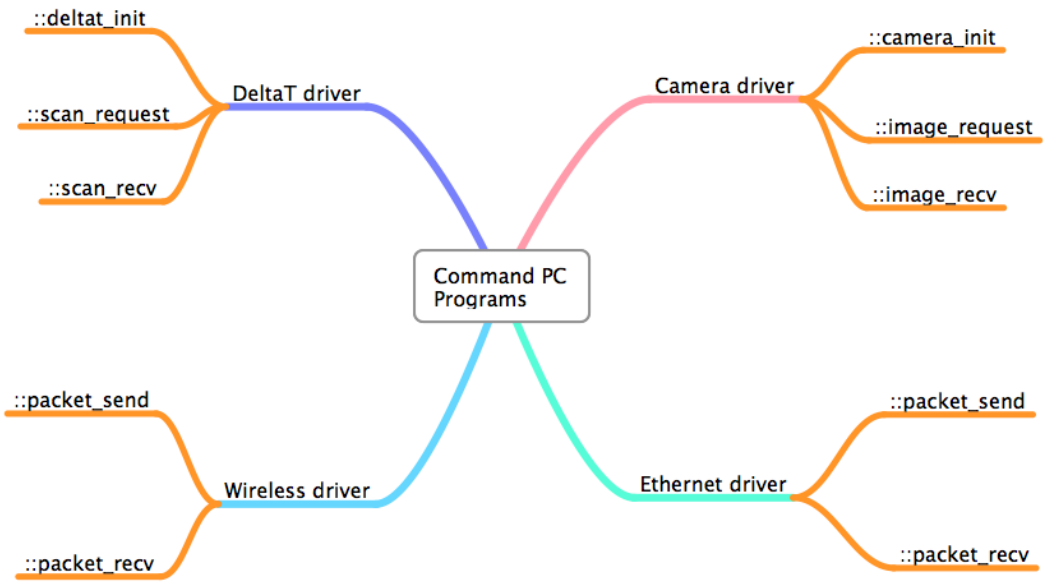

Fig. 5.10. Command PC software structure; Functions and libraries implemented using C++ programming language in MS Visual Studio

The mission controller communicates with the other processes over a self made protocol using files and Ethernet. At the start of the survey, the mission controller reads the initialization file and configures the camera and sonar accordingly by sending appropriate commands to their drivers. The controller passes the current vehicle mode information to the other programs through a file and the Ethernet handler. Every program running in the vehicle is aware of the current operation mode and takes the appropriate action individually. The protocol also mentions the current folder name so that the individual programs can log the data into the appropriate folders which makes it easier for processing. Once the data is collected the mission controller runs the algorithms and generates new files as required by the next stage in the survey. For instance, after wide area scanning and data processing, the mission controller generates a new waypoint file and changes the mode of the vehicle to high resolution scanning mode. The initialization file is also copied to the Control PC. After receiving the mode information from the mission controller, the vehicle controller sets the vehicle to the right speed and altitude until the next waypoint is met. The micron DST is configured by the Control PC based on parameters in the initialization file. The obstacle avoidance data is directly read by the vehicles motion control to take appropriate action in case of emergency. The survey is thus executed in stages by the vehicle mission controller by setting the right mode, collecting the data and processing it for analysis and decision making.

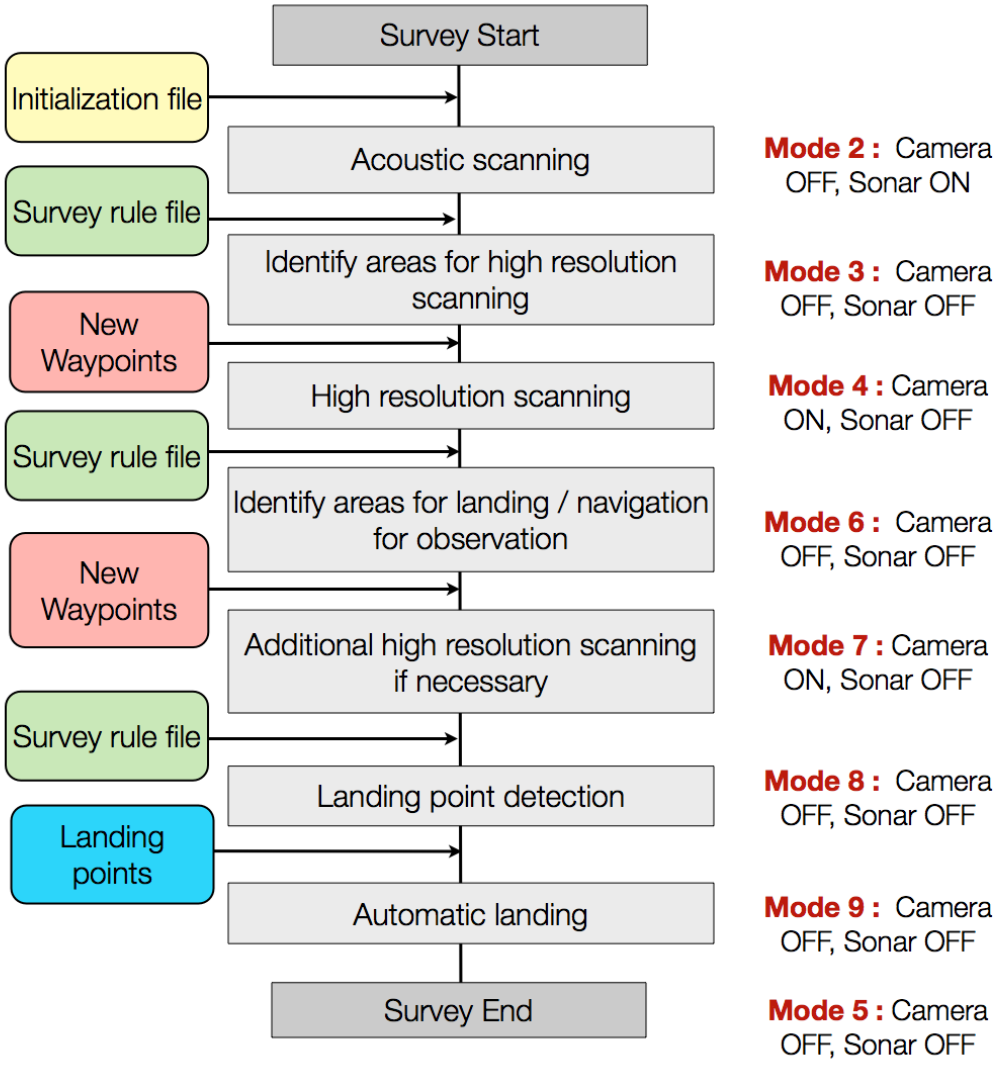

Fig. 5.11. Modes of operation of the vehicle used for implementing the survey method. The modes decide the status of the vehicle sensors and the action to be taken

5.7 Detailed vehicle specifications

The Table. 5.2 provides specifications of the navigation and scanning sensors used by the vehicle and its hardware components. Specifications of the vehicle electronic components are also given.

Table 5.2. Vehicle and sensor specifications

Property	Specifications
Vehicle hardware	
Size and mass	2.2m(L) x 1.0m(W) x 0.5m(H), 125Kg
Depth rating	750m
Vehicle navigation	
Velocity	RDI Workhorse Navigator WH-DVL1200kHz
Altitude	RDI Workhorse Navigator beams
GPS receiver	USBGPS2
Depth	Menstor6000 series
FOG	JG-35FD
Acoustic Scanning	
Multi-beam sonar	Imagenex DeltaT
Operating frequency	260kHz
Beam width	120° x 3°
Number of Beams	120°
Maximum range	100m
Range resolution	0.2% of range
Laser Scanning	
Lighting	LED Panel custom built
Camera	PointGrey Chameleon
	CMLN-13S2M/C-CS (mono)
	1.3MP, (max) 1296x964 at 18FPS
Operating resolution	640x480 at 25FPS
Laser	GreenLyte Green Laser 50mW
	MV-Excel/532/50/90/A/2000
Propulsion	
Surge thrusters	Tecnadyne 220W, 24VDC (2 sets)
Heave, Sway thrusters	Tecnadyne 100W, 24VDC (2 sets)
Computing power	
Command PC	Advantech PCM-3363D-1GS8A1E Intel AtomD525
Control PC	Advantech PCM-9382F-00A1E Intel Core2Duo
H8 MCU	Hitachi AE-3067F
Power	
Internal	Li-ion Custom designed $24V$, 10Ah (4 packs)
External	$24V$, $10A$ power source

6

Validation experiments

This chapter explains in detail the experiments performed to evaluate the proposed intelligent multi-resolution survey method using the developed landing vehicle. Various experiments were performed in steps to test and analyze different stages of the method and the vehicle hardware development. Experiments were conducted in a tank environment by creating different scenarios using artificially made objects. Initial experiments conducted were to test the performance of the landing vehicle. The hardware functionality of the vehicle, control system and the core software architecture were evaluated. The next set of experiments were performed to test and analyze the high resolution scanning stage of the system. The feature detection and landing algorithm implemented on the developed vehicle was evaluated in the tank on an artificially created landing area for its accuracy and computational time. Experiments were then conducted to verify the wide area acoustic scanning system and feature detection algorithm. The final part of this chapter provides details on the experiments used to evaluate the full survey method on an artificially generated seafloor scenario. The method was evaluated under different scenarios by changing the scanning waypoints and also for the same scenario by changing the scanning rules. For each set of experiments, the experimental details and results are provided along with analysis.

6.1 Experiments for vehicle hardware testing

The assembled vehicle was first tested for basic hardware and software functionality. Experiments were initially conducted to test the vehicle navigation sensors by connecting a tether and lowering the vehicle into the water. The vehicle was connected to an external computer using Ethernet and powered using an external power source. A graphical user interface (GUI) was built to operate the thrusters and view values from the sensors. The front end of the GUI prepared can be seen in the Fig. 6.1. The values measured include the vehicle roll, pitch, heading, depth, X-Y position, altitude, thruster revolution rate and battery voltages. The power switches to control the lights, laser and the navigational sensors were also tested by use of the GUI. The functionality to move the vehicle along all axis by setting the desired thrust value was also added to the GUI. The vehicle navigation sensor

data was collected in and out of the water to estimate the drift in the sensor measurement by keeping the vehicle stationary.

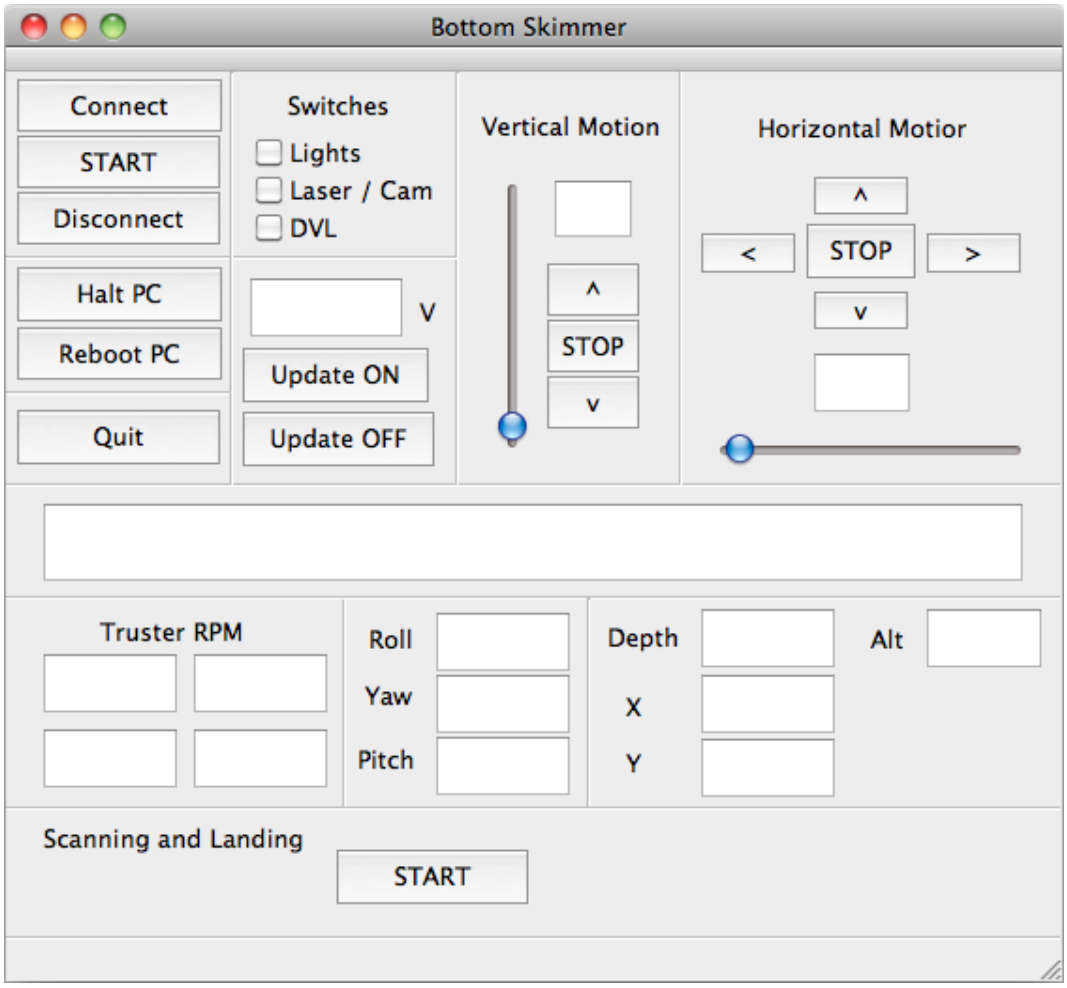

Fig. 6.1. GUI for pool testing; Communication was performed using wireless or tether using the GUI

The depth controller of the vehicle was tested by making it maintain a constant depth and changing between different depth levels. The controller was also tested for its depth control during forward motion. Heading controller was tested by making the vehicle maintain constant heading and changing between different headings. Once the gains of the controllers were tuned, waypoint navigation was tested. The navigation system of the vehicle was tested by deploying the vehicle in a tank environment. It was tested by giving random waypoints for navigation through a waypoint file. The vehicle navigation along a square shaped waypoint pattern can be seen in the Fig. 6.2. The vehicle was also made to perform depth control and landing on the tank floor using manual control which can also be seen in Fig. 6.3. The tail ends observed at the corners during the turning motion of the vehicle were caused due to mismatch in the vehicle centre of mass and the DVLs position

measurement point. The vehicle heading and depth controller was successfully tested to perform waypoint navigation.

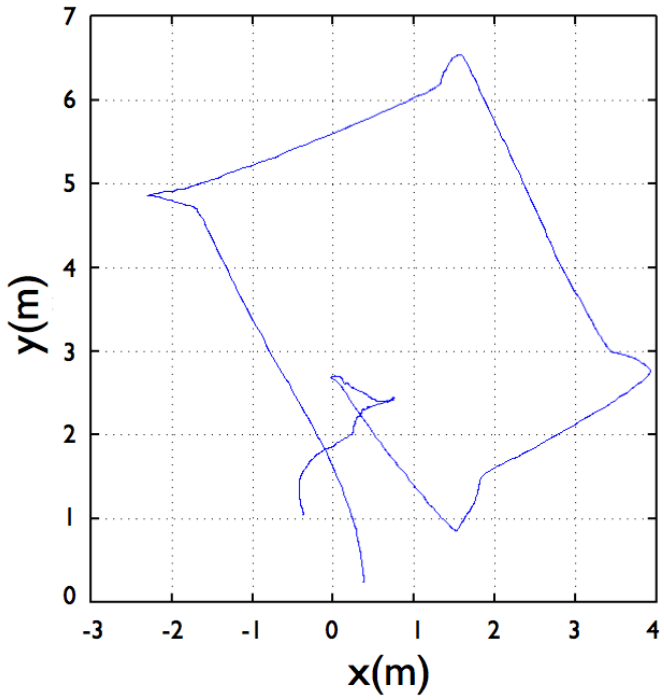

Fig. 6.2. Waypoint navigation testing of the vehicle conducted in a tank environment

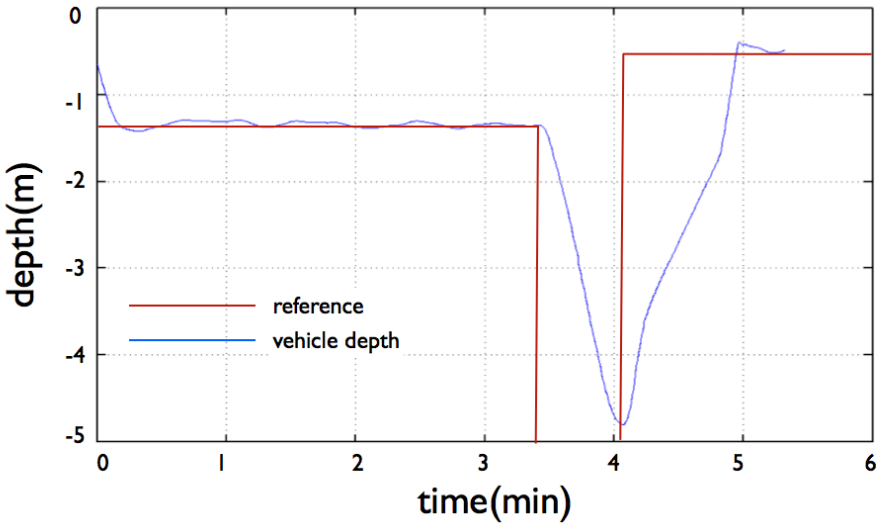

Fig. 6.3. Depth and landing control test conducted in a tank environment

6.2 Experiments for high resolution scanning

This section explains the experiments performed to evaluate various aspects of the high resolution scanning and landing system. The results obtained were analyzed to make evaluations about the hardware and software performance.

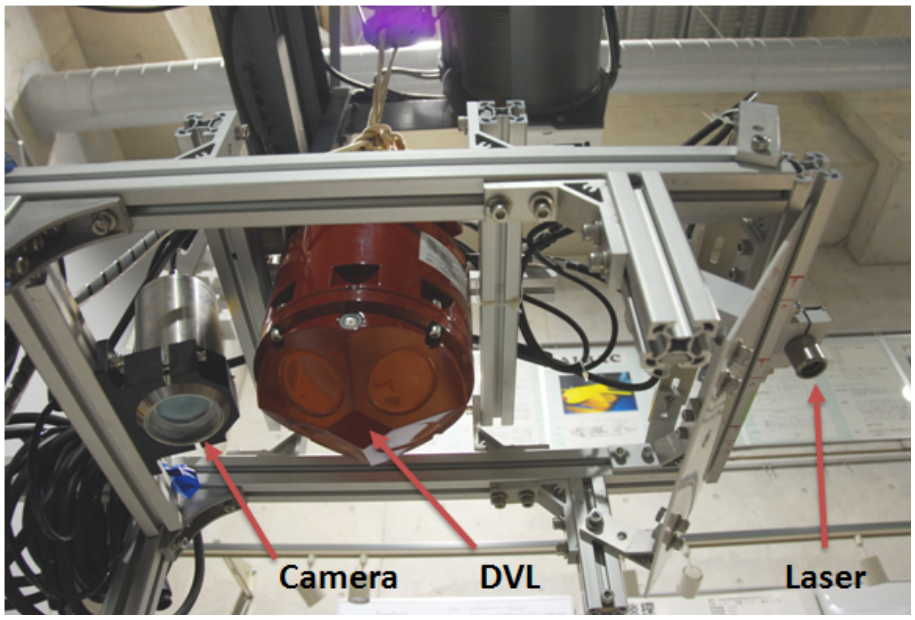

Fig. 6.4. Setup for high resolution scanning tests; Sensors for high resolution scanning mounted on a jig and towed using a crane

6.2.1 Testing the scanning hardware

Experiments were then conducted to evaluate the performance of the high resolution scanning system. The accuracy and resolution of the profiling system was computed by placing objects of known sizes on the bottom of the tank and scanning them. The high resolution scanning laser profiling system was mounted on an Aluminum frame as can be seen in the Fig. 6.4 to perform the experiments. The sizes of the objects estimated from the generated three dimensional point cloud were then compared to the original sizes. The results were also used to calibrate the profiling system. The Fig. 6.5 shows the laser scan and point cloud generated for a plastic object and a metal weight placed and scanned on the tank floor.

The average height measured of the plastic object using the laser scanning system was found to be 392mm while its actual height was measured as 398mm. The height of the metal weight was measured as 189mm while its actual height measured was 193mm. The laser scanning system was found to be reliable within 10% of the actual height of the bathymetry.

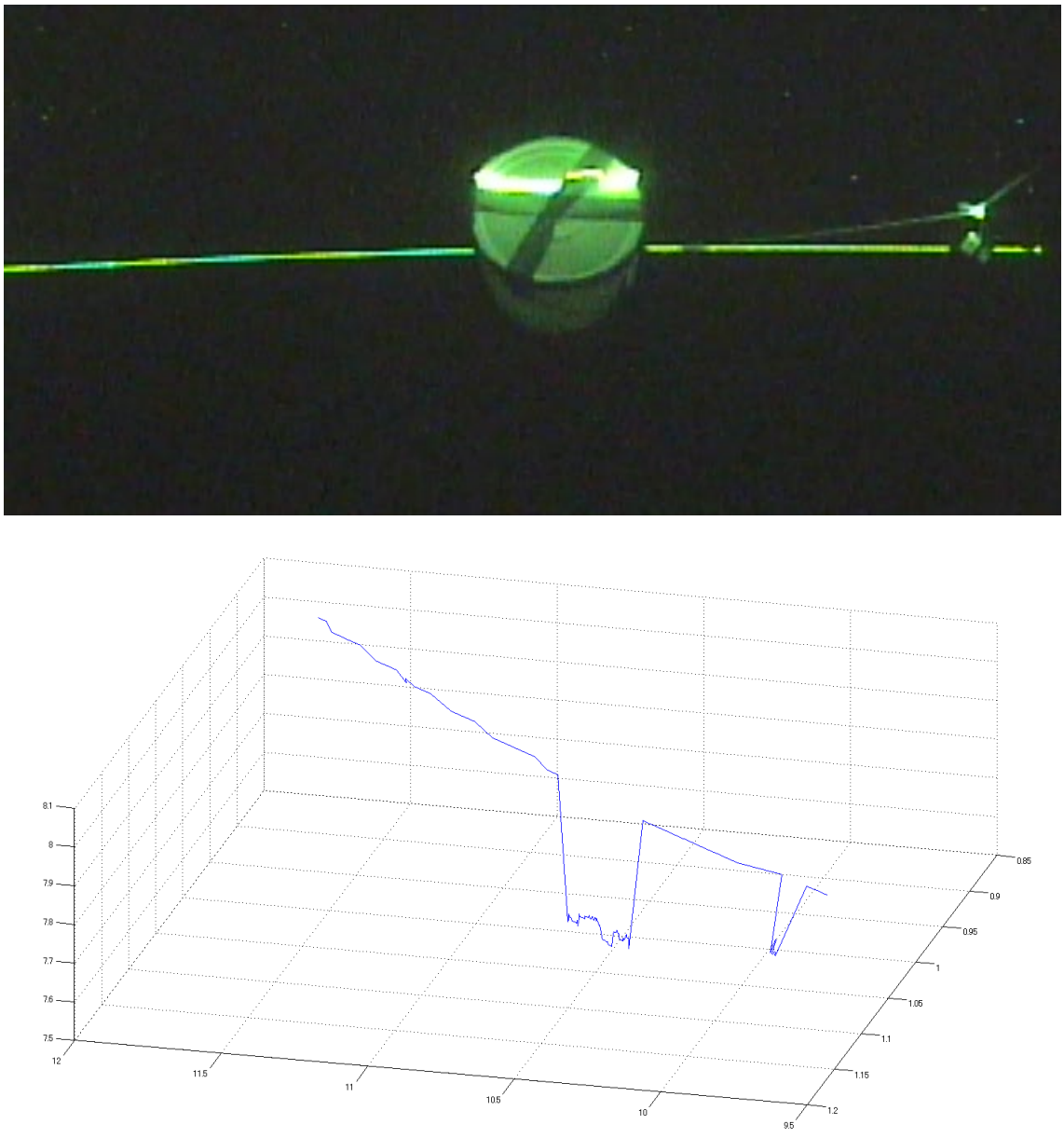

Fig. 6.5. Objects scanned on the seafloor for evaluating the performance of the laser profiling high resolution bathymetry generation system

6.2.2 Testing the landing system

The landing algorithm was evaluated for its ability to detect flat areas in the scanned bathymetry and select the appropriate landing coordinate and heading. The vehicles ability to perform landing on the selected coordinate with the correct heading was also tested. Experiments were conducted at the tank facility available at the IIS, The University of

Tokyo. An artificial terrain was constructed and lowered to the bottom of the pool for performing the experiments. The results obtained were then analyzed to test the accuracy of the system and occurrence of errors. The accurate determination of the landing coordinate and heading was evaluated by comparing the detected landing coordinate with the ideal landing point in the setup. Observations and analysis were made based on these results.

6.2.2.1 Setup of the experiment

The experimental tank used had dimensions of 8m×8m with a depth of 8m. Considering the tank dimensions, a 3m×2m area was considered for scanned for the landing experiments. To simulate the seafloor, artificial terrain was generated using wooden panels and corrugated sheets. The corrugated sheets have 90mm bumps which are the non-landing area while the flat wooden sheets make up landing patch. Each panel was approximately 1m × 1m in dimension. In total four corrugated sheets and two wooden panels were fixed together on a metal frame to form a 3m × 2m scanning surface. The wooden panels were placed between the corrugated sheets to have a landing area in the central region of the terrain. The terrain was lowered into the water at a depth of 3m from the water surface and secured using ropes. The constructed artificial scanning terrain can be seen in the Fig. 6.6.

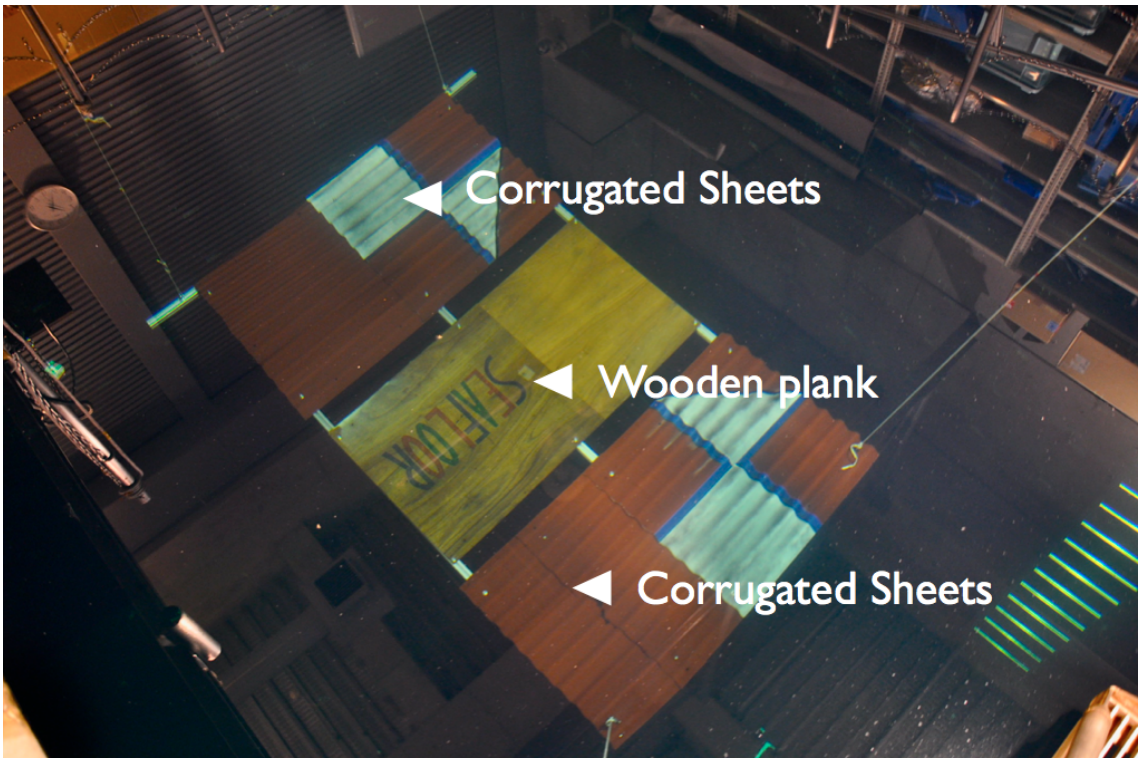

Fig. 6.6. Experimental scenario in the tank for performing high resolution scanning and landing

6.2.2.2 Experimental procedure

The AUV was placed at the water surface at one end of the artificial terrain and made negatively buoyant. The vehicle was tested with slight negative buoyancy. Scanning was performed along the length of the terrain which was initiated by a command from the external GUI using a tether. The tether also supplied power to the vehicle. The scanning altitude was set to 2m from the artificial terrain giving a laser swath of 2.2m. The heading orientation for the scanning path along the artificial terrain was measured prior to the experiment and given as the scanning heading for the vehicle control system. The scanning velocity was at 0.1m/s to obtain sufficient resolution in the laser profiles in the forward direction. Once in scanning mode, the vehicle would perform autonomous operation and execute the scanning and landing sequence. The terrain would be scanned across the length of the setup as shown in the Fig. 6.7 during which the vehicle would use its heading and depth controller to maintain course along the scanning path. A 4m length of the terrain would be scanned by maintaining constant heading and depth. Once scanning is completed the heading and depth would be maintained during which the landing algorithm would compute the landing coordinate and heading. Once the landing point was decided by the algorithm, the landing control system would navigate the vehicle to the selected coordinate and align the vehicle heading. The vehicle would then descend to landing point while maintaining its position and heading. In the shown setup, the vehicle would have to select the wooden plank as the landing area and generate the appropriate landing coordinate and heading.

6.2.2.3 Results of the experiments

The AUV performed autonomous scanning of the artificial terrain successfully and generated the three dimensional bathymetry as can be seen in Fig. 6.8. The vehicles control system maintained constant selected depth and heading While performing the scanning. The accurate reconstruction of the floor was then measured and compared to the actual setup. The comparison results can be seen in the Table .6.1. The landing algorithm computed the landing point correctly in 21 seconds, close to the ideal landing point. The intermediate steps involved in computing the landing coordinate can also be seen in the Fig. 6.9.

6.2.3 Observations from the experiments

The vehicle retraced back to the computed point and landed on the terrain surface successfully within the safe landing area by making use of its negative buoyancy as seen in Fig. 6.10. The error in the landing point was measured by comparing the ideal landing point coordinate based on the setup in the tank to the computed landing point which can also be seen in the comparison table. The landing heading computed and the ideal landing heading are also shown. From the experiments it was observed that the landing algorithm could successfully detect the coordinate and heading in a reasonable amount of time. During these experiments some of the code was still implemented in Matlab which increased the

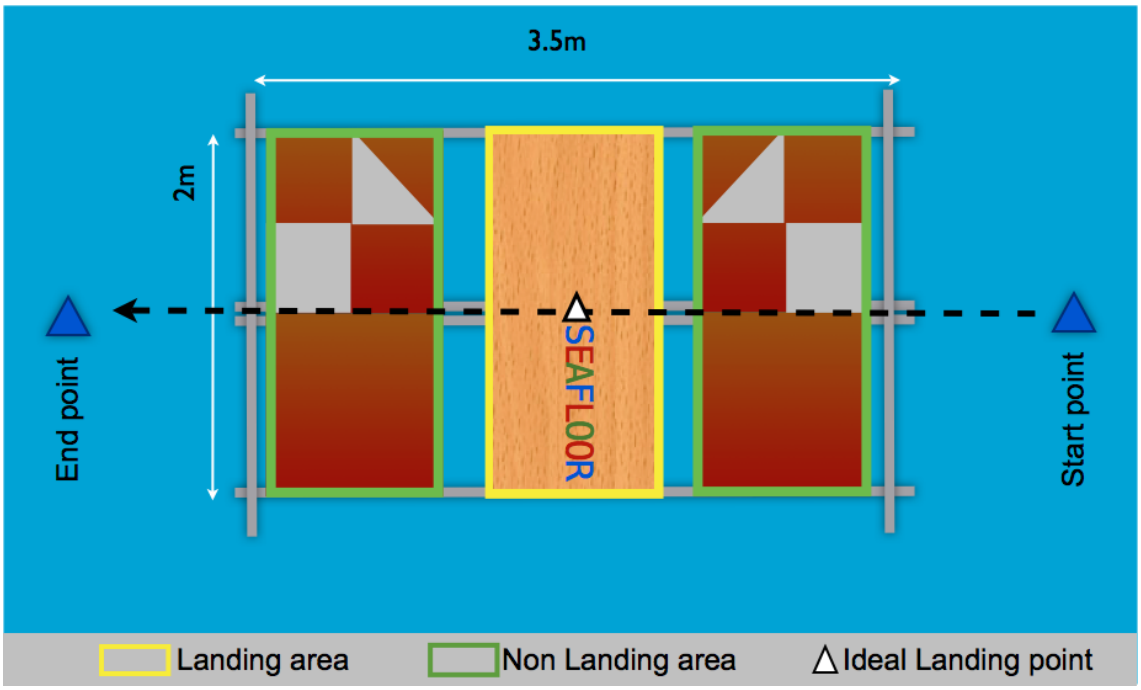

Fig. 6.7. Experimental scheme; Scanning direction and location of the ideal landing point

processing time of the algorithm. Although the landing point could be detected within of the actually landing point, it was observed that the algorithm is still sensitive to outliers which can cause significant error. Also the exact nature of the bathymetry generated was depending on the reliability of the laser line detection algorithm. The data collected was also used to enhance the algorithms and tune the camera hardware. During the experiments the vehicle was operated using a tether which created drag in the motion specially during turning. A few centimeters before landing the vehicle thrusters were cut off which caused the tether cable to change the heading.

Table 6.1. Comparison of measured values

Property	Actual	Measured
Height of Corrugations	90mm	85mm
X-point	0.5m	0.67m
Y-point	1.50m	1.41m
Heading after landing	90°	79°

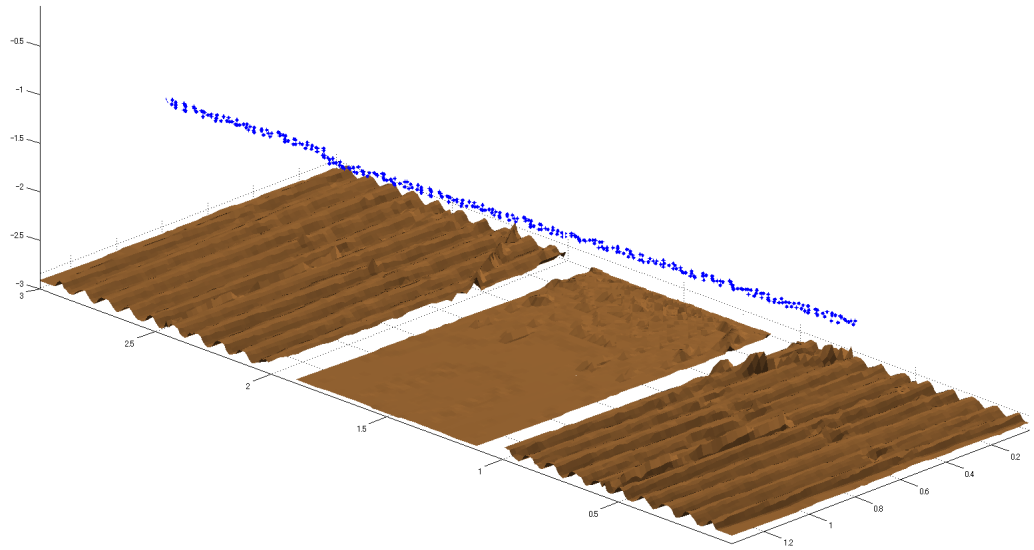

Fig. 6.8. 3D scanned bathymetry; Blue line: navigation path of the vehicle

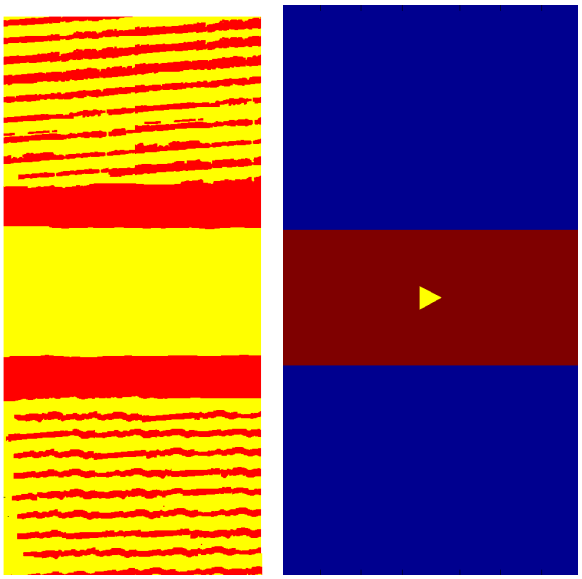

Fig. 6.9. Left: Detecting flat landing area, Right: Computed landing point

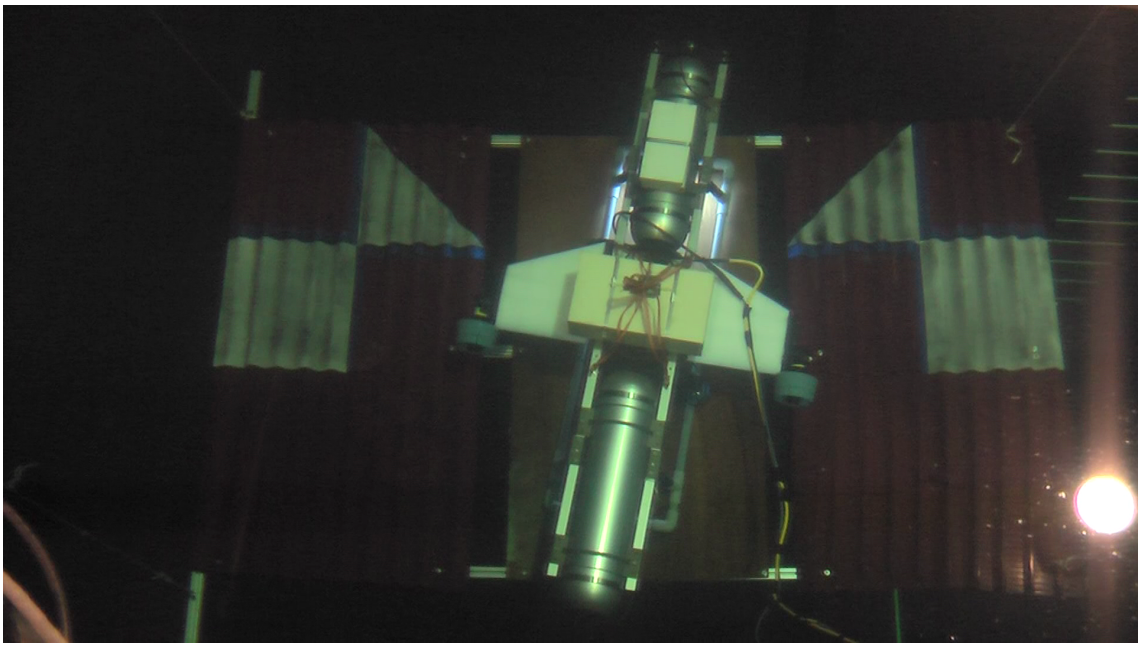

Fig. 6.10. Vehicle performing landing on the artificially created scenario

6.3 Experiments for wide area scanning

6.3.1 Testing the scanning hardware

Experiments were conducted at the pool available at the Chiba experimental Station belonging to the University of Tokyo for testing the scanning system mounted on the developed underwater vehicle. The scanning system was tested for its accuracy in generating the three dimensional bathymetry. Data collected from the scans was also used to tune the sonar gains. The navigation performance of the vehicle during scanning was also analyzed. As a scanning target, a 12m$\times$2.4m long wooden structure was constructed using Aluminum frame and wooden planks as can be seen in the Fig. 6.11. Each wooden plank used has a size of 1.2m $\times$ 2.4m.

The structure comprised of sloping areas and flat surfaces. Slopes of different angles were made. It was then lowered to the bottom of the pool at a depth of 5m. Scanning was performed from one end of the structure to the other lengthwise along the waypoints provided to the vehicle. The scanning altitude was set to 4m and the scanning speed was set to 0.3m/s. The waypoints were provided to the vehicle in a file and run as a test script which could be easily modified. Vehicle was operated in tethered mode. The vehicle successfully scanned the region between the points to collect the sonar data and log it. After scanning along the full length of the structure, bathymetry was generated as seen in Fig. 6.12. The generated bathymetry was compared to the previous measured dimensions of the structure. The reflection intensities of the scans observed during the experiments were used to adjust the scanning gain of the sonar for further experiments.

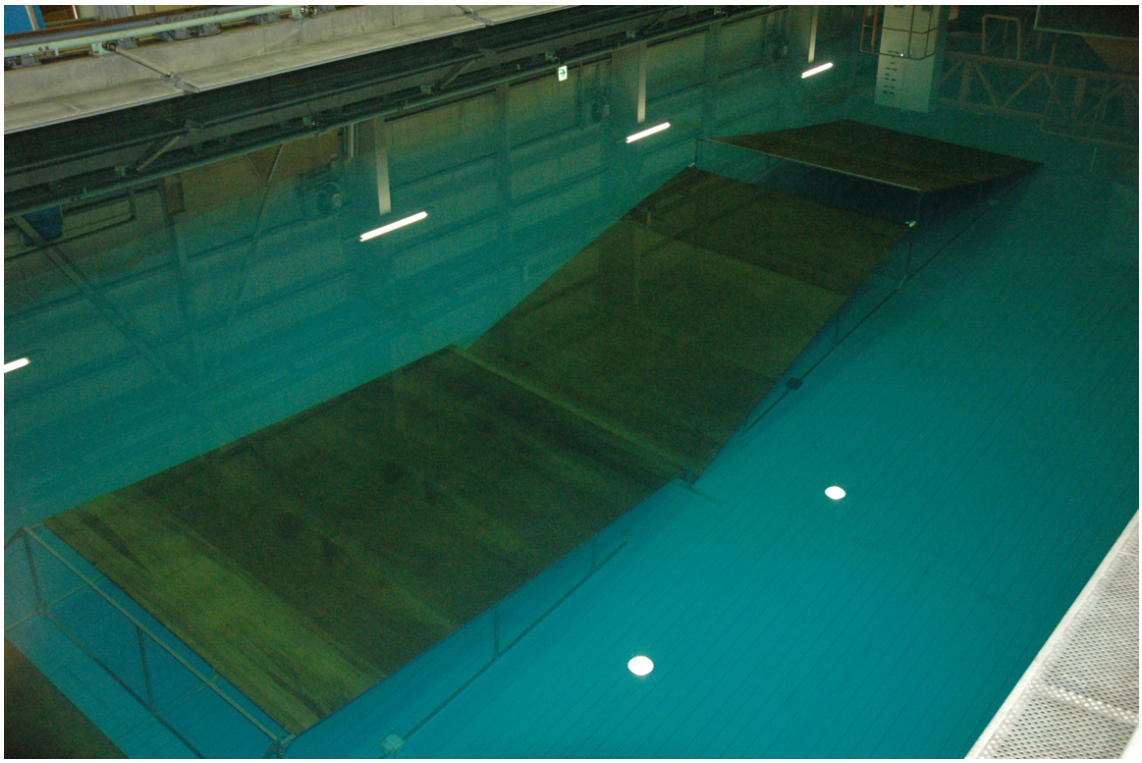

Fig. 6.11. Setup constructed for wide area scanning

6.3.2 Testing the bathymetry analysis algorithm

The main purpose of this experiment was to evaluate the wide area acoustic scanning stage of the survey method [48]. The scanning sensor was tested for its functionality. The program to generate three dimensional data was tested to generate real-time bathymetry after scanning the artificially generated terrain. The algorithm to detect features was implemented in semi real-time to process the scanned bathymetry and detect a suitable area for high resolution scanning. In this case, to evaluate the system, the area selected for high resolution scanning would be the flat area detected within the features. The way point generation algorithm was also implemented to generate coordinates where the vehicle would perform high resolution scanning for analyzing the performance of the system.

6.3.2.1 Setup of the experiment

The tank facility available at IIS, The University of Tokyo was used to perform these experiments on an artificially generated seafloor scenario. An artificial seafloor 3m $\times$ 2m in size was setup in the central part of the pool along with three 50cm $\times$ 40cm $\times$ 40cm boxes on either sides of this surface to be scanned and analyzed using the landing vehicle in real-time. These boxes could be detected with the sonar system used during the experiments. The artificial terrain was generated using wooden panels and corrugated sheets and plastic

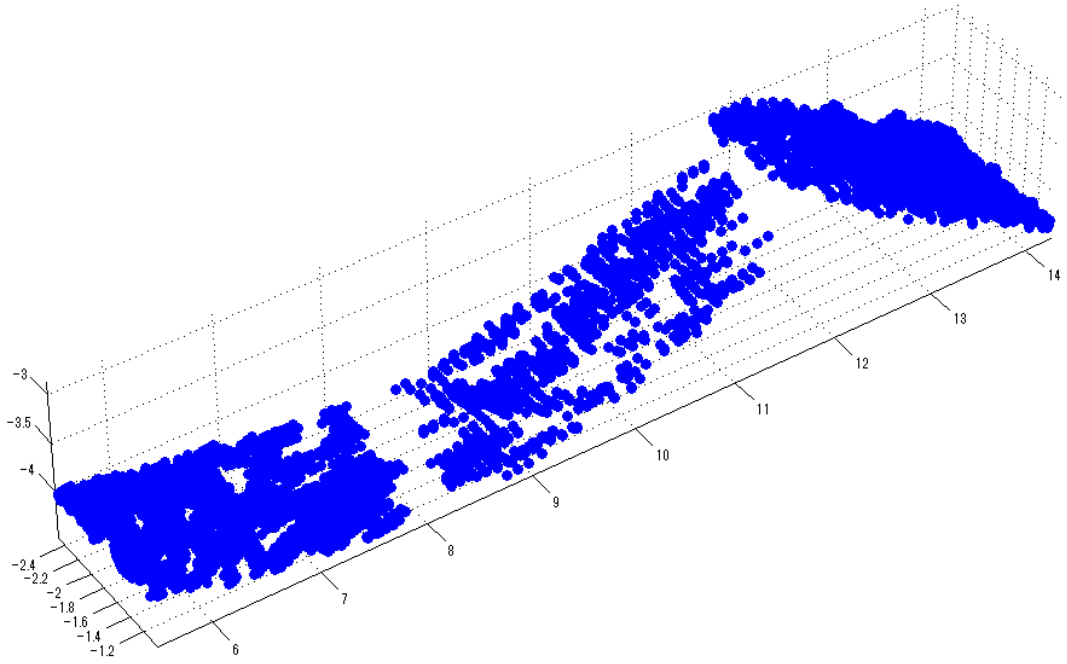

Fig. 6.12. Generated 3D point cloud

obstacles. The corrugated sheets had bumps of 90mm and was considered as the non landing area. These bumps could not be detected using the sonar system because of insufficient resolution. The resolution of the laser profiling system was high enough to detect them. Two corrugated sheets were fixed side by side in the central part of an aluminum frame. The wooden panels were placed on either ends of the terrain which were possible landing sites. A plastic obstacle was attached onto one of the wooden planks, which served as an obstacle to the landing operation. The orientation of the sheets was such that the landing area was normal to the direction of scanning. The terrain was lowered into the water at a depth of 8m from the surface and placed on the tank bottom, securing it using ropes. The setup placed at the bottom of the pool can be seen in the Fig. 6.13.

6.3.2.2 Experimental procedure

The AUV was made slightly negatively buoyant by 3Kgf and lowered into one end of the tank. The vehicle electronics were powered by an external tether but the thrusters were powered by an internal battery pack. The scanning sequence start command was given via an external computer through the GUI interface. For these experiments, the scanning altitude was set to 5m and the scanning speed was set to 0.25m/s. The scanning speed was kept so because of the small dimensions of the experimental tank so as to minimize the risk of accidents. These parameters and the initial and final waypoints were

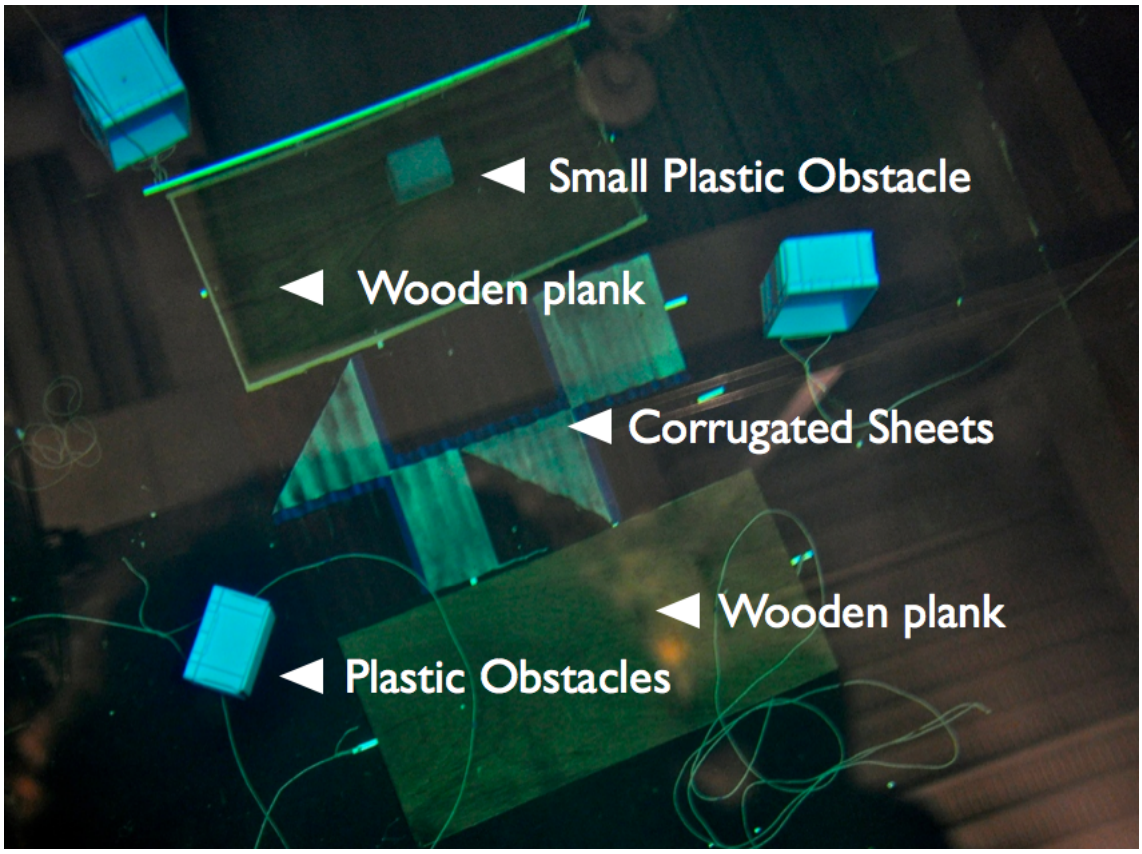

Fig. 6.13. Setup for evaluating the acoustic scanning and feature detection

provided to the vehicle though the initialization file. Once the command was given, the tank bottom surface would be scanned by the vehicle along the provided waypoints to capture acoustic measurements and generate bathymetry data after the scanning was completed. The data would be then analyzed autonomously using the algorithm to detect areas for high resolution scanning. For these experiments, the flat landing area between the features was to be identified by the algorithm as the high resolution scanning areas. The algorithm would then generate new waypoints for scanning the selected area. The vehicle would then scan the area between the selected waypoints using a laser profiling system to generate high resolution bathymetry. For scanning with high resolution, the scanning altitude was set to about 2m and the scanning speed was set to 0.1m/s. The bathymetry generated was then analyzed to see if the correct flat area was scanned by the vehicle.

6.3.2.3 Results of the experiments

The vehicle scanned the tank floor using the multi-beam sonar by following the provided waypoints accurately. The vehicle control system was successful in maintaining the proper heading and speed calculated by the navigation system. The sonar system functioned

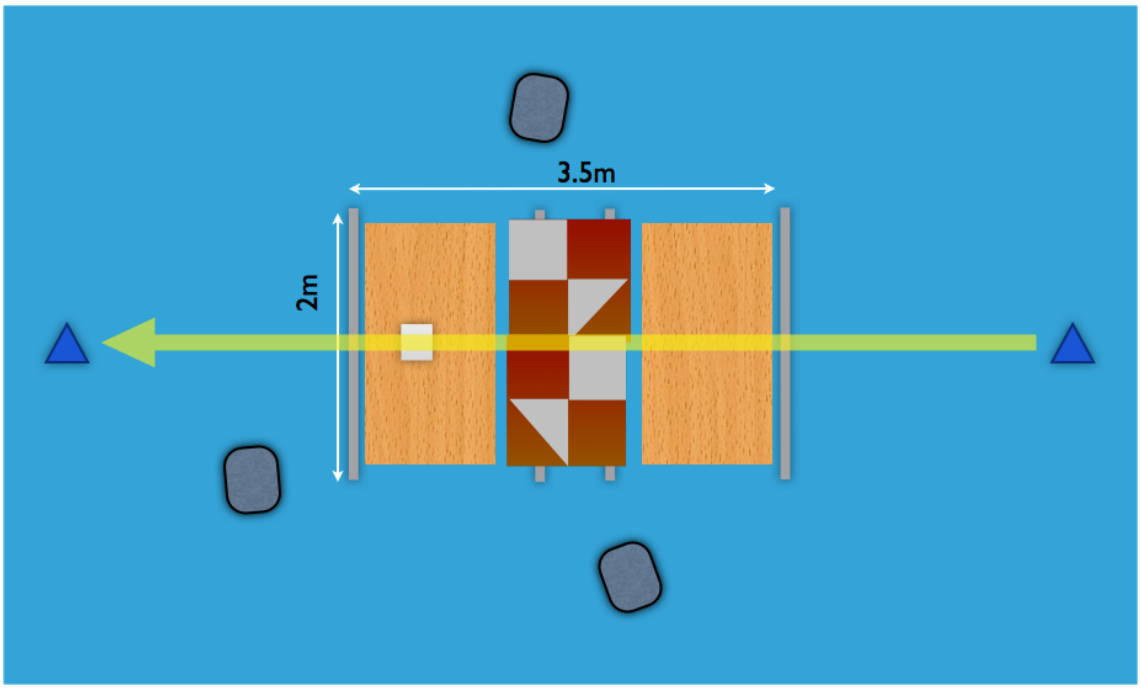

Fig. 6.14. Experimental procedure for wide area scanning

properly as well as the software driver. The bathymetry was generated after scanning was completed. The box features could be spotted in the sonar data but not the corrugated sheets of the wooden planks.

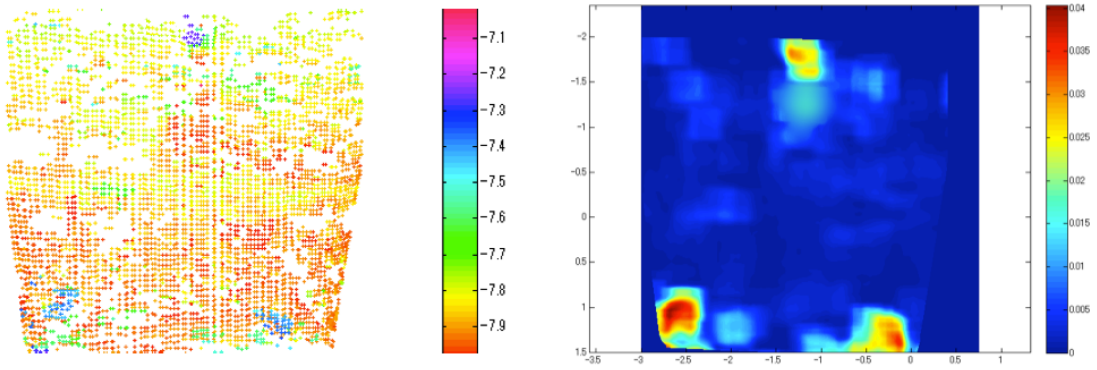

Fig. 6.15. Wide area data collection and analysis; Left: Scanned point cloud, Right: Detected features

From the Fig. 6.15 it can be seen that the algorithm correctly identified the features from the scanned bathymetry. The flat area was identified so as the rectangular boxes. The

algorithm also detect the correct region between the boxes as the high resolution scanning area as required by the survey. The waypoints generated to scan the region can be seen in the Fig. 6.16.

The high resolution bathymetry scanned between the generated waypoints can be seen in the Fig. 6.17. The fine features in the artificial terrain such as the rope, the plastic box and the ripples on the corrugates sheets are clearly visible on the scanned bathymetry. As it can be seen, the area between the large plastic boxes was rightly selected for scanning. To evaluate the selection process, based on the placement on the boxes, the ideal scanning area of a particular size was evaluated. This was then analyzed in comparison to the area selected by the algorithm.

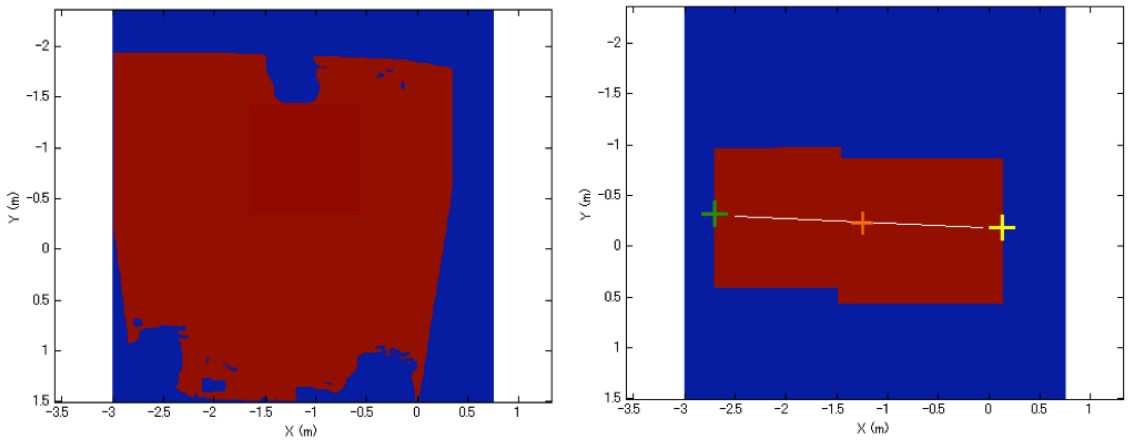

Fig. 6.16. Left: Flat area detected, Right: Scanning area selected

The vehicle successfully identified the flat area between the objects as the area for high resolution scanning. The nature of the objects was correctly identified from the wide area bathymetry. However, since the tank used was small, sonar reflections from the side walls caused the data to become full of outliers. The outliers in some of the trials generated errors in the variance map causing the wrong area to be identified for high resolutions scanning. A small filter was later implemented based on depth and variance to reduce the outliers. It was difficult to operate the vehicle at a higher speed due to safety concerns.

6.4 Experiments for evaluating the survey method

This section is about the main experiments performed to evaluate the proposed method. The experiments mentioned in the previous sections were used to develop, edit and enhance the algorithms and to tune the parameters of the scanning system. For these experiments, the vehicle was operated with the tether with no external monitoring or communication. The data collected from the vehicle after completion of the experiments was plotted and analyzed.

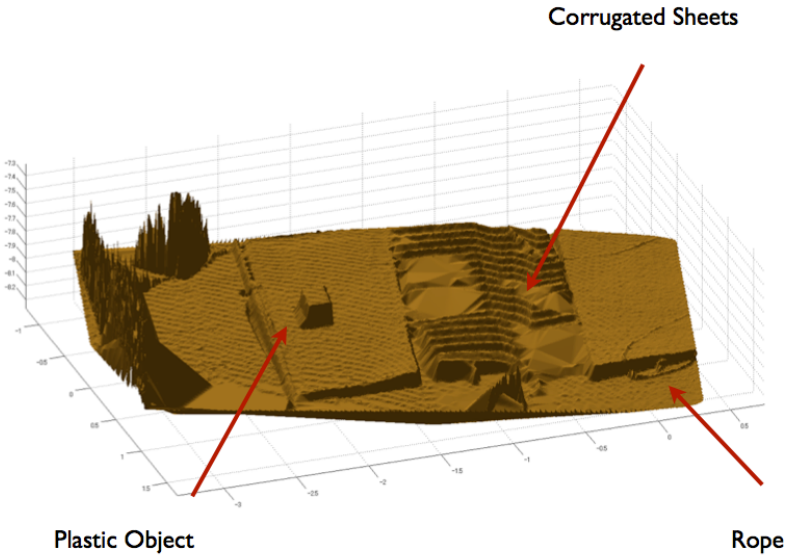

Fig. 6.17. High resolution bathymetry scanned between the generated waypoints

6.4.1 Objectives of the experiments

The experiments were performed to have an overall analysis of the survey method. Different stages of the method were analyzed in detail under different experimental scenarios. The main objectives of the experiments were to test the decision making process for changing the scanning resolution from acoustic scanning to high resolution scanning.

The main objectives of the experiments are as follows:

- The wide area scanning stage was evaluated for its robustness and correctness in scanning the bathymetry. The algorithm to detect features was evaluated for its ability to detect the features correctly and to select the appropriate high resolution scanning area based on the rules of the survey. The algorithm was also tested for its computation time.
- The waypoint generation algorithm was evaluated to generate suitable waypoints for scanning the selected region with high resolution. The computation time of the algorithm was also measured.
- The accuracy of the high resolution scanning stage in generating the correct bathymetry was tested. The area detected by the landing algorithm as the flat landing area was analyzed and compared to the ideal scenario case. The feature detection algorithm was also tested.
- The landing area decision making algorithm was evaluated for its selection of the most suitable area based on the survey rules.

To perform analysis on the above mentioned points, experiments were performed in a tank environment at the Chiba Experimental Station belonging to the The University of Tokyo. Setup was made on the tank floor using artificially created objects. Experiments

were performed on the same scenario by changing the survey rules and evaluating the change in the generated multi-resolution map generated by the system. Experiments were also performed on the same scenario by changing the initial scanning waypoints of the wide area scan to analyze its influence on the area selected for high resolution scanning based on the same survey rules. The experimental tank used for the experiments had a width of 10m, length 50m with a constant depth of 5m. Setup was made on the tank floor using artificially built features constructed using aluminum frames, wooden panels, plastic and metal objects to create different scenarios. Various structures were constructed whose dimensions have been mentioned in Table. 6.2. The objects used for the experiments can be seen in the Fig. 6.18.

The altitudes and speeds for scanning using the multi-beam sonar and laser profiling system were provided in the initialization file. The altitude for acoustic scanning was set at 4.25m. The horizontal resolution obtained was about 12.5cm. The sonar range was set to 10m with a vertical resolution of 2cm. The refresh rate obtained was 5 scans/second. The vehicle scanning speed was set at about 0.4m/s to obtain a forward resolution of 12.5cm. The Micron DST sonar, mounted on the front of the vehicle for obstacle avoidance was operated with its scanning sector set to 90° and range of 5m. The laser used for profiling the seafloor has a fan angle of 64° in water. The camera mounted on the vehicle has an inclination of 68° to the vertical with a baseline of 845mm between the camera and laser. The scanning altitude for laser profiling was set at 3.0m. Images from the camera were captured at 20fps at 640x480 pixel resolution. The horizontal across track resolution obtained was about 5mm. The vertical resolution obtained was 8mm. To have a sufficient resolution of 5mm in the forward direction, the scanning speed was set to 0.1m/s.

The initial and final points were also provided to the vehicle in the file along with the survey rules. For this particular scenario, the rules of the survey were to find ridge like features, land on the highest flat area of the feature and also identify and land on a bottom next to the highest flat area. These rules were encoded into the rule file and also uploaded in to the vehicles main computer. The vehicle then performed the survey based on these rules to detect the most suitable location for high resolution scanning based on the features identified.

6.4.2 Experimental Scenario A

The first scenario was made to simulate a terrain where the vehicle has to perform seafloor observation after landing on the top and bottom of the feature for comparison of the observed data. Such scenario can be seen in cobalt rich crust slabs along the edges of underwater sea-mounts where the thickness measurements of the manganese crusts have to be obtained and compared. Another application of this scenario would be for radiation measurements in areas on the seafloor where features have been observed. In these areas it is essential to measure the radiation levels on the top and bottom of the feature to analyze the effects of the features on the generation of hotspots.

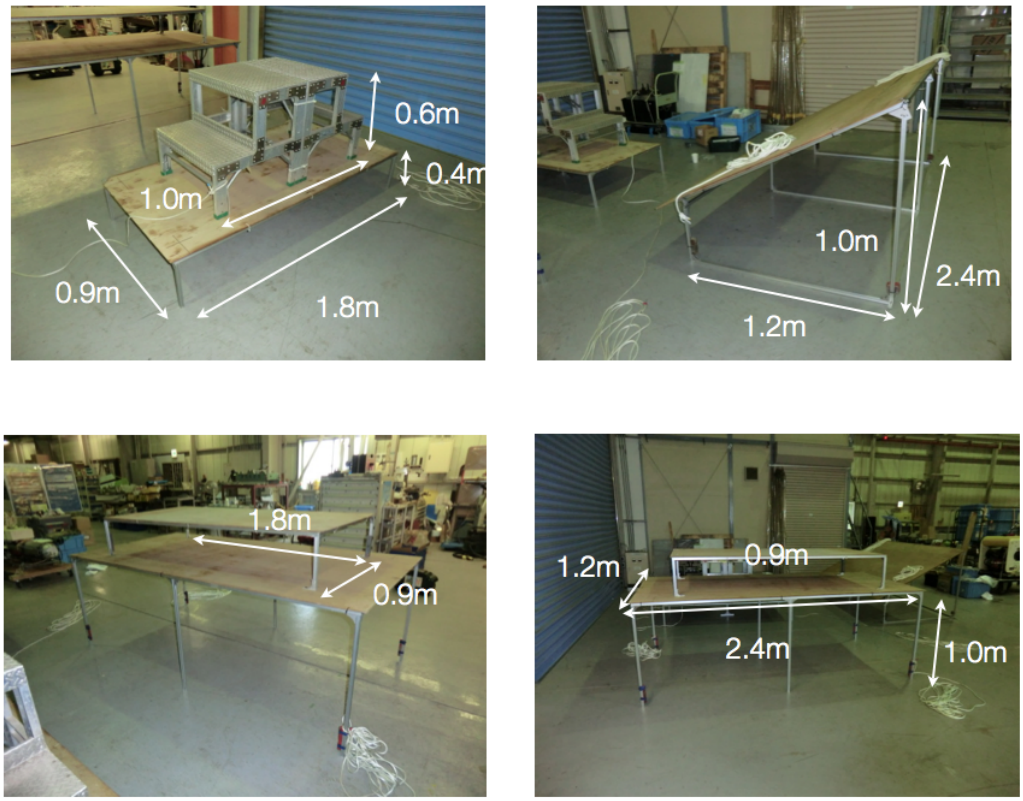

Fig. 6.18. Objects created for generating scenarios

6.4.2.1 Scenario setup and initialization

Setup was made on the tank floor using the objects built as described in Table. 6.2. The final configuration of the setup can be seen in the Fig. 6.19. The setup was spread over an area of 15mx10m.

Table 6.2. Objects used for generating the Scenario A

Object Type	Name	Dimensions
Slope	A	2.4m x 1.2m at 45°
Large flat platform	B	2.4m x 1.2m x 1.0m
Small flat platform	C	1.8m x 0.9m x 0.5m
Small flat platform	D	1.8m x 0.9m x 0.5m
Blue box	E	0.9m x 0.6m x 0.6m

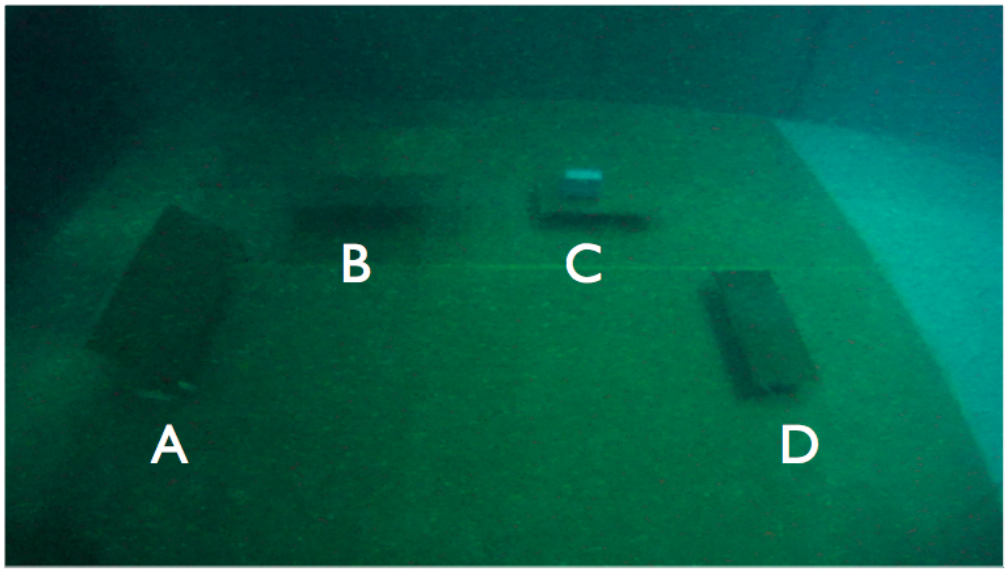

Fig. 6.19. Experimental scenario on the tank floor

6.4.2.2 Experimental scheme

For this experiment the vehicle was operated in a fully autonomous mode without tether. The initial and final waypoints for wide area acoustic scanning were given to the vehicle though the initialization file. The safe area box was also defined. The survey rule file was also provided to the vehicle. Experiments were repeated by changing the initial scanning waypoints but keeping the same rule file to see its influence on the multi-resolution map generated. The vehicle would scan the survey area by following the waypoints using the multi-beam sonar. The bathymetry would be then be generated automatically after the scanning is completed during which the vehicle would remain stationary and maintain its depth and heading. The data would be analyzed to detect the features on the seafloor and select the area for high resolution scanning based on the rules. The algorithm would then generate the waypoints for scanning with a high resolution. The vehicle would then scan the selected area from a lower altitude and speed as mentioned in the initialization file using a laser profiling system. The high resolution bathymetry would then be analyzed again to detect the features in more detail and also to detect landing areas. The vehicle would then perform automatic landing on the selected landing spot. The survey scheme for the experiment is shown in the Fig. 6.20

6.4.2.3 Experimental results

The multi-resolution map generated during the experiments can be seen in the Fig. 6.21. The depth plot can be seen in the Fig. 6.22. As seen, the vehicle autonomously scanned (blue track) the area between the given initial waypoints acoustically to generate a point

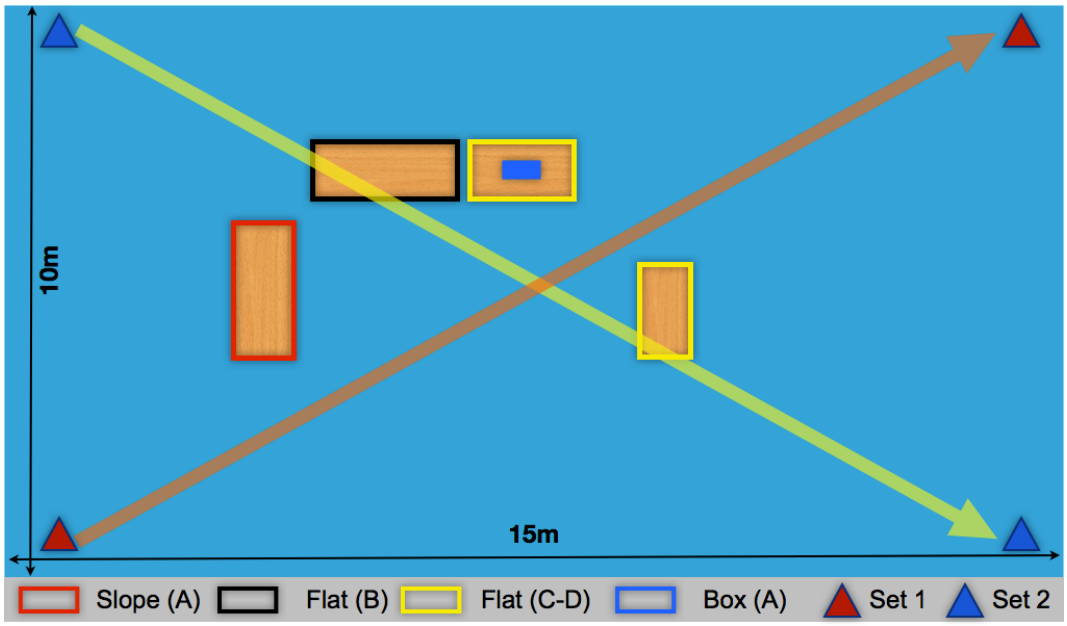

Fig. 6.20. Scenario A experimental scheme

cloud. This data was automatically analyzed and the algorithm was successful in generating suitable waypoints for scanning the correct area with high resolution based on the survey rules. High resolution scanning was then performed (red track) along the new waypoints and this data can be seen overlaid over the acoustic scan. The high resolution bathymetry data was also successfully analyzed for identifying the attributes of the features on the tank floor and detecting the flat area on the top of the table as the landing area. To complete the mission based on the rules, the algorithm successfully generated new waypoints for scanning more area around the feature with high resolution for finding additional landing points. The landing algorithm correctly determined landing points at two locations on the top of the larger table (Point A) and at the bottom of the table (Point B) on the tank floor along with landing orientations. Autonomous landing was finally performed at these points (orange track). The experiment was repeated by changing the initial scanning direction and the vehicle was found to successfully generate a similar map in each case. The vehicle landed on the tank floor and the table can be seen in the Fig. 6.23.

6.4.2.4 Analysis of results

The experiments evaluated the concept of adaptive multi-resolution survey. The different modes of operation of the vehicle performed without any errors to complete the overall survey. The vehicle successfully generated the wide area map by scanning with a constant speed and altitude automatically. In the absence of the tether, the vehicle motion was smoother and waypoints could be reached without any difficulty. The algorithm to analyze the wide area bathymetry detected the correct area as required by the survey rules. The area was the connected tables.

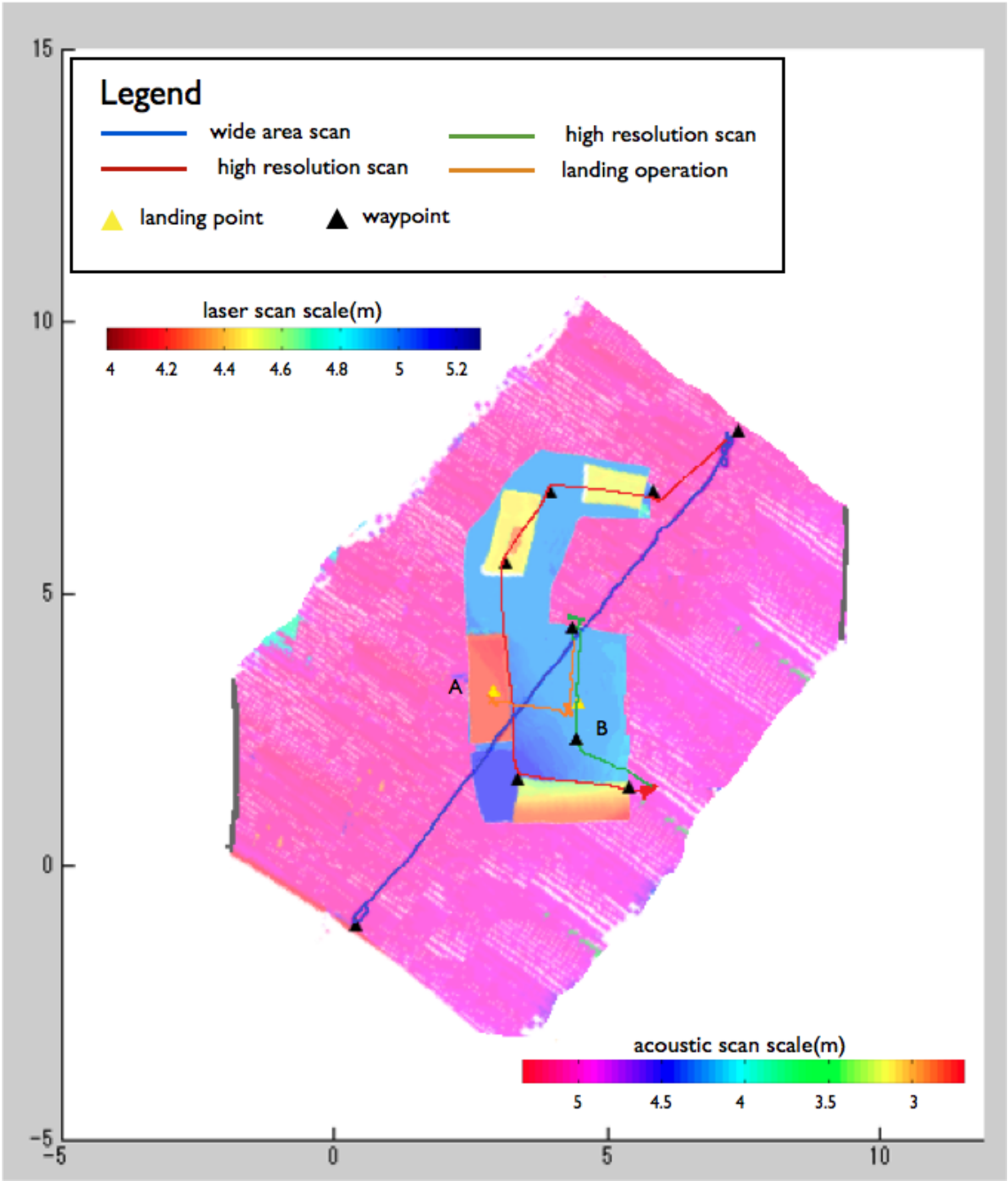

Fig. 6.21. Multi-resolution map generated of scenario A

The high resolution scanning was also successfully performed automatically at this selected area on the newly generated waypoints. The landing algorithm could detect the landing areas as required by the survey for data comparison. The landing system managed

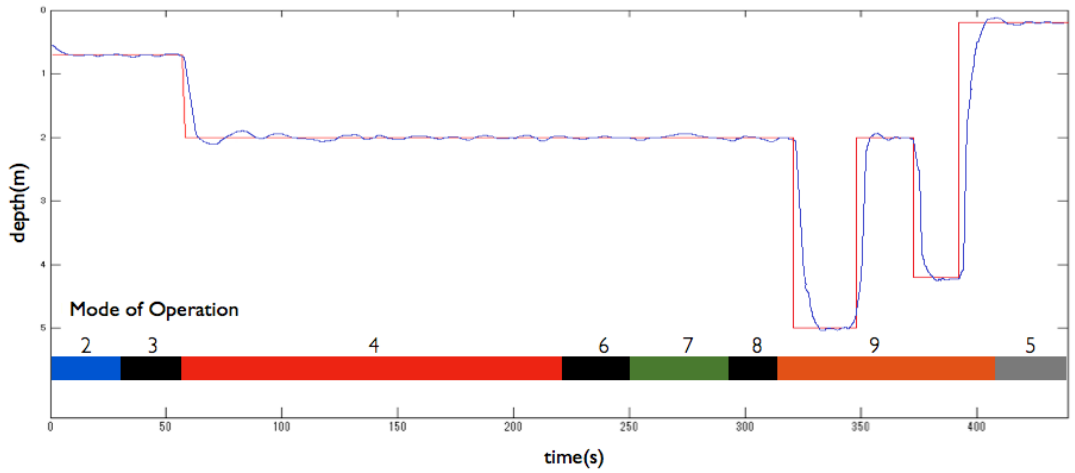

Fig. 6.22. Depth plot of the experimental scenario A

Fig. 6.23. Vehicle landing on the tank floor and the table

to perform autonomous landing at these areas successfully. The small tank environment made it difficult to test the system over larger scenario. The effect of the drift in the navigation sensors and the generated bathymetry was small and could not be thoroughly analyzed for very wide area surveys. The outliers and errors in bathymetry affected the bathymetry significantly. The reflection of acoustic signal from the tank walls also caused error but it was reduced by having a range filter. The vehicle was operated at a slower speed than possible because of safety reasons. Also since the vehicle did not scan the entire table feature accurately, the landing point generated was not exactly in the central part of the table.

Mode	Time(s)	Distance(m)	Speed(m/s)	Activity
2	30.6	10.87	0.355	Wide area scanning
3	15.3			Wide area processing
4	176.2	14.80	0.084	High res scanning
6	28.5			High res processing
7	42.2	3.67	0.087	High res scanning
8	20.1			Landing point calculation
9	93.9			Autonomous landing

Fig. 6.24. Timings for different experimental steps during scenario A

6.4.3 Experimental Scenario B

The second scenario was made to simulate a terrain where the vehicle has to obtain seafloor observation or generate high resolution color bathymetry around a feature. Such scenario can be seen in areas rich with hydrothermal vents where the vehicle has to detect the vents from a wide area scan but obtain high resolution 3D bathymetry, photo-mosaics by scanning with a high resolution. The vehicle might also need to take chemical samples around these areas.

6.4.3.1 Scenario setup and initialization

To simulate a similar structure on the tank floor, setup was made using some of the objects constructed as mentioned before. The dimensions of the objects used to prepare the setup can be seen in the table 6.3. The setup was made over an area of 15mx10m.

Table 6.3. Objects used for generating the Scenario B

Object Type	Name	Dimensions
Slope	A	2.4m x 1.2m at 45°
Large flat platform	B	2.4m x 1.2m x 1.0m
Small flat platform	C	1.8m x 0.9m x 0.5m
Small flat platform	D	1.8m x 0.9m x 0.5m
Metal Steps	E	1.0m x 0.6m x 0.6m

6.4.3.2 Experimental scheme

The initial and final waypoints for wide area acoustic scanning were given to the vehicle though the initialization file. The safe area box was also defined. The survey rule file

was also provided to the vehicle. Experiments were repeated by changing the rules of the survey file but keeping the same scenario to see its influence on the multi-resolution map generated. The vehicle would scan the survey area by following the waypoints using the multi-beam sonar. The bathymetry would be then be generated automatically after the scanning is completed during which the vehicle would remain stationary and maintain its depth and heading. The data would be analyzed to detect the features on the seafloor and select the area for high resolution scanning based on the rules. The algorithm would then generate the waypoints for scanning with a high resolution. The vehicle would then scan the selected area from a lower altitude and speed as mentioned in the initialization file using a laser profiling system. The high resolution bathymetry would then be analyzed again to detect the features in more detail and also to detect landing areas. The vehicle would then perform automatic landing on the selected landing spot. The survey scheme for the experiment is shown in the Fig. 6.25. The rules of the survey were to find the larger feature and land along the longest sides of the feature to obtain seafloor measurements.

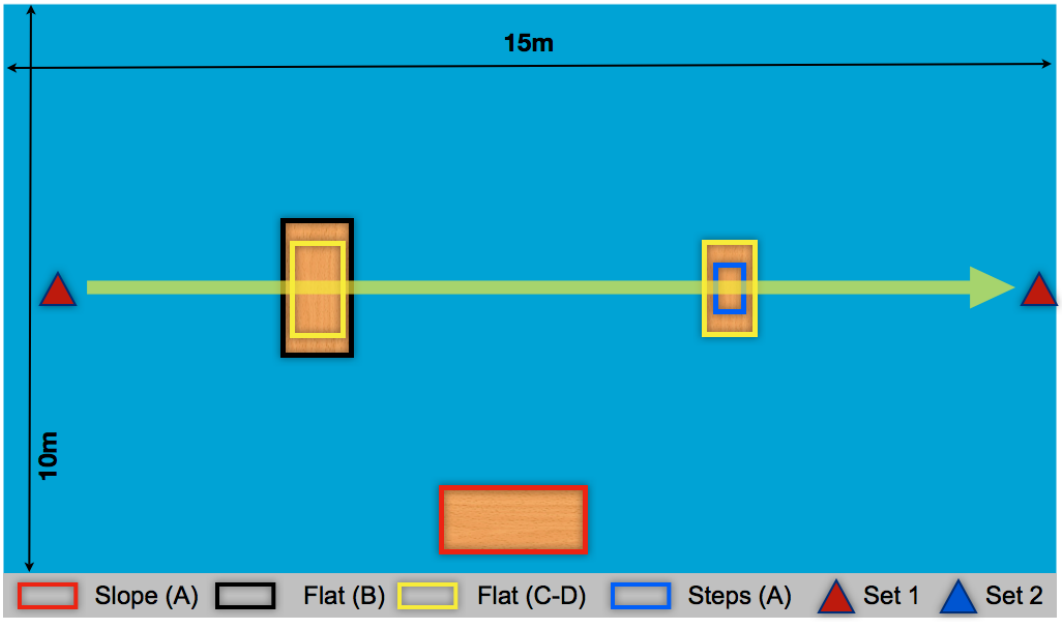

Fig. 6.25. Scenario B experimental scheme

6.4.3.3 Experimental results

The multi-resolution map generated during the experiments can be seen in the Fig. 6.26. The depth plot of the vehicle during the experiment can be seen in the Fig. 6.27. As seen, the vehicle autonomously scanned (blue track) the area between the given initial waypoints acoustically to generate a point cloud between the initially provided waypoints. This data was automatically analyzed to identify the larger of the feature. The algorithm was successful in generating suitable waypoints for scanning the correct area around the large table with high resolution based on the survey rules.

High resolution scanning was then performed (red track) along the new waypoints. This was overlaid on the wide area map to show the area with high resolution. The high resolution bathymetry data was also successfully analyzed for identifying the attributes of the features on the tank floor and detecting the flat area around the larger table. To complete the mission based on the rules, the algorithm successfully generated new waypoints for scanning more area around the feature with high resolution for finding additional landing points. Additional region on the upper side of the table had to be scanned for obtaining sufficient bathymetry to detect a landing point (green track). The landing algorithm correctly determined landing points at two locations on either side of the table. Autonomous landing was then performed at these locations (orange track).

6.4.3.4 Analysis of results

The experiments evaluated the concept of adaptive multi-resolution survey. The vehicle successfully generated the wide area acoustic bathymetry map of the tank setup. The algorithm was successful in identifying the correct feature for high resolution scanning. The acoustic reflection from the tank walls introduces noise in the bathymetry generated which affected the results in some of the trials. The navigation system of the vehicle was successful in maintaining the right heading and depth for scanning. The area scanned was small and the time required for the experiment to be performed was short. The sensor drifts were not significant. The high resolution scanning was successfully performed at the larger table. The landing points were correctly generated on either sides of the table. In some trials the landing point was incorrectly identified due to wrongly generated bathymetry. This was caused due to the refection of the laser from the metallic part of the Aluminium frame resulting in error in laser line detection. Overall the system was found to be reliable and experiments were repeated many times to successfully identify the correct region for scanning and landing based on the rules.

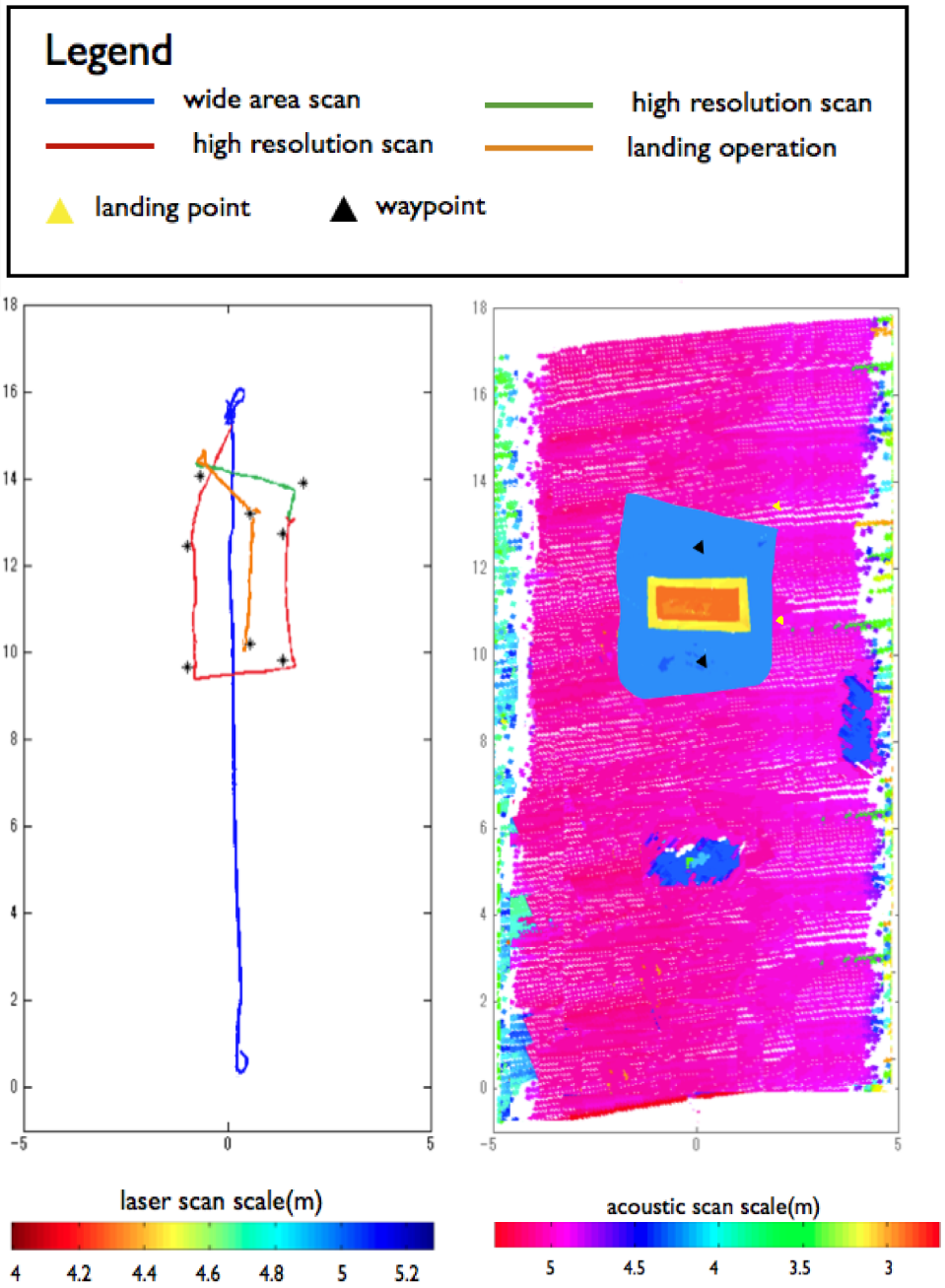

Fig. 6.26. Multi-resolution map generated of scenario B

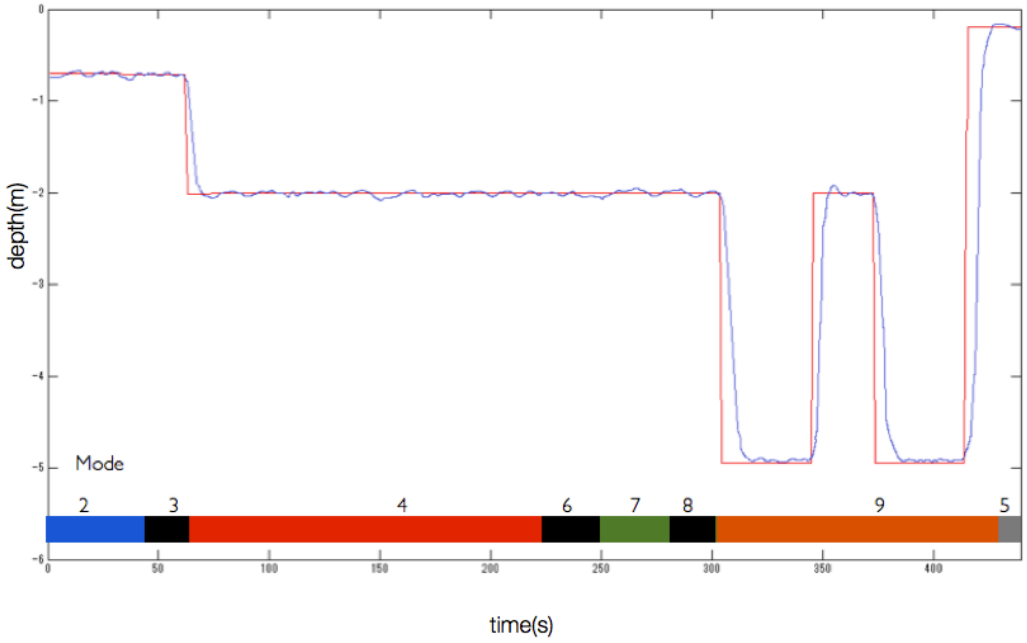

Fig. 6.27. Depth plot of the experimental scenario B

Mode	Time(s)	Distance(m)	Speed(m/s)	Activity
2	43.5	15.8	0.36	Wide area scanning
3	18.8			Wide area processing
4	158.2	13.6	0.086	High res scanning
6	25.2			High res processing
7	31.7	2.88	0.091	High res scanning
8	20.6			Landing point calculation
9	126.5			Autonomous landing

Fig. 6.28. Timings for different experimental steps during scenario B

7

Observations and discussions

This chapter provides observations based on the results obtained from the experiments performed in the tank environment as seen in Chapter 6. Observations are made based on different aspects of the survey method to evaluate its performance. The final part of this chapter provides discussion on practical difficulties in implementation of the method for real ocean applications.

7.1 Survey time

The time required to perform the survey and its advantages are analyzed in this section. In the Scenario A of the experiments, the total distance covered by the vehicle during wide area scanning was found to be about $100m^2$. The vehicle took about 407 seconds to perform the survey. If the complete scan was performed using high resolution without landing, it would take over 600 seconds.

The algorithm to analyze the wide area bathymetry would take about 77 seconds to process an area of 50m x 10m. This is considering a sonar system with swath of 10m and a forward transit of 50m. Although the time required is not extremely significant, during this time the vehicle will have to hover above its last position. This may be possible in a tank environment but not possible in real ocean environments due to currents. Also during this period, the drift from sensors such as IMU and DVL would be significant causing further errors in data processing. To avoid this problem, the area will have to be scanned in small sections. Another solution would be to process the data in real time along with data acquisition.

7.2 Landing point error

The landing point calculated by the landing system on the table top is analyzed for estimating the accuracy and difficulties. The ideal landing point on the top of the table is the centre of the table. The table used is made from plywood with dimensions $2.4\text{m} \times 1.2\text{m}$. With these dimensions, the landing point would be 1.2m x 0.6m at the centre of the table.

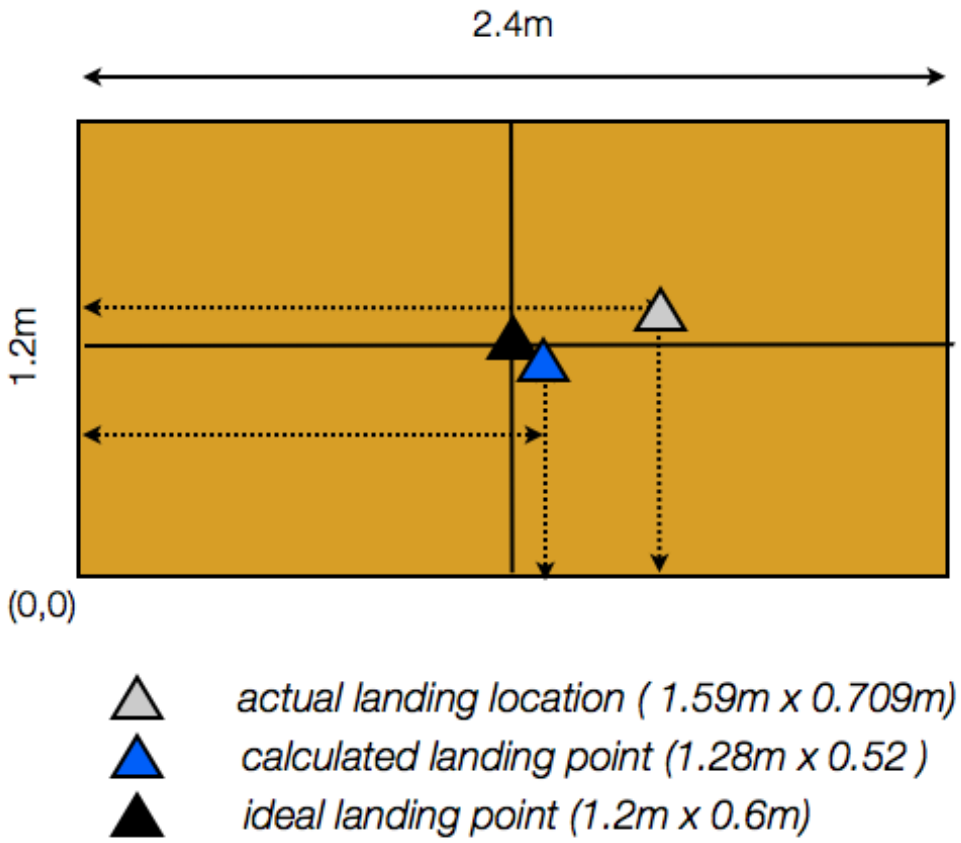

Fig. 7.1. Landing algorithm error estimated from tank observations

The landing algorithm calculated the landing point at 1.28m×0.52m. The error in the value of the landing point calculated by the system is because of the green line laser detection, the minimum 8mm resolution of the system and the the vehicle navigation path. It was also observed that the vehicle missed a part of the table while performing scanning causing a slight shift in the landing point.

The landing point where the vehicle actually performed landing after retracing was found to be worse than the computed point. The final landing point of the vehicle was 1.59m×0.709m. This gives an error of 0.39m in the x direction and 1.09m in the y direction. The reasons for errors in the landing point were attributed to two parameters, the sensor drift as well as the navigation accuracy of the vehicle. The time required for the vehicle between computing the landing point and final landing was over thirty seconds. During this time, the DVL sensor would have drifted causing an error in the landing point finally retraced. Furthermore, the vehicle switches off its thrusters when performing landing on the floor about 0.5m above the bottom. The residual motion of the vehicle also causes and error in the final landing point. To overcome this problem, a vision based or SLAM based

algorithm for retracing the original point is required. This error will become substantial in the real ocean environments with large drifts in sensors.

7.3 Observations from experiments

This section provides the observations made from the experiments conducted in the tank environment to evaluate the system.

7.3.1 Environment

Experiments were conducted in a controlled tank environment to demonstrate the survey method proposed by this research. The tank waters are calm and current free making them ideal for setting up seafloor scenarios for evaluating the system. In the absence of waves and currents, the control system of the vehicle could perform navigation effectively to scan the seafloor. By maintaining a straight scanning line, a nearly rectangular area of the tank bottom could be scanned. The algorithms at present require the scanned bathymetry to be free from areas with no data and almost rectangular in shape. In real ocean scenario, it may be difficult for an underwater vehicle to maintain constant heading and speed in presence of currents. This shall affect the scanning resolution considerably and will make it difficult to implement the proposed algorithms in their current form. The features detected in the tank were sharp and easy to identify which may not be the case with real seafloor features.

7.3.2 Computation time

The area covered during the experiments was between 15m-20m and the processing time for analyzing this data was close to 30seconds for wide areas scanning and close to 1minute for analyzing the high resolution bathymetry. In such a small area the drifts from navigation sensors such as DVL and FOG were not considered during scanning the newly generated waypoints or performing landing. When performing experiments over a wide area, the drifts would be substantial and retracing back the waypoints as well as landing could become an issue. A more robust data processing algorithm for localization using bathymetry or image based SLAM would have to be implemented for better positioning accuracy.

7.3.3 Data outliers

The scanned bathymetry is filtered for outliers using a simple depth and mean filtering algorithm. Even after filtering the data, some outliers tend to remain. During the experiments, the outliers in the acoustically scanned bathymetry are mainly generated due to the multi-path reflections from the walls of the tank. In the laser profiling system scanned bathymetry, outliers are caused due to the particles in the water reflected by the laser and detected by the camera system. Outliers can create problems in the decisions made by the

landing algorithm. In presence of outliers a flat area can be detected as one having features and rejected for landing. In wide area bathymetry, the presence of outliers can cause the detection of a wrong area for high resolution scanning. A robust outlier detection algorithm is essential for data filtering without increasing the computational load.

7.3.4 Vehicle hardware

At present the developed vehicle is a test platform not fully capable of operations at sea. The vehicle has to be equipped with GPS, radio and satellite communications for data communication and safe operation. The vehicle also needs a more robust navigation system against currents specially during hovering and slow speed scanning.

8

Conclusions and future work

8.1 Research contributions

This research has proposed a survey method allowing autonomous underwater vehicles to generate multi-resolution maps of a survey area by adapting the scanning resolution in real-time. Most survey techniques currently used allow autonomous underwater vehicles to either generate wide area low resolution maps or observe small areas with high resolution, but not both. The use of autonomous underwater vehicles in complex underwater missions has been explored by developing a method to detect seafloor features autonomously and take appropriate actions based on the seafloor parameters being measured. The type of seafloor properties measured and their relation to the seafloor bathymetry has been used for allowing autonomous vehicles to make real-time survey decisions which are usually taken manually. This research has also provided a means for underwater vehicles to land on the seafloor autonomously without the need of human observation. By providing the landing feature, these underwater vehicles shall acquire the capability to perform seafloor observation using in-situ sensors which usually require a ROV with a human operator. By allowing the user to change the actions taken by the vehicle based on the interest of the survey using a rule file, the use of underwater vehicles in fully automated seafloor observations shall be enhanced. The method developed can be easily applied to real world scenarios such as radiation detection, hydrothermal vent field observation, analysis of manganese crust sea mounts etc by simply changing the payload sensor for seafloor observation and the survey rule file. This research has provided a tool for autonomous exploration of various seafloor features for scientific, economic and environmental purposes.

8.2 Conclusions

This research proposed a new survey method and hardware for obtaining multi-resolution information from the seafloor based on the sensor used for measurement and the interest of the survey. To implement data analysis and decision making, various algorithms were developed to analyze the bathymetry data collected by an underwater vehicle. The algorithms were designed to be made simple for easy implementation on an underwater

vehicle. A new decision making system was developed which allows the users to influence the actions taken by an underwater vehicle by changing the payload sensor and modifying the survey rule file. A prototype underwater vehicle capable of performing the survey was designed and developed with specially designed hardware and software. Hardware for autonomous landing on the seafloor and scanning with different resolutions was implemented. A software architecture was designed for the vehicle to perform and manage the data processing and analysis using the developed algorithms fully autonomously. The system was tested in a tank environment to successfully demonstrate the multi-resolution map generation and decision making process. The system was validated using different seafloor scenarios resembling real ocean environments.

8.3 Future Work

The research at present only uses the bathymetry data acquired using the multi-beam sonar for seafloor analysis. Recent advances have also been made in estimating the seafloor physical characteristics by processing the sonar back-scatter. This can easily be implemented on the developed system and the back-scatter classification data can be used in the decision making process along with the bathymetry data. The camera system used on the vehicle during the experiments captured black and white images of the seafloor. Although this camera has good sensitivity and makes the laser line detection easier, it looses on the color information which can also be extracted from the images. The camera has been mounted on the vehicle such that a part of it looks vertically downwards. The part of the images corresponding to the area looking vertically downwards can be stitched together to generate photo-mosaics in color. Advances have also been made recently in generating three dimensional color bathymetry from laser profiling system. The color information can be used in the decision making process while deciding the areas for landing or seafloor observation. Based on the shape of the bathymetry and the color, classification can be made on an object level basis and used in deciding in taking the appropriate action. The algorithms developed during the experiments can be enhanced for better outlier detection and correction since the detected areas are influenced by their presence. The algorithm also does so not compensate for large pieces of missing data in the scanned acoustic or high resolution bathymetry which needs to be tackled in real world scenarios. Robustness in the algorithms detecting the suitable area for seafloor observation in presence of bad data, missing data and outliers has to be implemented.
The positioning errors of the vehicle are not dealt with during the analysis of the algorithms. During large area surveys in real ocean environments, drifts in position estimates of the vehicle would become substantial and cause errors in relocation of the selected landing areas or scanning areas accurately. Positioning techniques for navigating the vehicle back to the correct landing sites can developed based on image and feature matching. A simultaneous localization and mapping (SLAM) based algorithm based on the images or features obtained in the multi-beam sonar and high resolution bathymetry can be implemented for obtaining better positioning estimates of the vehicle. The experiments

were conducted in a tank environment which is free of currents and easy to monitor the status of the underwater vehicle. The system has to be made sea worthy by having a GPS, stronger wireless and satellite messaging service for communication. The vehicle will also have to be fitted with an emergency ballast release system to surface in case of system failure. An SSBL or USBL system for tracking the vehicle or an underwater modem for acoustic communication would also be essential for safe operation in sea environment. For better hydrodynamic properties and reduction in the drag coefficient during the forward motion of the vehicle, the hull can be covered in a streamlined fairing. Mounting for sensors required for seafloor observation have also to be designed. Experiments can be conducted around several sites around Japan with various applications of the system to different environments. The system can be used to perform radioactivity measurements around various locations around the Fukushima No.1 nuclear plant. Further experiments can also be performed Kagoshima bay underwater hydrothermal vents and other such sites.

A

Scanning hardware details

This appendix provides details on the sensors used for scanning the seafloor with different resolutions. The first part of this appendix explains the hardware for acoustic wide area scanning. Specifications of the sensor have been provided. The section also provides details on the equations used to generate three dimensional bathymetry from the sonar scans. The selection of scanning speeds and sensor resolutions for generation bathymetry have been explained. The later half of the chapter provides details on the sensor to scan the seafloor with high resolution. The hardware and operation procedure have been explained to elaborate on the working of the system. The process of generation of bathymetry from the sensor data has been elaborated. The parameters affecting the scanning resolution and the selection of scanning speed and altitude for the system have been mentioned in the last section.

A.1 Wide area scanning system

For this research, a multi-beam sonar has been used for generation of wide area bathymetry. The sensor used is an Imagenex Delta-T multi-beam sonar whose specifications have been mentioned in the Fig. A.2. The sensor has been mounted on to the lower part of the vehicle facing downwards with the scanning beam normal to the direction of motion of the vehicle.

A.1.1 Scanning hardware

The multi-beam sonar scans the seafloor at about 5 scans/second using an external trigger command. For the purposed of beam forming the software provided by the manufacturer (Deltat.exe) has been used. This is an proprietary software from Imagenex whose source code is not available and runs only using Microsoft windows. An external protocol for interacting with the software has been provided by the manufacturer which communicates over Ethernet TCP. The external command allows the setting of the gain, sector size, beam-width, averaging, sound velocity, output format, operation mode etc. The sonar can be operated in the sector, linear, perspective, profile or beamtest mode. For this research, the sonar was operated in the profile mode.

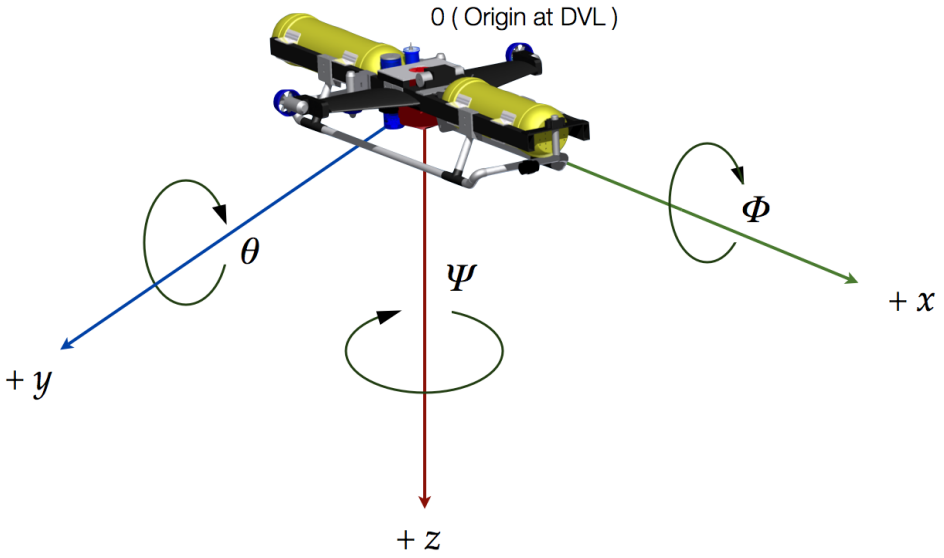

Fig. A.1. Coordinate system used for calculations and data processing

The sonar captures one scan of the seafloor each time a trigger command is given. The format used to capture the data is the 83B beam output format developed by Imagenex. The format provides the scan data as well as sonar parameters such an beams, sector size, sound velocity, range, range resolution, ping no, etc. Each beam of the sonar is divided into 500 bin ranges. For each beam, the bin intensity is provided as a 0-255 value with 255 being the maximum intensity.

Beams width	120° x 3°
No. of beams	120
Opening angle	120°
Range resolution	0.2% Range
Minimum range	0.5m
Maximum range	300m
Frame rate	20 fps max
Interface	Ethernet

Fig. A.2. Delta-T Imagenex multi-beam sonar and its specifications

A.1.2 3D bathymetry generation

A flat tank bottom was scanned using the sonar. A 120 beam x 500 bin intensity reflection captured by the sonar can be seen in the Fig. A.4. The corresponding scan in the frame of reference of the sonar can be seen as well in which the tank bottom appears flat.

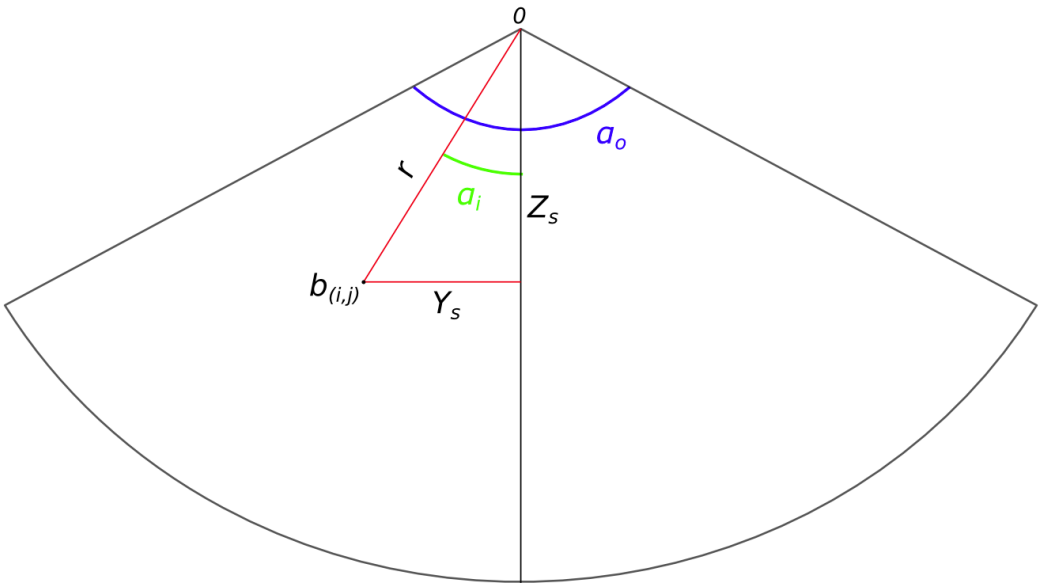

Fig. A.3. Sonar beam geometry and description of related parameters

To process the sonar data, the geometry of the beam is considered and triangulation is performed to calculate the horizontal and vertical distance of each point from the sonar centre. Consider the sonar beam swath seen in Fig. A.3. The sensor location is considered to be at the origin 0.

For every beam i and every bin j, the X_s, Y_s and Z_s positions of point $b_{(i,j)}$ have to be calculated in the frame of reference of the robot. α_o is the complete opening angle of the sonar and α_i is the angle made by the i^{th} beam and r is the range to point $b_{(i,j)}$. The current position and orientation state of the robot is defined by ϕ, θ, ψ, X_{rob}, Y_{rob}, Z_{rob}. If the range resolution of the sonar is r_{res} then we can compute as follows:

$$
\begin{aligned}
r &= r_{res} \times j \\
\alpha_i &= \frac{-\alpha_o}{2} + 0.5 + (i-1) \\
X_s &= 0 + x_{off} \\
Y_s &= r \times sin(\alpha_i) + y_{off} \\
Z_s &= r \times cos(\alpha_i) + z_{off}
\end{aligned}
$$

To select only the required points for generation of bathymetry points, a threshold is applied to the intensity values. Only the bins with values above a certain intensity (between 0-255) are converted to bathymetry points. The rest are rejected. After the entire beam is processed, the three dimensional points are logged as seen in the Fig. A.5.

$$
\begin{bmatrix} X_{temp} \\ Y_{temp} \\ Z_{temp} \end{bmatrix} = \begin{bmatrix} cos\phi cos\theta & cos\phi sin\theta sin\psi - sin\phi cos\psi & cos\phi sin\theta cos\psi - sin\phi sin\psi \\ sin\phi cos\theta & sin\phi sin\theta sin\psi + cos\phi cos\psi & sin\phi sin\theta cos\psi + cos\phi sin\psi \\ -sin\theta & cos\theta sin\psi & cos\theta cos\psi \end{bmatrix} \times \begin{bmatrix} X_s \\ Y_s \\ Z_s \end{bmatrix}
$$

$$
\begin{bmatrix} X_w \\ Y_w \\ Z_w \end{bmatrix} = \begin{bmatrix} X_{temp} \\ Y_{temp} \\ Z_{temp} \end{bmatrix} + \begin{bmatrix} X_{rob} \\ Y_{rob} \\ Z_{rob} \end{bmatrix}
$$

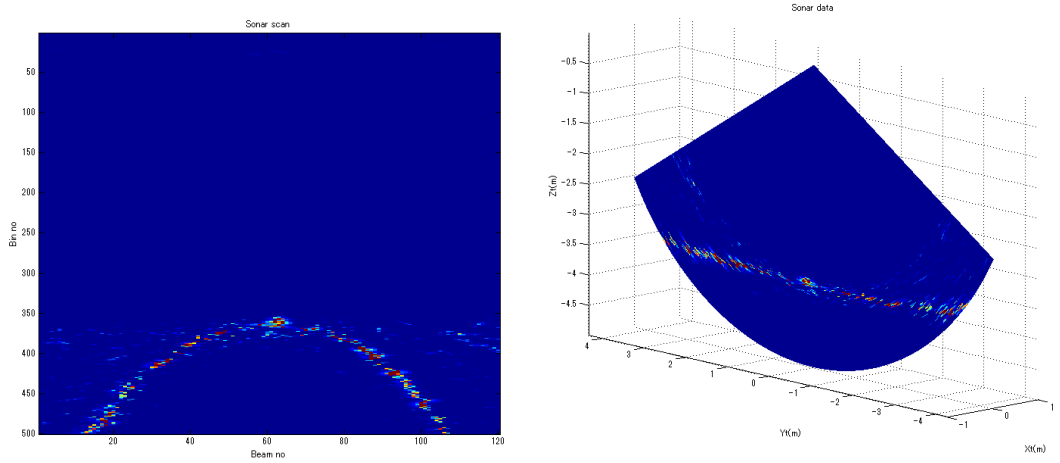

Fig. A.4. Multi-beam sonar data processing; Left:Scanned original data Right:Data corrected for beam geometry

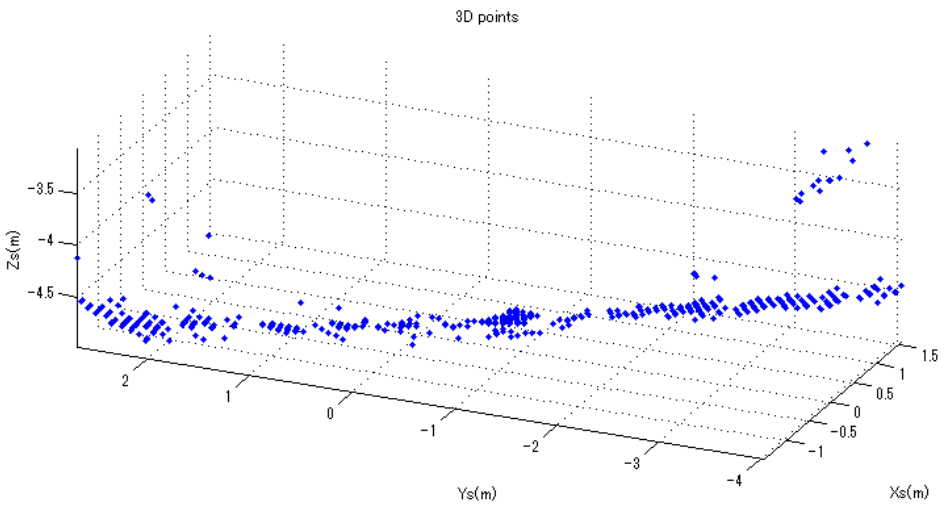

Fig. A.5. Generated bathymetry 3D point cloud after data processing

A.2 Laser profiling system

The laser profiling system is a light sectioning method for generating millimeter resolution bathymetry [49]. The system requires the use of a camera to capture images of the laser projections on the seafloor. As a result, this system cannot be used from high altitude scanning because of difficulty in detecting the laser line.

A.2.1 Profiling hardware

The laser profiling system uses a camera and sheet laser assembly as seen in the Fig. A.6. The laser used is a sheet laser which projects vertically downwards as a fan. The camera is mounted at an angle to the laser to capture the projection of the laser on the ground. The laser falls on the underlying surface as a single line profile [50] [51]. This projection is photographed and recorded by the camera along with the navigation data of the vehicle which is the three axis position and orientation and time stamp in $yyyy-mm-dd-hh-mm-ss-msec$. The images with the sheet laser projection are then processed to generate high resolution bathymetry.

A.2.2 Bathymetry generation

At first the laser line from the image is extracted. In color images, the pixels in each vertical column with the highest green value are extracted and their average vertical position is considered. In black and white images, they are first threshold to a binary imagine with the white pixels representing the laser line. The average value of the white pixels in each column is considered as the detected laser line. Once the pixel values representing the laser are extracted the following triangulation method is applied for converting these to the

robot coordinates [52]. To convert the detect the laser line into bathymetry, triangulation is used. At first, for a particular lens of a camera and the baseline between the camera and the laser, a camera point model is established.

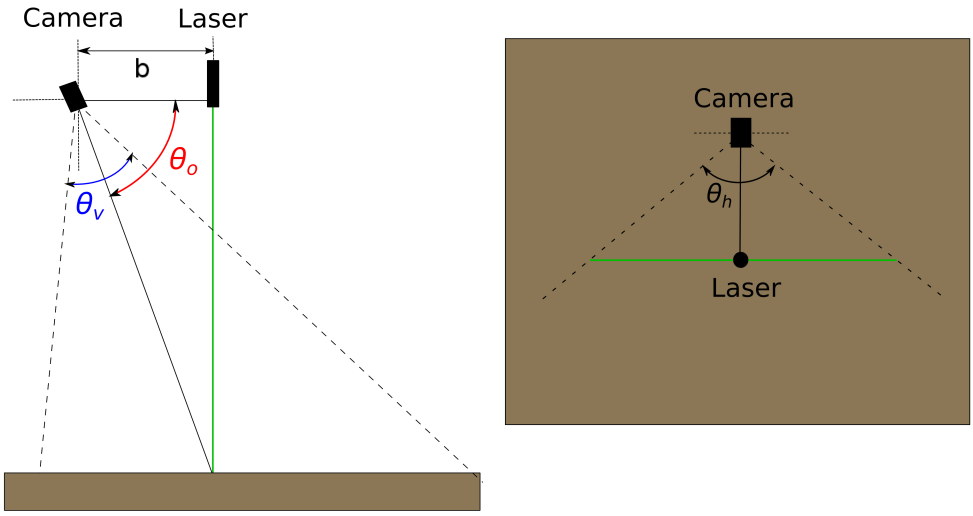

Fig. A.6. Light sectioning based laser profiling technique; Left: Side view of the setup, Right: Top view of the setup

For processing the data, consider a camera with pixel resolution in the horizontal and vertical direction as $P_h \times P_v$. The opening angles of the camera system along the two axis are $\theta_h \times \theta_v$. The baseline b is the spacing between the camera and the laser assembly. The mounting angle of the camera system with respect to the vertical plane is θ_o. For every pixel i in the vertical plane of the camera going from 0 to $P_v - 1$, the appropriate angle and the range bins made is calculated.

$$\theta_{vi} = \theta_o - \frac{\theta_v}{2} + \frac{\theta_v}{P_v - 1} \times i$$
$$Z_i = b \times \tan(\theta_{vi})$$

For every pixel j in the horizontal plane of the camera going from 0 to $P_h - 1$, the new baseline is first calculated. The new baseline is then used to find the horizontal angle made by the pixel and the range bin. The camera range point cloud can then be calculated and seen in the Fig. A.7.

$$b_j = \frac{b}{\cos(\theta_{vi})}$$
$$\theta_{hj} = \theta_o - \frac{\theta_h}{2} + \frac{\theta_h}{P_h - 1} \times j$$
$$Y_i = b_j \times \tan(\theta_{hj})$$
$$X_i = 0$$

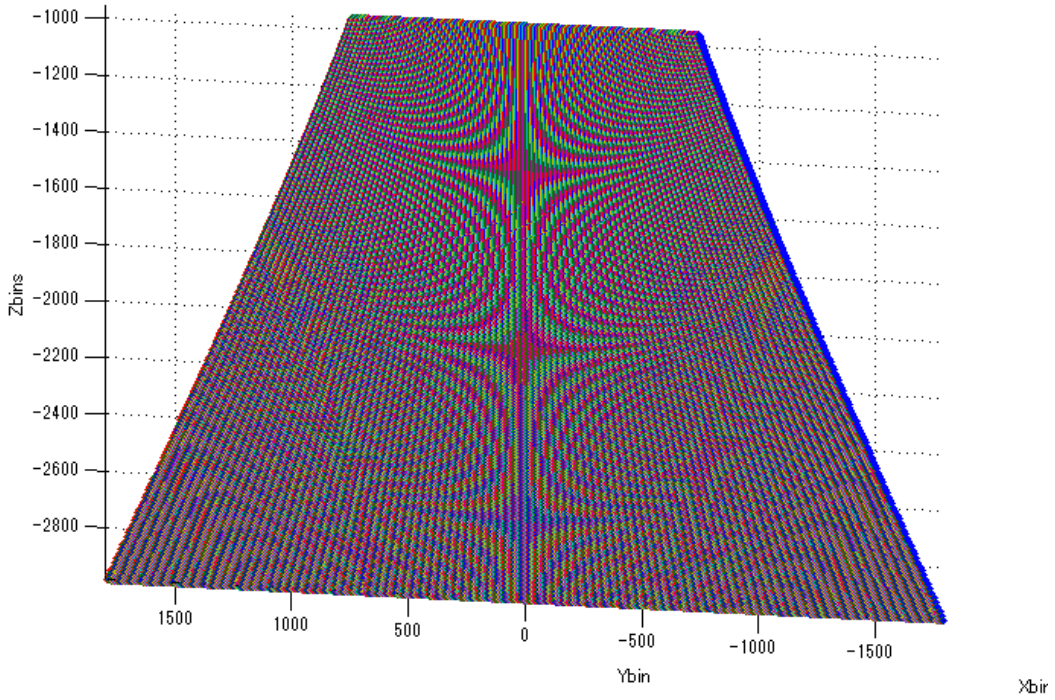

Fig. A.7. Ranges calculated for each pixel of the camera image based on the geometry of the setup

The points in the green laser then identified are then selected and the corresponding values of x_t,y_t,z_t are selected from the matrix. The coordinates generated are in the robot frame of reference. To transform them into the earth frame of reference, coordinate transformation is performed. For better results, a coupled roll, pitch, way system is assumed during coordinate transformation. The equations for transformation are provided below. The roll(ϕ), pitch(θ) and yaw (ψ) of the robot position are measured at the time when the laser profile was obtained. For the points extracted from the laser profiles, geometrical transformation can be obtained to generate a point cloud in the vehicles frame of reference. If the current state of the robot at time of taking the image is defined by roll(ϕ), pitch(θ), yaw (ψ), X_{rob} , Y_{rob} , Z_{rob} then we can compute as follows:

$$\begin{bmatrix} X_{temp} \\ Y_{temp} \\ Z_{temp} \end{bmatrix} = \begin{bmatrix} cos\phi cos\theta & cos\phi sin\theta sin\psi - sin\phi cos\psi & cos\phi sin\theta cos\psi - sin\phi sin\psi \\ sin\phi cos\theta & sin\phi sin\theta sin\psi + cos\phi cos\psi & sin\phi sin\theta cos\psi + cos\phi sin\psi \\ -sin\theta & cos\theta sin\psi & cos\theta cos\psi \end{bmatrix} \times \begin{bmatrix} X_i \\ Y_i \\ Z_i \end{bmatrix}$$

$$\begin{bmatrix} X_h \\ Y_h \\ Z_h \end{bmatrix} = \begin{bmatrix} X_{temp} \\ Y_{temp} \\ Z_{temp} \end{bmatrix} + \begin{bmatrix} X_{rob} \\ Y_{rob} \\ Z_{rob} \end{bmatrix}$$

For every laser profile acquired during the scan between the waypoints, bathymetry point cloud in the earth frame of reference is generated and logged. This data is then processed using the algorithm explained in the next section of this chapter. The laser profile of a scanned plastic object Fig. A.8 and the generated point cloud can be seen in the Fig. A.9.

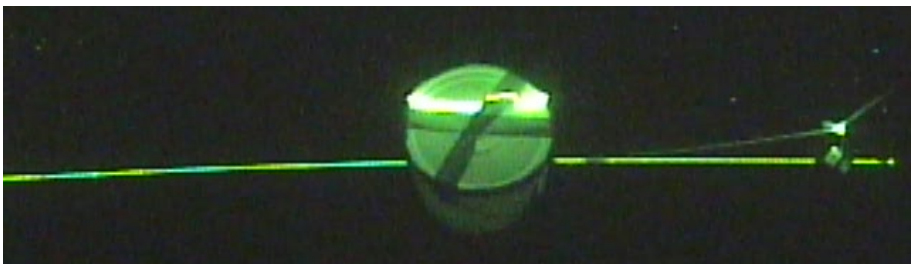

Fig. A.8. Bucket scanned using a laser profiling system

A.3 Bathymetry meshing algorithm

To find the new z values of the bathymetry at the point B_n on the new mesh, the inverse distance squared rule is applied. Consider the original point cloud and meshed grid in Fig. A.10. For every point B_n, the number of points from the original bathymetry in the adjacent squares are identified and their distance from the point are computed. In this case $r1$, $r2$, $r3$, $r4$ are the distances computed from B_n to points with z values z_1, z_2, z_3, z_4 respectively. Then the new value of Z_b is computed using the following:

$$Z_b = \frac{z_1\left(\frac{1}{r_1^2}\right) + z_2\left(\frac{1}{r_2^2}\right) + z_3\left(\frac{1}{r_3^2}\right) + z_4\left(\frac{1}{r_4^2}\right)}{\frac{1}{r_1^2} + \frac{1}{r_2^2} + \frac{1}{r_3^2} + \frac{1}{r_4^2}}$$

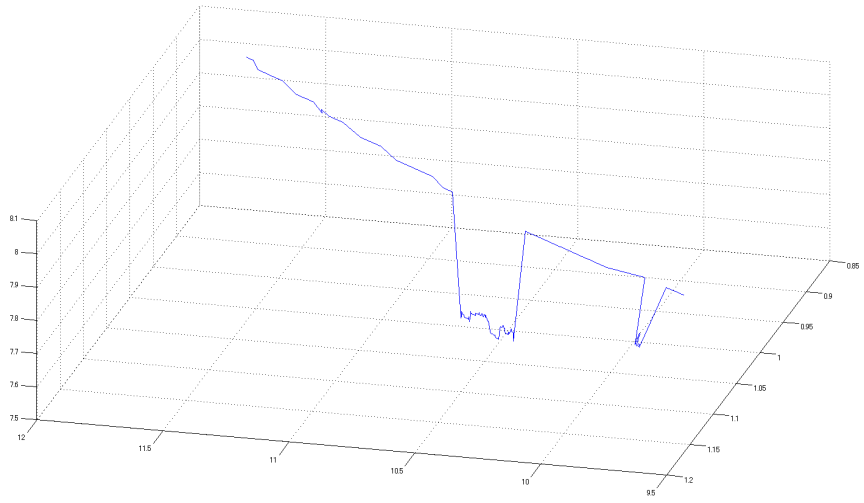

Fig. A.9. Generated bathymetry 3D point cloud after data processing

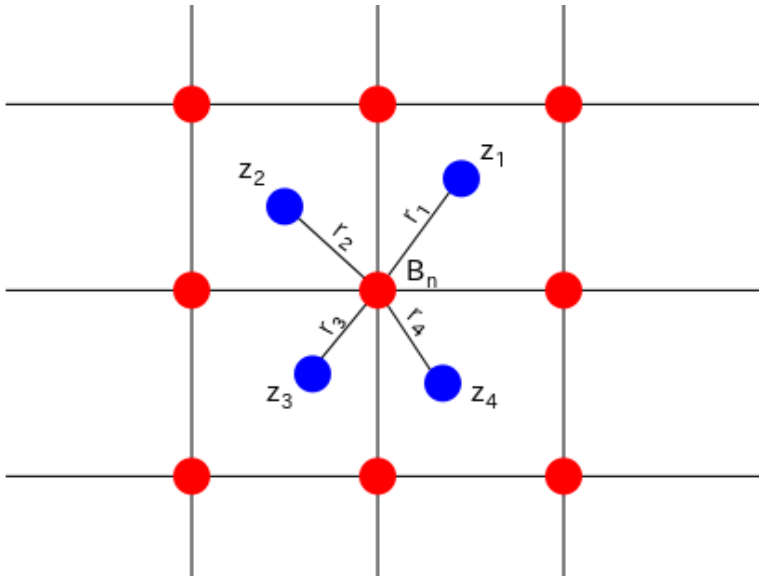

Fig. A.10. Point cloud meshing using inverse distance squared rule. Red point are on the new meshed grid. Blue points are those from originally scanned data.

This process is applied to estimate the values of all the points on the new bathymetry mesh. For those points who do not have sufficient points in the neighborhood, the values are interpolated in a second round of processing using the bathymetry values of newly computed points.

B

Vehicle mechanical assembly and electronics

This chapter provides details on the mechanical and electrical design components of the vehicle. The overview of the electronics architecture of vehicle are shown along with the stacking arrangement in the electronics hull. These can be seen from Fig. B.1 to Fig. B.3. The circuit diagrams for individual parts of the electronic circuits are shown with explanations. The later part of the chapter has mechanical drawing of the main cylinders, the skeleton, wings, landing skids and the overall assembly.

B.1 Electrical schematics

Fig. B.1: Electronics tray design and arrangement

Fig. B.2: Electronics tray components mounting A to D

Fig. B.3: Electronics tray components mounting E to G

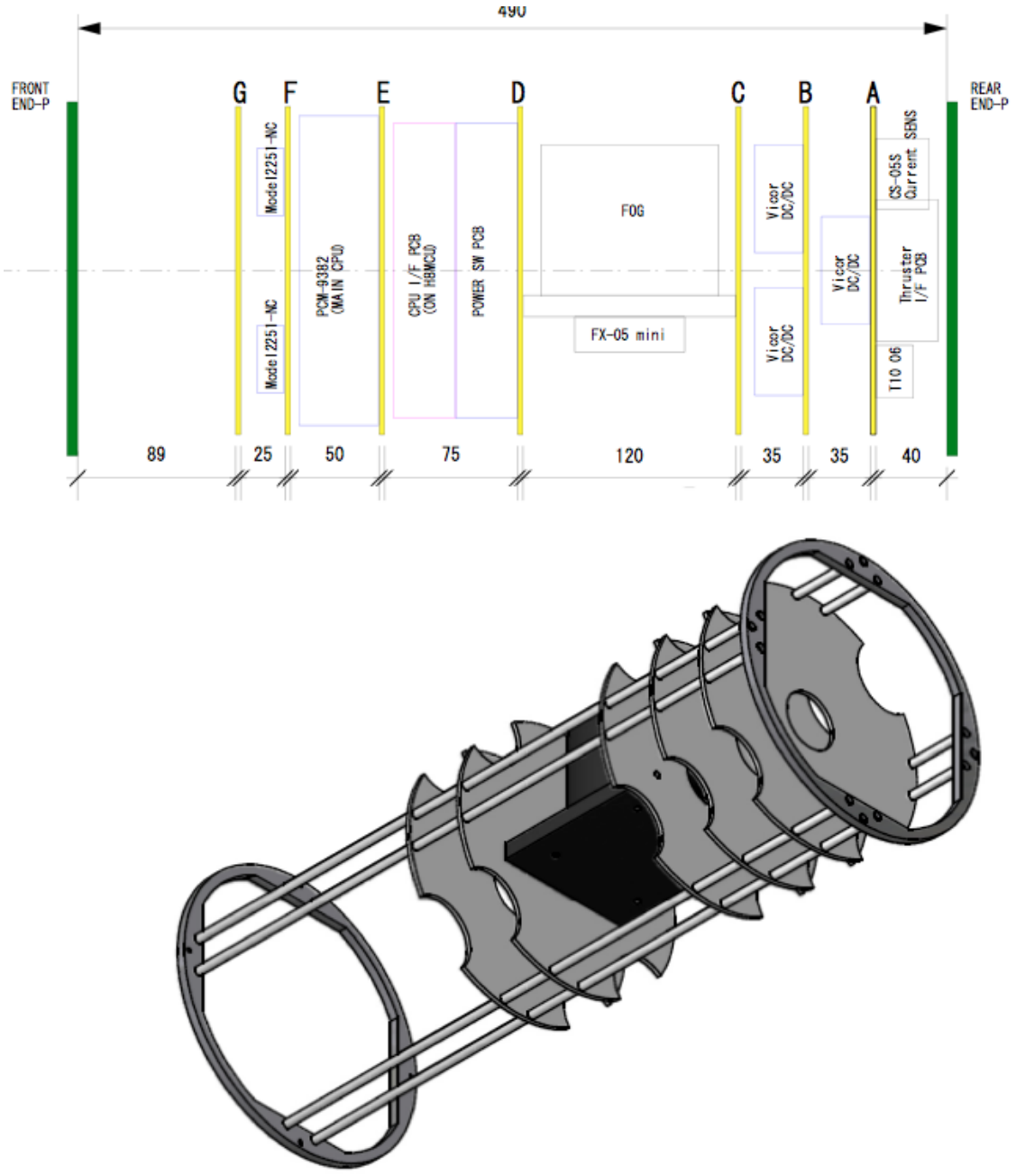

Fig. B.1. Electronics tray design and arrangement; Up: Circuit board arrangement order, Bottom: CAD drawing of the electronics tray

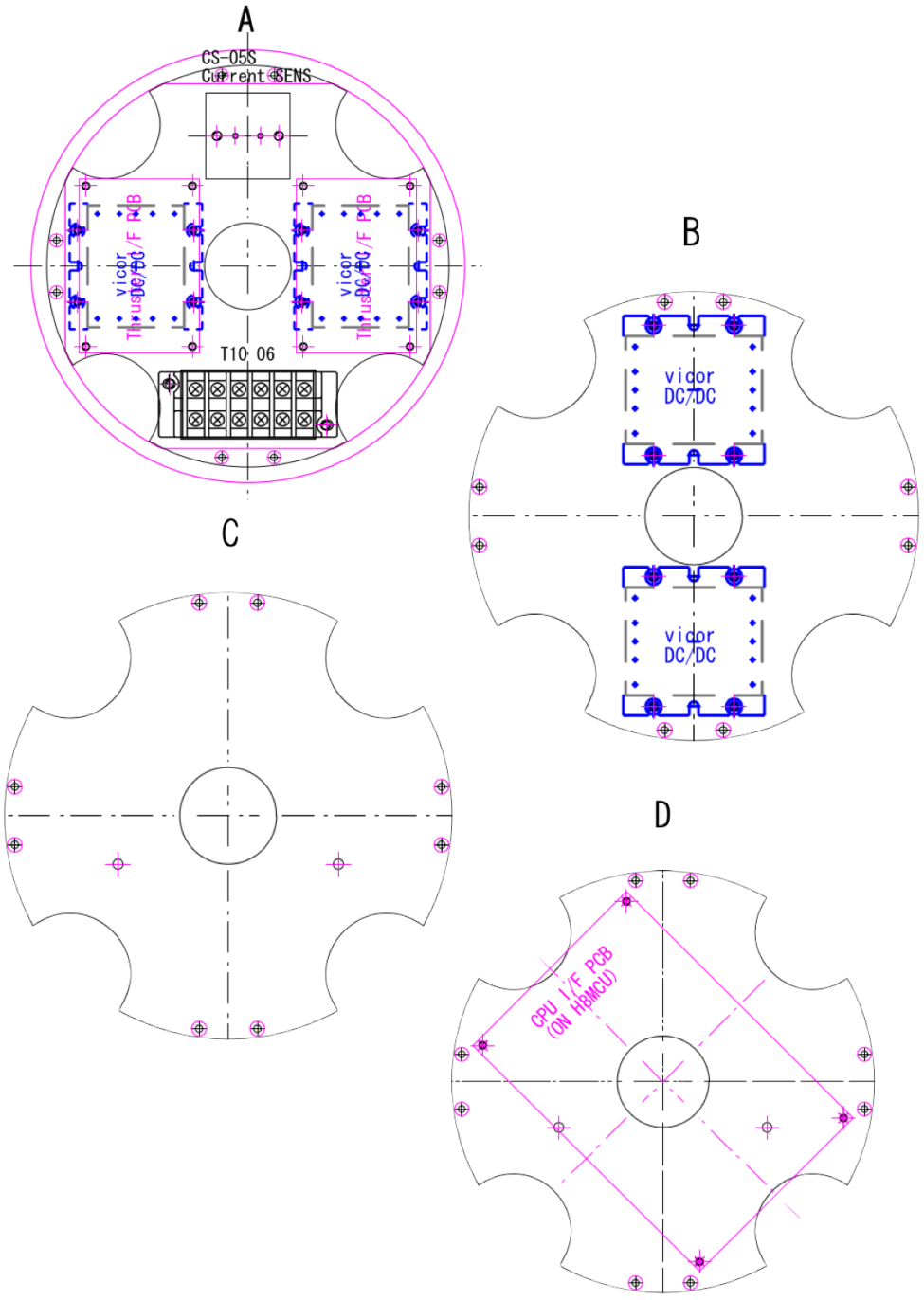

Fig. B.2. Electronics tray components mounting A to D

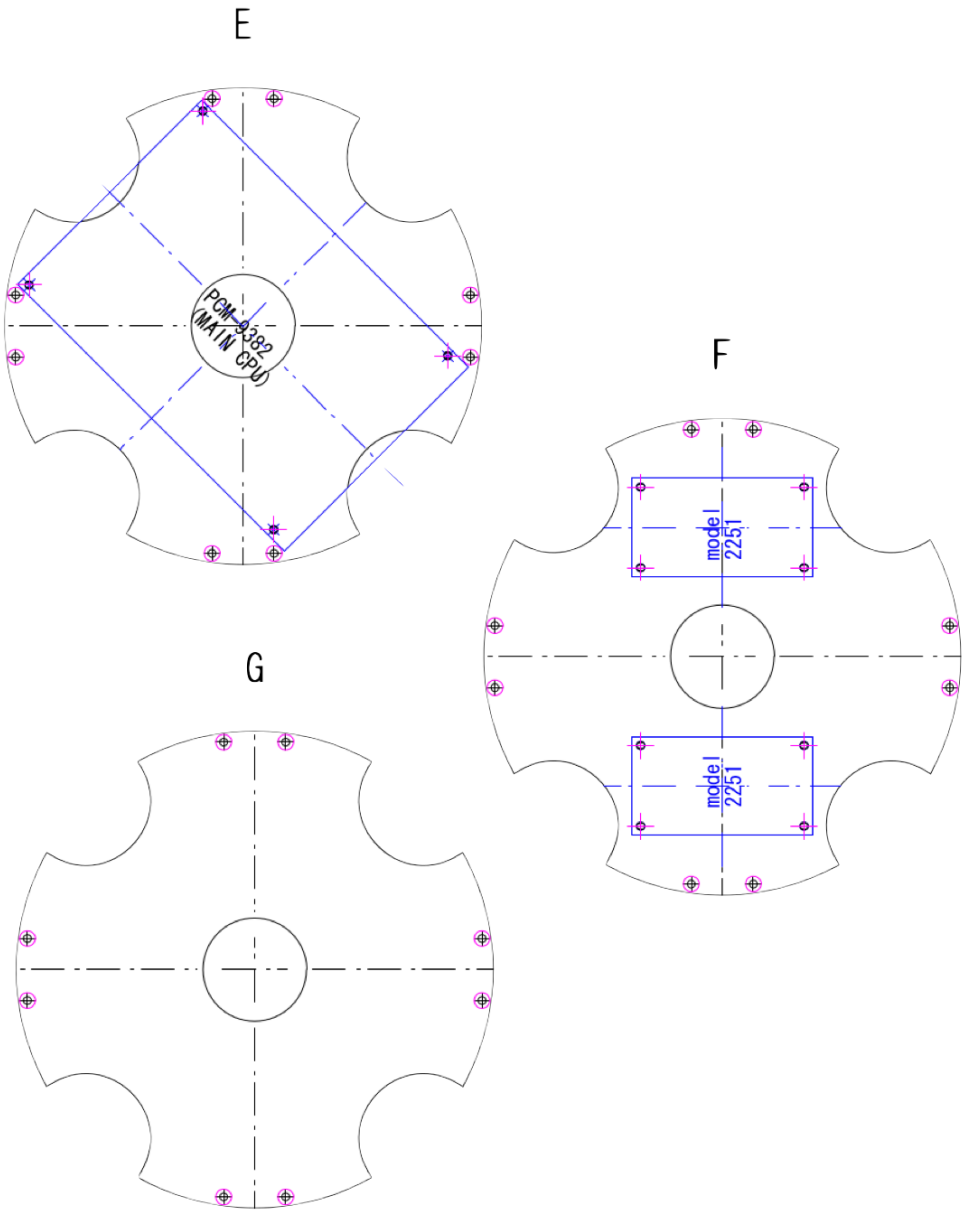

Fig. B.3. Electronics tray components mounting E to G

B.1.1 Thruster power and control circuits

The thruster control circuit translates the digital to analog output 0V to +5Vfrom the MCU to a −5V to +5V using a potential divider and shifter. The revolutions of the thruster area measured though a digital to analog converter and measured by the MCU. The thruster main power is provided from the batteries only. The instrumentation power is provided though a DC-DC isolator. Each thruster has an independent driver as seen in the Fig. B.4. When the vehicle is powered using an external source, the thrusters are always powered using the internal batteries as seen in Fig. B.5

Fig. B.4: Control circuits for thrusters implemented in the vehicle

Fig. B.5: Power circuits for thrusters implemented in the vehicle

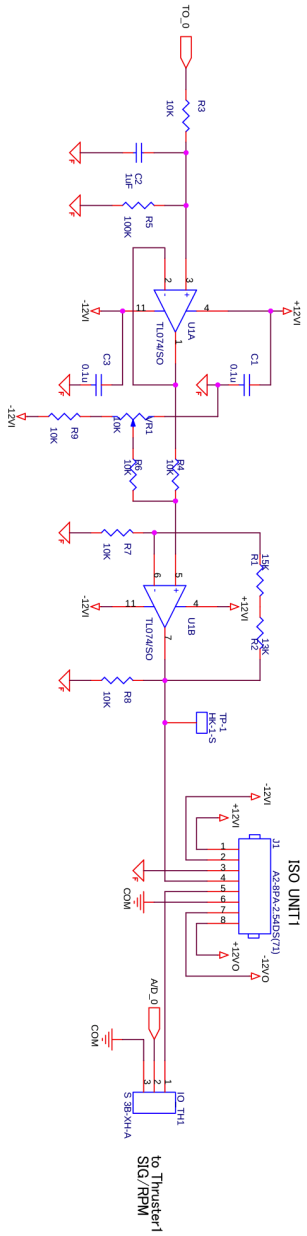

Fig. B.4. Control circuits for thrusters implemented in the vehicle

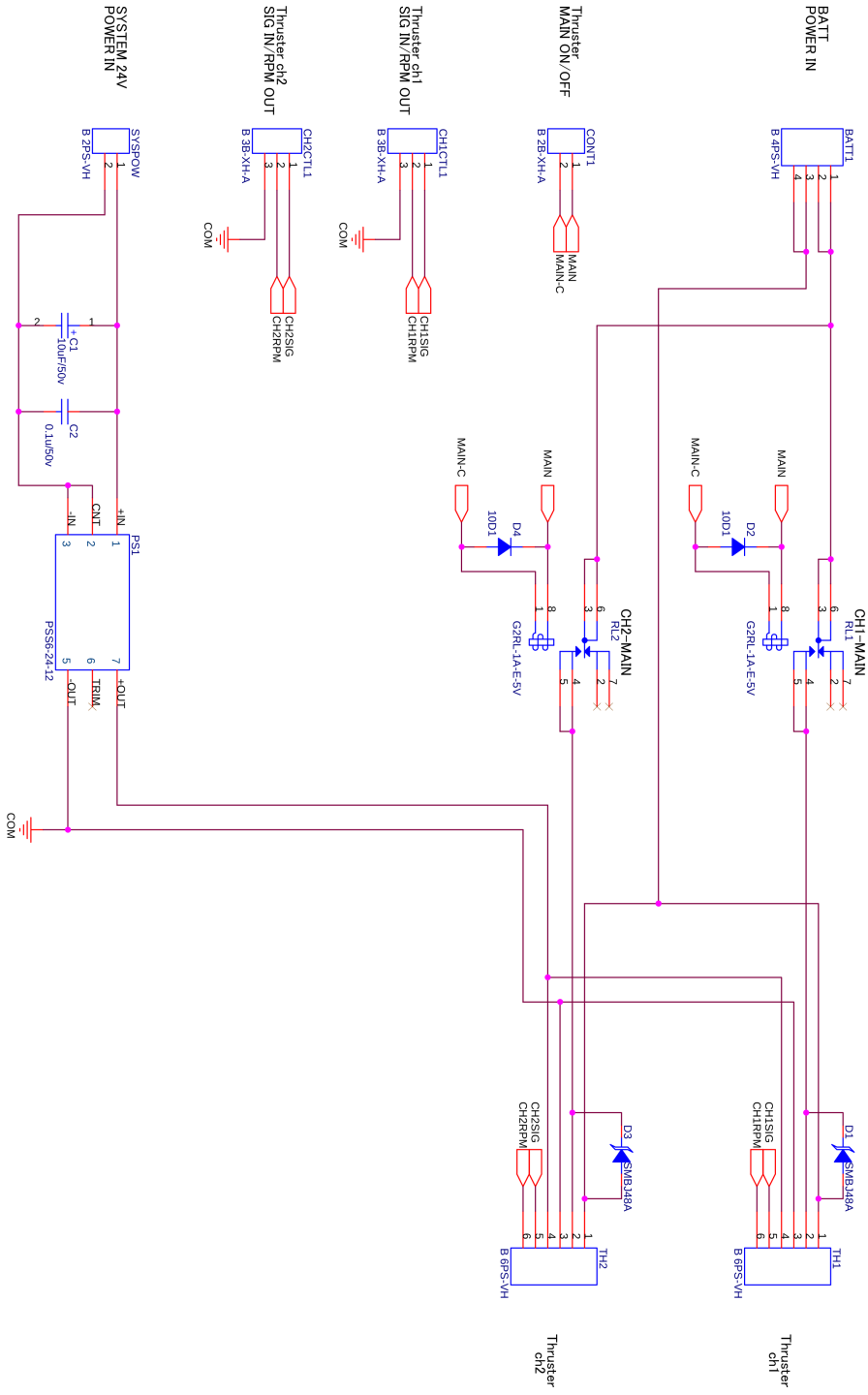

Fig. B.5. Power circuits for thrusters implemented in the vehicle

B.2 Mechanical drawings

B.2.1 Wing structure

The AUV has a winged structure designed to generate lift during forward motion of the vehicle. The NACA 651412 profile has been used to generate the basic shape of the wing. An asymmetrical profile has been selected so that life can be generated without any angle of attack since the vehicles pitch always remains constant. The profile of the wing and the finalized three dimensional drawing can be seen in the Fig. B.6.

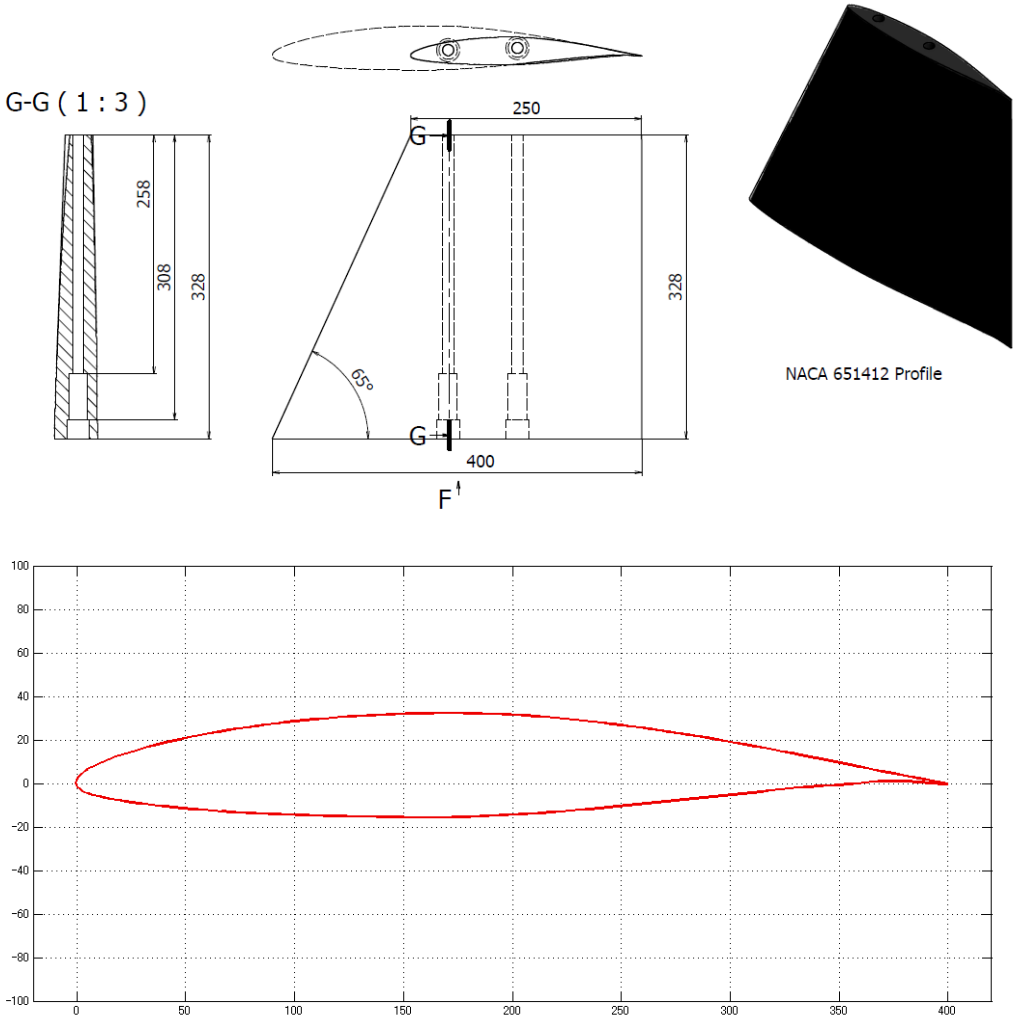

Fig. B.6. Wing profile and CAD design of the wing skeleton and assembly

B.2.2 Landing skids

The landing skids were designed using PVC pipes to keep the structure lightweight and easily replaceable as seen in Fig. B.7. The design of the skids has been made similar to those of a helicopter. They are slightly expandable being made from PVC but offer good rigidity to the robot structure. The sensors required for seafloor observation need a flat stable ground below them for acquiring data, hence a flat design for the skids was considered.

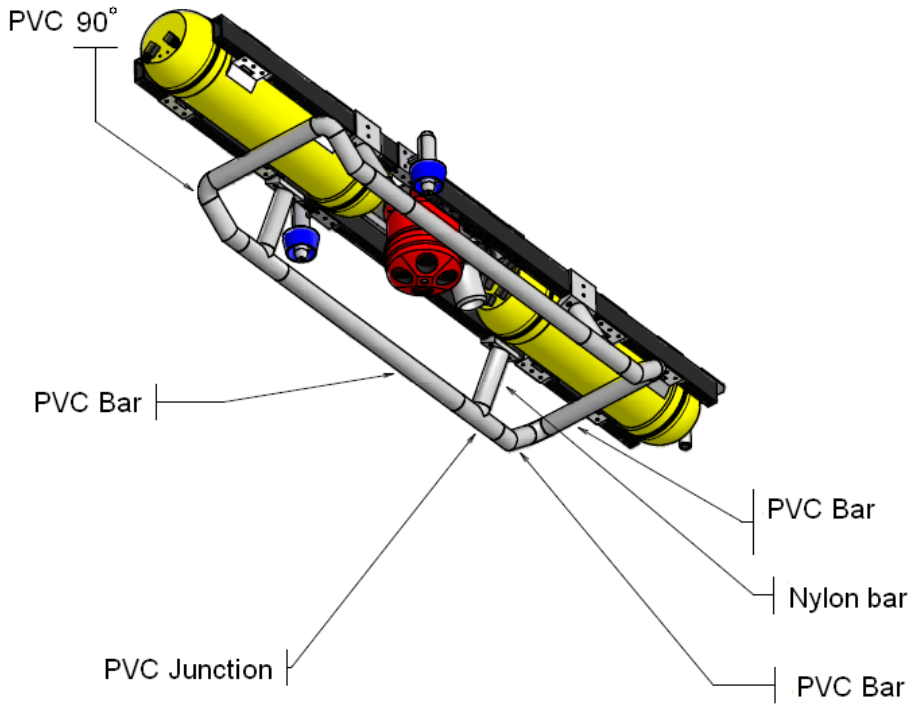

Fig. B.7. Design and assembly of the landing skids

B.2.3 Main cylinders and assembly

The two main cylinders of the vehicle house the electronic components and batteries. The main cylinder has been made from Aluminum 5056 grade. The design of the cylinders can be seen in the Fig. B.8.

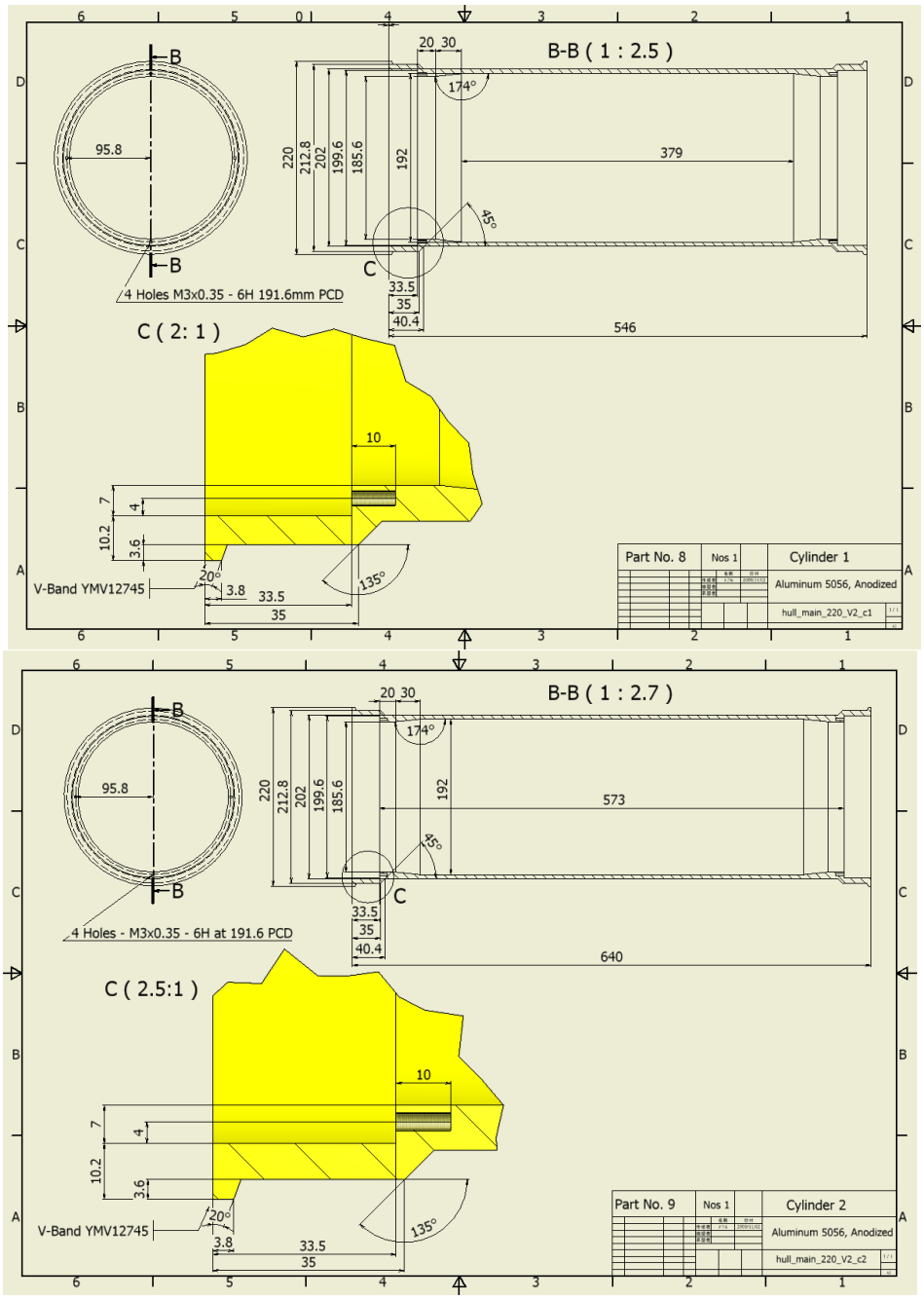

Fig. B.8. Mechanical drawing of the vehicles main cylinders. Top: Electronics cylinder, Bottom: Battery cylinder

Each cylinder has a cap on each end with O-rings for water sealing. The end caps have a partial flat surface for mounting underwater connectors. The connectors also have O-rings for sealing. The design of end caps can be seen in Fig. B.9 and Fig. B.10.

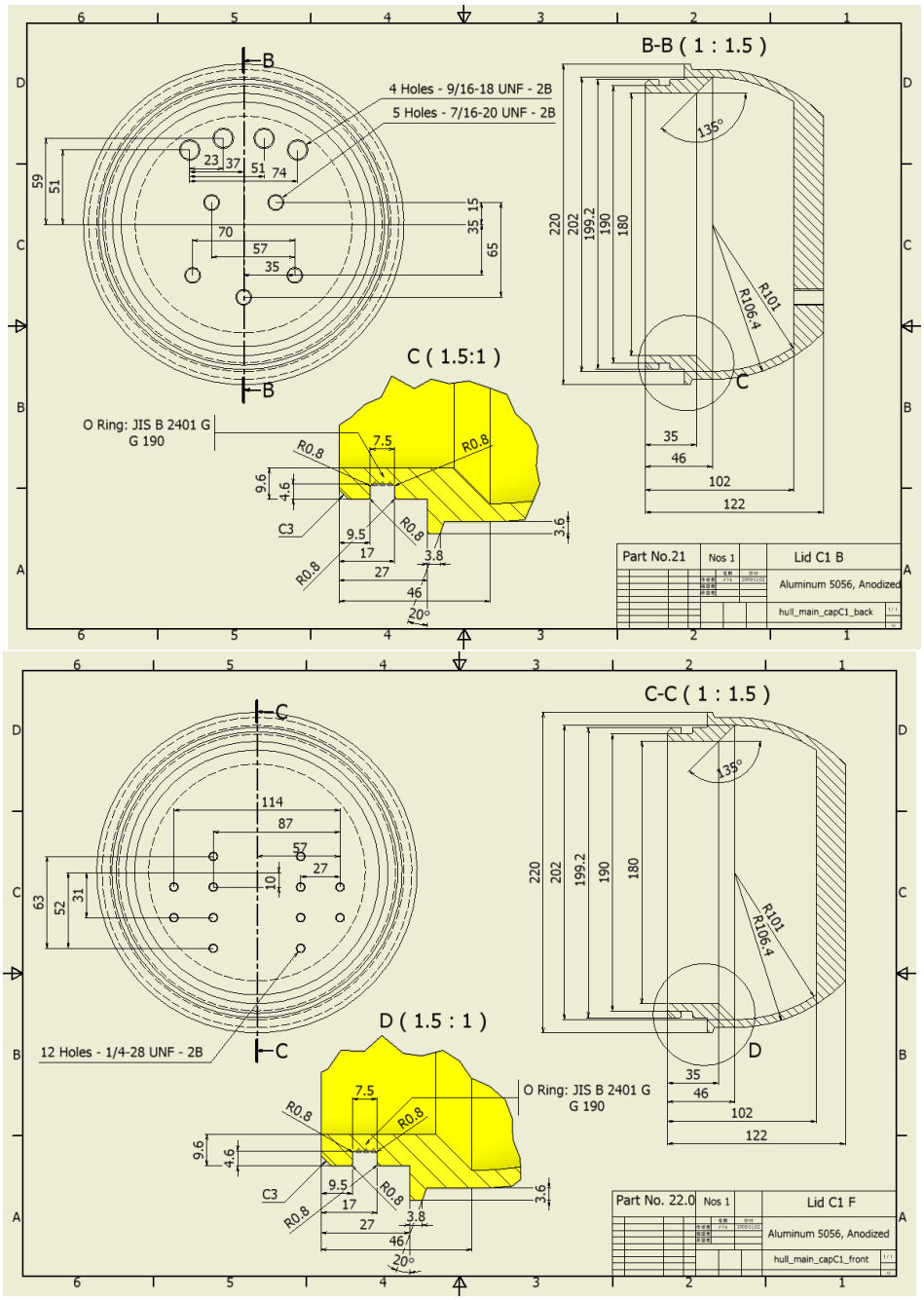

Fig. B.9. Electronics cylinder hull front and back end caps

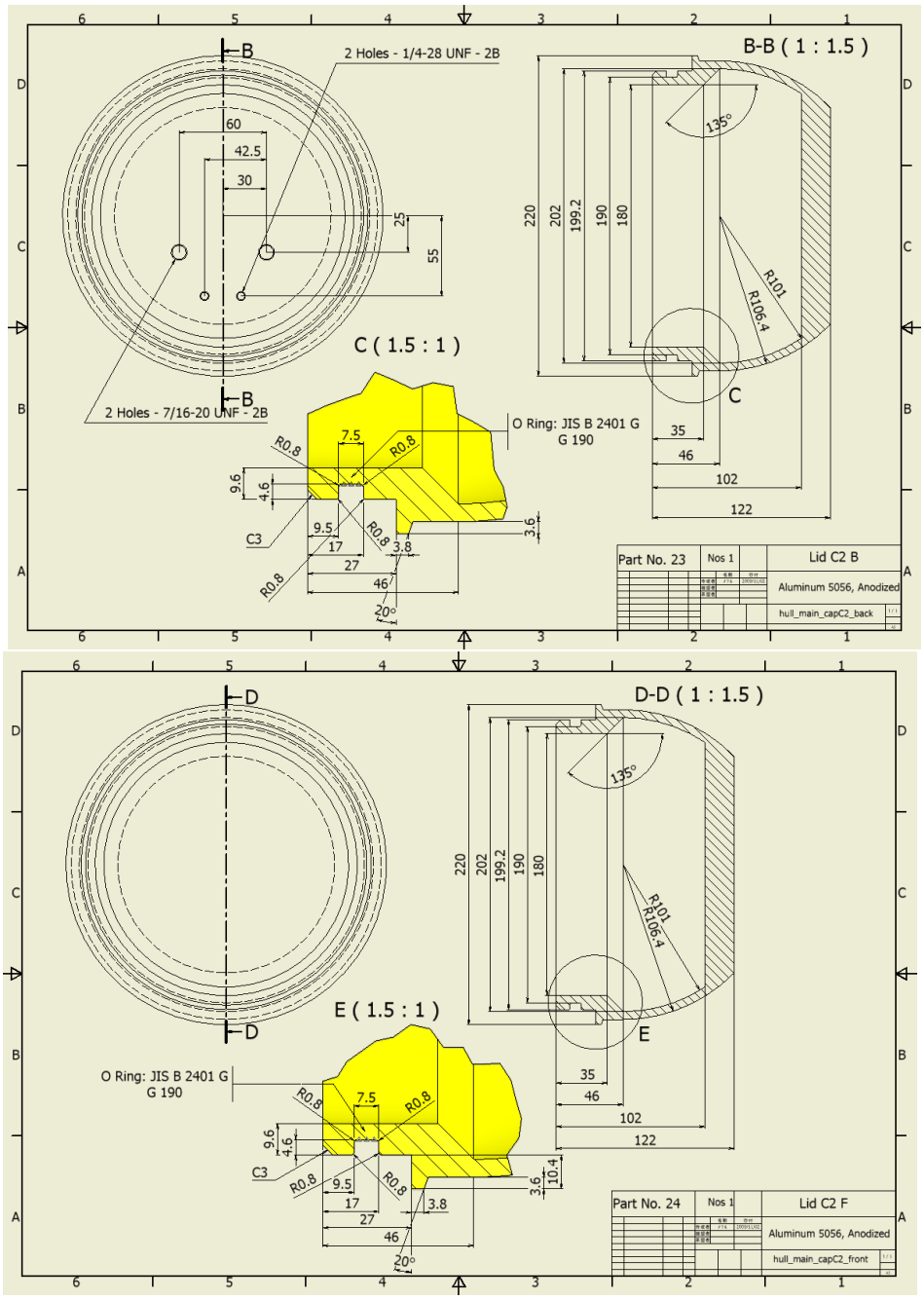

Fig. B.10. Battery cylinder hull front and back end caps

The main skeleton of the vehicle has been made from Aluminum bars anodized for oxidation protection. The bars are hollow and have been filled with two nylon bars of equal sizes. The detailed assembly of the main skeleton can be see in the Fig. B.11. Holes have been made for fixing the remaining components on the frame. Special clamps have been made for fixing the main cylinders with bands. The assembly of the cylinders on the main skeleton can be seen in the Fig. B.12.

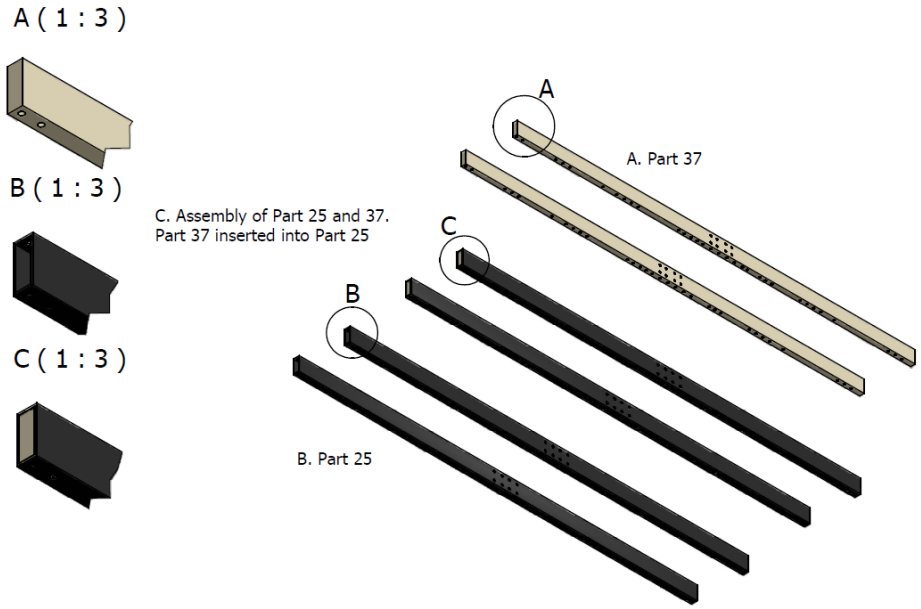

Fig. B.11. Vehicle main frame design and assembly

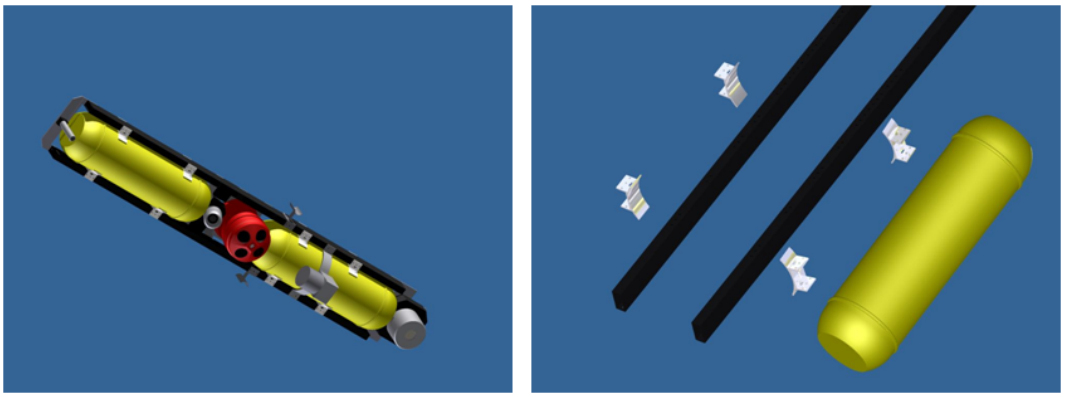

Fig. B.12. Vehicle main structure assembly

Special mounting jigs have been using nylon for mounting the camera and and laser assemble. A nylon wedge has been made to provide the camera the exact mounting angle with the vertical. The camera and laser assembly can be seen in the Fig. B.13.

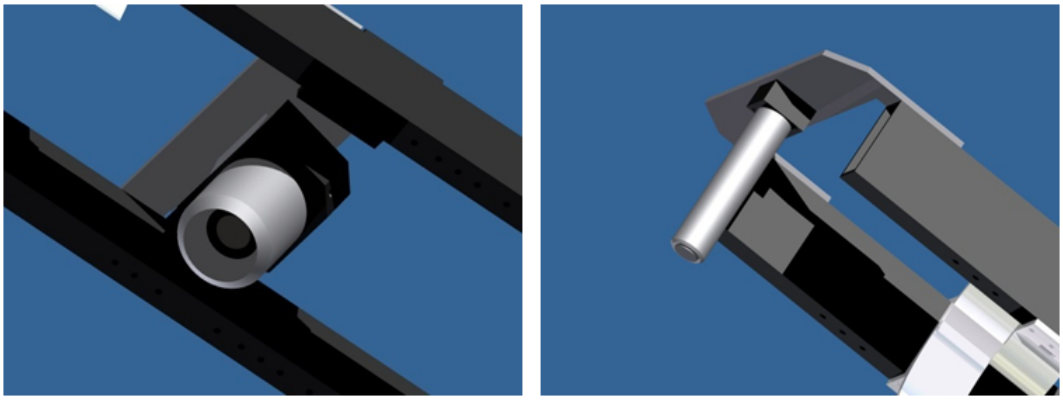

Fig. B.13. Camera and laser assembly

An Aluminum frame has been designed for mounting the DVL and depth sensor on the main skeleton. The thrusters are connected to the main frame using two Aluminum rods which pass through the wing assembly. The DVL, depth sensor and thruster assembly can be seen in the Fig. B.14.

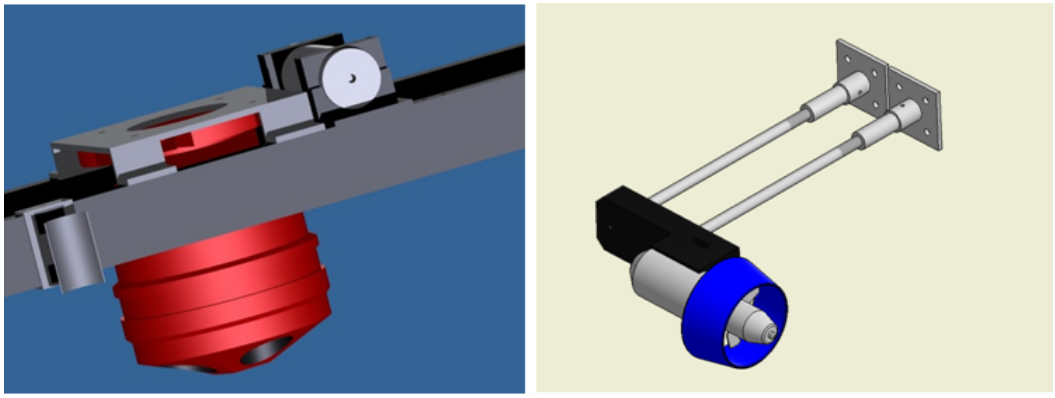

Fig. B.14. DVL, depth sensor and thruster assembly

C

Vehicle survey files

This appendix provides details on the initialization and rule files which are provided to the vehicle for performing the required survey. The structure of the files has been described along with the parameters explained in detail. Examples of the files which were used during the experiments have also been included. The next part of this appendix shows the database structure for recording the features detected during the wide area acoustic bathymetry analysis. The last part explains the database structure used for storing the analysis results of the high resolution bathymetry.

C.1 Initialization file

The initialization file is uploaded into the vehicle at the start of the mission. The file structure is based on an XML. XML which is a markup language primarily used for encoding documents.

Fig. C.1. Parameters for navigation provided in the initialization file

The format of the file has been modified to provide mission details and sensor initialization parameters to the vehicle. The area to be covered is provided to the vehicle in the form of waypoints and a safe navigation bounding box as seen in the Fig. C.1. The different paremeters for vehicle navigation and sensor initializaion are mentioned in the Table. C.1.

Table C.1. Initialization file navigation parameters

Property	**Nomenclature**	**Units**
No. of waypoints	n	
Waypoints	$x_0\ y_0\ z_0$	meters
	$x_n\ y_n\ z_n$	meters
Safe point a	$x_a\ y_a$	meters
Safe point b	$x_b\ y_b$	meters
Safe point c	$x_c\ y_c$	meters
Safe point d	$x_d\ y_d$	meters

The XML structure of the file is given as below:

<?xml version="1.0" encoding="UTF-8"?>
<user>*Username and Institution Name*</user>
<mission>
<name>*Missionname*</name>
<mode>*Mode of operation: Automatic, Manual*</mode>
<point><nops>*Number of waypoints*</nops>
$x_0\ y_0\ z_0$
$x_n\ y_n\ z_n$
</point>
<area>
$x_a\ y_a$
$x_b\ y_b$
$x_c\ y_c$
$x_d\ y_d$
</area>
</mission>
</user>

Table C.2. Initialization file sensor parameters

Property	Nomenclature	Units
Wide area scanning		
Scanning altitude	W_{alt}	meters
Scanning speed	W_{vel}	m/s
Sonar gain	S_{gain}	percentage
Sonar mode	x_b y_b	Point mode (P)
Scan beam angle	a_0	°
Scan range	R	meters
High resolution scanning		
Scanning altitude	H_{alt}	meters
Scanning speed	H_{vel}	m/s
Camera gain	C_{gain}	percentage, Auto (A)
Horizontal opening angle	θ_h	°
Vertical opening angle	θ_v	°
Camera mounting angle	θ_o	°
Baseline	b	percentage
Camera horizontal resolution	H_{res}	pixels
Camera vertical resolution	V_{res}	pixels
Laser opening angle	θ_l	°
Obstacle avoidance		
Scan range	R_o	meters
Scan beam angle	a_0	°
Sonar gain	S_{gain}	percentage

</area>

</mission>

<scanning>

<sonar>

Scanning altitude in m

Scanning speed in m/s

Sonar gain in percentage

Sonar operation mode

Scan beam angle

Scan range in m

</sonar>

<lprofile>

Scanning altitude in m

Scanning speed in m/s

Camera gain in percentage or Auto(A)

Camera horizontal opening angle in deg

Camera vertical opening angle in deg

Camera mounting angle in deg

Baseline in millimetres

Camera horizontal resolution in pixels

Camera vertical resolution in pixels

Laser opening angle in deg

</lprofile>

<oas>

Sonar range in m

Scan beam angle

Sonar gain in percentage

</oas>

</scanning>

An example of the initialization file used during one of the experiments conducted in the tank environment at the Chiba Experimental station is as follows:

<?xml version="1.0" encoding="UTF-8"?>
<user>MNS, IIS</user>
<mission>

<name>Test1</name>

<mode>Auto</mode>

<point><nops>2</nops>

1.56 1.00 0.00

1.78 2.20 1.29

</point>

<area>

0.0 0.0

0.0 10.0

10.0 10.0

10.0 0.0

</area>

</mission>

<scanning>

<sonar>

5

0.35

50

P

120

5

</sonar>

<lprofile>

2.5

0.1

A

```
            60.5
            52.5
            68
            835
            640
            480
            90
        </lprofile>
        <oas>
            5
            90
            80
        </oas>
</scanning>
```

Currently these are the parameter values that can be configured using the initialization file. Additional specifications and parameters can be easily incorporated into the file and the file parsing program.

C.2 Survey rule file

This section of the appendix gives details on the structure of the survey rule file. The rule file provides the vehicle information about the interest of the survey. This allows the vehicle to take suitable action once features on the seafloor are detected. The interest of the survey is decided based on the seafloor property being measured by the seafloor observation sensor carried by the vehicle. For certain sensors to work reliably, they need contact with the seafloor. Since landing on the seafloor is time consuming, the areas which are best suited for observation based on the bathymetry features should be given priority. The survey rule file provides the vehicle information which enables it to make decisions for most effective survey outcome. Similar to the initialization file, the survey rule file is an XML based file. There are several advantages of using an XML based file system. Parsers for reading these files are easily available. Structured data makes programing easy. The file is a progressive

file and sections can be added or removed as per the user. It is easy to add new features in the future making it suitable for performing future enhancements to the developed system. The basic structure of the rule file has been given below:

```
<?xml version="1.0" encoding="UTF-8"?>
<user>Username and Institution Name</user>
<mission>
    <name>Missionname</name>
    <sensorid>Type of sensor being used</sensorid>
    <prop>Measured seafloor property</prop>
 <widescan>
    <feature>
        <shp>Nature of feature for scanning</shp>
        <sha>Area of feature for scanning</sha>
        <shc>Connected or isolated</shc>
        <sho>Orientation of the feature</sho>
    </feature>
    <highscan>
        <feature>
            <shp>Shape of feature for scanning</shp>
            <shz>Size of feature for scanning</shz>
            <landing>
                <nop>Minimum number of points</nop>
                <shp>Shape of feature for landing</shp>
                    <lattr>
                    <lupdw>Landing on top or bottom</lupdw>
                    <lsds>Landing on sides of feature</lsds>
                    </lattr>
```

```
            </landing>
        </feature>
    </highscan>
</widescan>
</mission>
```

To explain the making of the rule file for different scenario, we can consider the file used for one of the experiments. In this case, the scenario was to simulate landing around artificial reefs to collected radiation measurements. The mission was to locate rectangular features and land on the largest of the sides to obtain seafloor measurements. The first stage required scanning of the scenario using an acoustic wide area sonar to detect individual objects which are rectangular in shape. The next was to select the largest of the object and scan that with a high resolution. The last step was to find landing points along the largest sides and performing landing for obtaining seafloor observations. The file provided to the vehicle for this mission can be seen as follows:

```
<?xml version="1.0" encoding="UTF-8"?>
<user>MNS, IIS</user>
<mission>
    <name>Tankexp1</name>
    <sensorid>G</sensorid>
    <prop>Rad</prop>
<widescan>
    <feature>
        <shp>rect</shp>
        <sha>+2.5</sha>
        <shc>iso</shc>
    </feature>
    <highscan>
        <feature>
            <shp>all</shp>
```

```
            <landing>
                <nop>2</nop>
                <shp>rect</shp>
                    <lattr>
                    <lupdw>0</lupdw>
                    <lsds>l+2</lsds>
                    </lattr>
            </landing>
        </feature>
    </highscan>
</widescan>
</mission>
```

In the header, the G indicates the Gamma radiation sensor and Rad the radiation measurement. A list of abbreviations for sensor types has been made. At present this information is not used. In future work, the sensor type and seafloor property measured will be used to make presets of the types of features required for a particular sensor. The area of the feature to be scanned should be more than 2.5sq.m. The code l+2 indicated finding landing points along the largest 2 sides. The code 0 for landing on up and down indicates that the vehicle need not land on the top of the feature.

Acknowledgements

This research was conducted at the Institute of Industrial Science, The University of Tokyo, Japan between October 2010 and March 2014. I am forever indebted to Prof. Tamaki Ura under the supervision of whom I started my Masters program and continued my Ph.D program. I am very thankful for his endless support and encouragement and for allowing me to pursue my ideas freely and explore solutions independently. Without his support and guidance this research would not have been possible. I would also like to sincerely thank him for allowing me to go on three research cruises during the time of my research. I also appreciate his help and support for helping me with some of my personal issues during my stay here in Japan. I would like to extent my gratitude and appreciation towards Prof. Takagawa and Prof. Maki for their guidance, encourage and support and patience during the final year of my program under whose supervision I shall be completing the program.

My sincere gratitude to Ms.Harumi Sugimatsu for her endless effort and help during the entire program and for making things easier for me whenever I needed help with paperwork and official formalities. I would also like to thank Ms.Minegishi and Ms.Takenaga for helping me on numerous occasions with forms and documents which I have usually forgotten to submit. I sincerely appreciate the inspiration and guidance provided to me by Dr. Blair Thornton at every step and also thank him for providing me suggestions and recommendations whenever necessary. I wish to thank Sakamaki san for helping me every time with hardware setup during my experiments on ship as well as in the pool. I would also like to extend by thanks to Adrian Bodenmann, P.V. Unnikrishnan, Nakatani san , Nose san , Kim san and other members of Ura Lab and Maki Lab for their help and for taking time out of their busy schedules to provide answers for my several inquiries. I would also like to thank all my close friends at IIS and around the world for boosting my moral and bringing be back on track when I was uncertain of my objectives and goals.

But above all, I would like to thank my father, Naresh Sangekar, for inspiring me since my childhood and guiding me all throughout my life for taking the right steps and being a good person. I would also like to thank him for allowing me to take risks in life and supporting me on any path I choose for myself. I will always be forever grateful to my loving mother, Aruna Sangekar, without her nourishment and care I would not be here. I could never forget the endless efforts she put in my studies and education when I was young. Without the endless care and efforts of my parents in my upbringing and education I would not have made it so far.

References

[1] Thomson C and Murray J. Report on the scientific results of the Voyage of H.M.S Challenger. *Order of her Majesty's Government*, 1(1), 1885. 2

[2] Christian Moustier and Haruyoshi Matsumoto. Seafloor acoustic remote sensing with multibeam echo-sounders and bathymetric sidescan sonar systems. *Marine Geophysical Researches*, 15(1):27–42, March 1993. 2

[3] Oscar Pizarro, Stefan B. Williams, Michael V. Jakuba, Matthew Johnson-Roberson, Ian Mahon, Mitch Bryson, Daniel Steinberg, Ariell Friedman, Donald Dansereau, Navid Nourani-Vatani, Daniel Bongiorno, Michael Bewley, Asher Bender, Nasir Ashan, and Bertrand Douillard. Benthic monitoring with robotic platforms - The experience of Australia. In *2013 IEEE International Underwater Technology Symposium (UT)*, pages 1–10. IEEE, March 2013. 3

[4] C. Roman, O. Pizarro, R. Eustice, and H. Singh. A new autonomous underwater vehicle for imaging research. In *OCEANS 2000 MTS/IEEE Conference and Exhibition*, volume 1, pages 153–156, September 2000. 3

[5] D G Jones. Development and application of marine gamma-ray measurements: a review. *Journal of environmental radioactivity*, 53(3):313–33, January 2001. 3

[6] David M Rubin, Henry Chezar, Jodi N Harney, David J Topping, Theodore S Melis, and Christopher R Sherwood. Underwater microscope for measuring spatial and temporal changes in bed-sediment grain size. *Sedimentary Geology*, 202(3):402–408, 2007. 3

[7] Blair Thornton, Akira Asada, Adrian Bodenmann, Mehul Sangekar, and Tamaki Ura. Instruments and Methods for Acoustic and Visual Survey of Manganese Crusts. *IEEE Journal of Oceanic Engineering*, 38(1):186–203, January 2013. 3

[8] Blair Thornton, Tetsuo Sakka, Tomoko Takahashi, Ayaka Tamura, Tatsuya Masamura, and Ayumu Matsumoto. Spectroscopic Measurements of Solids Immersed in Water at High Pressure Using a Long-Duration Nanosecond Laser Pulse. *Applied Physics Express*, 6(8):082401, July 2013. 3

[9] Blair Thornton, Adrian Bodenmann, Akira Asada, Tamaki Ura, Mehul Sangekar, Katsumi Ohira, and Daigo Kirimura. Acoustic and visual survey of manganese crusts using an underwater vehicle at #5 Takuyo seamount. In *2011 IEEE Symposium*

on Underwater Technology and Workshop on Scientific Use of Submarine Cables and Related Technologies, pages 1–9. The University of Tokyo, 4-6-1 Komaba, Meguro, Tokyo, IEEE, 2011. 5

[10] Chie Honsho, Tamaki Ura, and Akira Asada. Mapping the Bayonnaise knoll caldera and the Hakurei hydrothermal deposit with autonomous underwater vehicle using side-scan and multi-beam sonars. Number December, pages 1–8, 2013. 6

[11] Blair Thornton, Yusuke Yano, and Tamaki Ura. The Development of a Towed Sea-bed Gamma Ray Spectrometer. 2013. 6

[12] Blair Thornton, Seiki Ohnishi, Tamaki Ura, Naoteru Odano, and Tsuneo Fujita. Continuous measurement of radionuclide distribution off Fukushima using a towed sea-bed gamma ray spectrometer. 2013. 6

[13] K.P. Carroll, S.R. McClaran, E.L. Nelson, D.M. Barnett, D.K. Friesen, and G.N. William. AUV path planning: an A* approach to path planning with consideration of variable vehicle speeds and multiple, overlapping, time-dependent exclusion zones. In *Proceedings of the 1992 Symposium on Autonomous Underwater Vehicle Technology*, pages 79–84. IEEE, 1992. 8

[14] Y. Petillot, I. Tena Ruiz, D.M. Lane, Y. Wang, E. Trucco, and N. Pican. Underwater vehicle path planning using a multi-beam forward looking sonar. In *IEEE Oceanic Engineering Society. OCEANS'98. Conference Proceedings (Cat. No.98CH36259)*, volume 2, pages 1194–1199. IEEE, 1998. 9

[15] David P Williams. AUV-enabled adaptive underwater surveying for optimal data collection. *Intelligent Service Robotics*, 5(1):33–54, 2012. 9

[16] Beng Parijat D Deshpande,Mehul N Sangekar,Bharath Kalyan,Mandar Chitre,Shiraz Shahabudeen,Venugopalan Pallayil,Teong Koay. Design and Development of AUVs for cooperative missions. In *Defence Technology Asia*, Singapore, 2007. 9

[17] Andrea Munafo, Enrico Simetti, Alessio Turetta, Andrea Caiti, and Giuseppe Casalino. Autonomous underwater vehicle teams for adaptive ocean sampling: a data-driven approach. *Ocean Dynamics*, 61(11):1981–1994, July 2011. 9

[18] A Kume, T Maki, T Sakamaki, and T Ura. Path re-planning method for an AUV to image rough terrain by on-site quality evaluation. In *2012 Oceans - Yeosu*, pages 1–9. IEEE, May 2012. 9

[19] Andrew A Bennett, Associate Member, and John J Leonard. A behavior-based approach to adaptive feature detection and following with autonomous underwater vehicles. *Oceanic Engineering, IEEE Journal of*, 25(2):213–226, 2000. 9

[20] R. Camilli, B. Bingham, M. Jakuba, H. Singh, and J. Whelan. Integrating in-situ chemical sampling with auv control systems. In *Oceans '04 MTS/IEEE Techno-Ocean '04 (IEEE Cat. No.04CH37600)*, volume 1, pages 101–109. IEEE, 2004. 9

[21] J.A. Farrell and R.M. Arrieta. Moth-inspired chemical plume tracing on an autonomous underwater vehicle. *IEEE Transactions on Robotics*, 22(2):292–307, April 2006. 9

[22] N K Yilmaz, C Evangelinos, P F J Lermusiaux, and N M Patrikalakis. Path Planning of Autonomous Underwater Vehicles for Adaptive Sampling Using Mixed Integer Linear Programming. *Oceanic Engineering, IEEE Journal of*, 33(4):522–537, 2008. 9

[23] Y.R. Petillot, S.R. Reed, and J.M. Bell. Real time AUV pipeline detection and tracking using side scan sonar and multi-beam echo-sounder. In *Oceans '02 MTS/IEEE*, volume 1, pages 217–222. IEEE, 2002. 9

[24] G R Cutter Jr., Y Rzhanov, and L A Mayer. Automated segmentation of seafloor bathymetry from multibeam echosounder data using local Fourier histogram texture features. *Journal of Experimental Marine Biology and Ecology*, 285-286(0):355–370, 2003. 9

[25] Bertrand Douillard, Navid Nourani-Vatani, Matthew Johnson-Roberson, Stefan Williams, Chris Roman, Oscar Pizarro, Ian Vaughn, and Gabrielle Inglis. FFT-based Terrain Segmentation for Underwater Mapping. In *Proceedings of Robotics: Science and Systems*, Sydney, Australia, 2012. 9

[26] B. Douillard, N. Nourani-Vatani, M. Johnson-Roberson, O. Pizarro, S. Williams, C. Roman, and I. Vaughn. Frequency-based underwater terrain segmentation. *Autonomous Robots*, 35(4):255–269, July 2013. 9

[27] W.I. Stewart, D. Chu, S. Malik, S. Lerner, and H. Singh. Quantitative seafloor characterization using a bathymetric sidescan sonar. *IEEE Journal of Oceanic Engineering*, 19(4):599–610, 1994. 9

[28] Li-Yuan Weng, Min Li, Zhenbang Gong, and Shugen Ma. Underwater object detection and localization based on multi-beam sonar image processing. In *2012 IEEE International Conference on Robotics and Biomimetics (ROBIO)*, pages 514–519. IEEE, December 2012. 9

[29] C.B. Lirakis and K.P. Bongiovanni. Automated multibeam data cleaning and target detection. In *OCEANS 2000 MTS/IEEE Conference and Exhibition. Conference Proceedings (Cat. No.00CH37158)*, volume 1, pages 719–723. IEEE, 2000. 9

[30] Takeshi Nakatani, Tamaki Ura, Yuzuru Ito, Junichi Kojima, Kenkichi Tamura, Takashi Sakamaki, and Yoshiaki Nose. AUV "TUNA-SAND" and its Exploration of hydrothermal vents at Kagoshima Bay. In *OCEANS 2008 - MTS/IEEE Kobe Techno-Ocean*, pages 1–5. IEEE, April 2008. 10

[31] T Ura, T Nakatani, and Y Nose. Terrain Based Localization Method for Wreck Observation AUV. *OCEANS 2006*, pages 1–6, 2006. 10

[32] Takeshi Nakatani, Tamaki Ura, Takashi Sakamaki, and Junichi Kojima. Terrain based localization for pinpoint observation of deep seafloors. In *OCEANS 2009 - EUROPE*, number 1, pages 1–6. IEEE, May 2009. 10

[33] Severin Stalder, Hannes Bleuler, and Tamaki Ura. Terrain-based navigation for underwater vehicles using side scan sonar images. In *OCEANS 2008*, pages 1–3. IEEE, 2008. 10

[34] Kouji Masuko, Ippei Takahashi, Shuhei Ogawa, Meng-Hung Wu, Atsushi Oosedo, Takaaki Matsumoto, Kenta Go, Fumihito Sugai, Atsushi Konno, and Masaru Uchiyama. Autonomous takeoff and landing of an unmanned aerial vehicle. In *2010*

IEEE/SICE International Symposium on System Integration, pages 248–253. IEEE, December 2010. 10

[35] Omer Cetin, Sefer Kurnaz, and Okyay Kaynak. Fuzzy Logic Based Approach to Design of Autonomous Landing System for Unmanned Aerial Vehicles. *Journal of Intelligent & Robotic Systems*, 61(1-4):239–250, November 2010. 10

[36] Marwan Shaker, Mark N.R. Smith, Shigang Yue, and Tom Duckett. Vision-Based Landing of a Simulated Unmanned Aerial Vehicle with Fast Reinforcement Learning. In *2010 International Conference on Emerging Security Technologies*, pages 183–188. IEEE, September 2010. 10

[37] S Wang, H Zhang, W Hou, J Liang, Publisher Taylor, H Zhangy, W Houy, and J Liangz. Control and navigation of the variable buoyancy AUV for underwater landing and takeoff. *International Journal of Control*, 80(7):1018–1026, 2007. 10

[38] Jonathan Byron and R. Tyce. Designing a vertical / horizontal auv for deep ocean sampling. In *OCEANS 2007*, pages 1–10, 2007. 10

[39] Bing Du, Yongxiang Jiang, and Hongwei Zhang. Dynamic analysis of landing autonomous underwater vehicle. *Transactions of Tianjin University*, 18(4):298–304, August 2012. 10

[40] Jeremy Breen, P A de Souza, Greg P Timms, Robert Ollington, and Paulo A De Souza Jr. Adaptive behaviour for an Autonomous Underwater Vehicle to perform chemical mappings. pages 1–6, 2010. 10

[41] Blair Thornton, Seiki Ohnishi, Tamaki Ura, Naoteru Odano, Shun Sasaki, Tsuneo Fujita, Tomowo Watanabe, Kaoru Nakata, Tsuneo Ono, and Daisuke Ambe. Distribution of local 137Cs anomalies on the seafloor near the Fukushima Dai-ichi Nuclear Power Plant. *Marine Pollution Bulletin*, 74(1):344–350, 2013. 17

[42] Matthew Johnson-Roberson, Oscar Pizarro, Stefan B Williams, and Ian Mahon. Generation and visualization of large-scale three-dimensional reconstructions from underwater robotic surveys. *Journal of Field Robotics*, 27(1):21–51, 2010. 39

[43] Jon Henderson, Oscar Pizarro, Matthew Johnson-Roberson, and Ian Mahon. Mapping Submerged Archaeological Sites using Stereo-Vision Photogrammetry. *International Journal of Nautical Archaeology*, 42(2):243–256, September 2013. 39

[44] M N Sangekar, B Thornton, T Nakatani, and T Ura. Development of a landing algorithm for autonomous underwater vehicles using laser profiling. In *OCEANS 2010*, pages 1–7, Sydney, Australia, 2010. IEEE. 43

[45] M. Dunbabin, J. Roberts, K. Usher, G. Winstanley, and P. Corke. A Hybrid AUV Design for Shallow Water Reef Navigation. In *Proceedings of the 2005 IEEE International Conference on Robotics and Automation*, pages 2105–2110. IEEE, 2005. 56

[46] Blair Thornton, Tamaki Ura, Mehul Sangekar, and Katsumi Ohira. A case study to demonstrate remote acoustic measurement of ferro-manganese crust thickness. In *Ocean Engineering Symposium*, Tokyo, 2009. 57

[47] M Sangekar, M Chitre, and T B Koay. Hardware architecture for a modular autonomous underwater vehicle STARFISH. In *OCEANS 2008*, pages 1–8, Quebec, Canada, 2008. IEEE. 63

[48] Mehul Sangekar, Blair Thornton, and Tamaki Ura. Wide area seafloor observation using an autonomous landing vehicle with adaptive resolution capability. In *OCEANS 2012*, pages 1–9, Hampton Roads, USA, October 2012. IEEE. 81

[49] Peter Axelsson. Processing of laser scanner data - algorithms and applications. *ISPRS Journal of Photogrammetry and Remote Sensing*, 54(2):138–147, 1999. 109

[50] G Inglis, C Smart, I Vaughn, and C Roman. A pipeline for structured light bathymetric mapping. In *Intelligent Robots and Systems (IROS), 2012 IEEE/RSJ International Conference on*, pages 4425–4432, 2012. 109

[51] A Bodenmann, B Thornton, T Ura, M Sangekar, T Nakatani, and T Sakamaki. Pixel based mapping using a sheet laser and camera for generation of coloured 3D seafloor reconstructions. In *OCEANS 2010*, pages 1–5, 2010. 109

[52] Adrian Bodenmann, Blair Thornton, Tamaki Ura, and Mehul Sangekar. Pixel mapping for generation of 3D coloured seafloor bathymetry using a single camera. In *Autonomous Underwater Vehicles AUV 2010 IEEEOES*, pages 1–9, USA, 2010. IEEE. 110

[53] S. Kuchler, J. K. Eberharter, K. Langer, K. Schneider, and O. Sawodny. Heave Motion Estimation of a Vessel Using Acceleration Measurements. MIlano, Italy, 2011.

[54] Chris Roman, Gabrielle Inglis, and Bryan McGilvray. Lagrangian floats as sea floor imaging platforms. *Continental Shelf Research*, 31(15):1592–1598, 2011.

[55] F Pohner, J Bakke, O Nilsen, T Kjaer, and Luciano Fonseca. Integrating Imagery from Hull Mounted Sidescan Sonars with Multibeam Bathymetry. In *U.S. Hydrographic Conference (US HYDRO)*, Norfolk, VA, USA, 2007.

[56] Hanumant Singh, Roy Armstrong, Fernando Gilbes, Ryan Eustice, Chris Roman, Oscar Pizarro, and Juan Torres. Imaging Coral I: Imaging Coral Habitats with the SeaBED AUV. *Subsurface Sensing Technologies and Applications*, 5(1):25–42, January 2004.

[57] Mitch Bryson, Matthew Johnson-roberson, Oscar Pizarro, and Stefan B Williams. Colour-Consistent Structure-from-Motion Models using Underwater Imagery. In *Science and Systems VIII*, pages 1–8, Sydney, Australia, 2012.

[58] C Roman, G Inglis, and J Rutter. Application of structured light imaging for high resolution mapping of underwater archaeological sites. In *OCEANS 2010 IEEE*, pages 1–9, Sydney, Australia, 2010.

[59] Hanumant Singh, Chris Roman, Oscar Pizarro, and Ryan Eustice. Advances in High Resolution Imaging from Underwater Vehicles. In S Thrun, Brooks RA, and Durrant-Whyte HF, editors, *Robotics Research: Results of the 12th International Symposium ISRR*, number 3, pages 430–448. Springer, 28 edition, 2007.

[60] Oscar Pizarro, Stefan B. Williams, and Jamie Colquhoun. Topic-based habitat classification using visual data. In *OCEANS 2009-EUROPE*, pages 1–8. IEEE, May 2009.

[61] StefanB. Williams, Oscar Pizarro, Michael Jakuba, and Neville Barrett. Auv benthic habitat mapping in south eastern tasmania. In Andrew Howard, Karl Iagnemma, and Alonzo Kelly, editors, *Field and Service Robotics*, volume 62 of *Springer Tracts in Advanced Robotics*, pages 275–284. Springer Berlin Heidelberg, 2010.

[62] Ricardo Leon, Luis Somoza, Teresa Medialdea, Adolfo Maestro, Victor Diaz-del Rio, and Maria Carmen Fernandez-Puga. Classification of sea-floor features associated with methane seeps along the Gulf of Cadiz continental margin. *Deep Sea Research Part II: Topical Studies in Oceanography*, 53(11-13):1464–1481, 2006.

[63] Toshihiro Maki, Ayaka Kume, Tamaki Ura, Takashi Sakamaki, and Hideyuki Suzuki. Autonomous detection and volume determination of tubeworm colonies from underwater robotic surveys. In *OCEANS 2010 IEEE - Sydney*, volume d, pages 1–8. Ieee, May 2010.

[64] W K Stewart, D Chu, S Malik, S Lerner, and H Singh. Quantitative seafloor characterization using a bathymetric sidescan sonar. *Oceanic Engineering, IEEE Journal of*, 19(4):599–610, 1994.

[65] Smriti H Bhandari and S M Deshpande. Feature Extraction for Surface Classification - An approach with Wavelets. *International Journal of Computer and Information Science and Engine*, 1(4):322–326, 2007.

[66] Neil C Mitchell, Maurice A Tivey, and Pascal Gente. Seafloor slopes at mid-ocean ridges from submersible observations and implications for interpreting geology from seafloor topography. *Earth and Planetary Science Letters*, 183(3-4):543–555, 2000.

[67] H. Singh, C. Roman, L. Whitcomb, and D. Yoerger. Advances in fusion of high resolution underwater optical and acoustic data. In *Proceedings of the 2000 International Symposium on Underwater Technology (Cat. No.00EX418)*, pages 206–211. IEEE, 2000.

[68] D. R. Yoerger, M. Jakuba, A. M. Bradley, and B. Bingham. Techniques for Deep Sea Near Bottom Survey Using an Autonomous Underwater Vehicle. *The International Journal of Robotics Research*, 26(1):41–54, January 2007.

[69] Matthew Johnson-Roberson, Oscar Pizarro, and Stefan Willams. Towards large scale optical and acoustic sensor integration for Visualization. In *OCEANS 2009-EUROPE*, pages 1–4. IEEE, May 2009.

[70] Neil Cunningham Dobson. Developmental deep-water archaeology: a preliminary report on the investigation and excavation of the 19th-century side-wheel steamer SS Republic, lost in a storm off Savannah in 1865. In *OCEANS, 2005. Proceedings of MTS/IEEE*, pages 1761–1769 Vol. 2, 2005.

[71] L.D. Stone, C.M. Keller, T.M. Kratzke, and J.P. Strumpfer. Search analysis for the underwater wreckage of Air France Flight 447, 2011.

[72] Michael L. Brennan, Robert D. Ballard, Chris Roman, Katherine C. Bell, Bridget Buxton, Dwight F. Coleman, Gabrielle Inglis, Orkan Y, and Tufan Turanli. Evaluation of the modern submarine landscape off southwestern Turkey through the documentation of ancient shipwreck sites. *Continental Shelf Research*, 43(0):55–70, July 2012.

[73] Andres Mora, Colin Ho, and Srikanth Saripalli. Analysis of adaptive sampling techniques for underwater vehicles. *Autonomous Robots*, 35(2-3):111–122, May 2013.

[74] Stephanie Kemna, Michael J. Hamilton, David T. Hughes, and Kevin D. LePage. Adaptive autonomous underwater vehicles for littoral surveillance. *Intelligent Service Robotics*, 4(4):245–258, July 2011.

[75] Donald P. Eickstedt, Michael R. Benjamin, Ding Wang, Joseph Curcio, and Henrik Schmidt. Behavior Based Adaptive Control for Autonomous Oceanographic Sampling. In *Proceedings 2007 IEEE International Conference on Robotics and Automation*, pages 4245–4250. IEEE, April 2007.